



# This is to certify that the

### dissertation entitled

# Intercalation of Transition Metal Complex Salts in Layered

Silicate Clays: Applications as Phase

Transfer Catalysts presented by

Abbas Kadkhodayan

has been accepted towards fulfillment of the requirements for

Ph.D. degree in Chemistry

Major professor

Dr. Thomas J. Pinnavaia

Date \_ Kine 25/994



RETURNING MATERIALS:
Place in book drop to remove this checkout from your record. FINES will be charged if book is returned after the date stamped below.

# INTERCALATION OF TRANSITION METAL COMPLEX SALTS IN LAYERED SILICATE CLAYS: APPLICATIONS AS PHASE TRANSFER CATALYSTS

By

Abbas Kadkhodayan

# A DISSERTATION

Submitted to
Michigan State University
in partial fulfillment of the requirements
for the degree of

DOCTOR OF PHILOSOPHY

Department of Chemistry

1984

### **ABSTRACT**

INTERCALATION OF TRANSITION METAL COMPLEX
SALTS IN LAYERED SILICATE CLAYS: APPLICATIONS
AS PHASE TRANSFER CATALYSTS

By

# Abbas Kadkhodayan

Several chelated transition metal complex salts as well as some organic salts have been intercalated in smectite clays (hectorite and montmorillonite). After the characterization of these systems by a variety of physical and chemical measurements, their utility as phase transfer catalysts was examined.

Among the complexes used in the present investigation tris-orthophenanthroline metal complexes of the type  $M(\text{phen})_3 XO_4$  (M-Ni,Fe,Zn) and  $(XO_4 = MoO_4^{2-}, CrO_4^{2-}, WO_4^{2-}, SO_4^{2-})$  and organic salts such as Nile Blue were capable of binding to smectite clay in excess of its cation exchange capacity (Intersalation reaction, see Chap. I). The adsorption isotherms demonstrate that the complexes have a marked affinity for the clay surfaces in aqueous suspension. Chemical analysis of  $M(\text{phen})_3^{2+}/XO_4^{2-}$ -hectorite indicates the presence of one equivalent of  $M(\text{phen})_3^{2+}$  to balance the layer charge of the clay and one equivalent as  $M(\text{phen})_3^{2+}/XO_4^{2-}$  ion pairs.

The solid state of these intersalated phases yield a d(001) spacing as high as  $\sim 30$  Å which is consistent with the presence of an anion layer sandwiched between two layers

of the complex cation within the interlayer of the smectite. Intercalation of various complex cations and anions showed that the intersalation reactions are dependent on the nature of the complex cation as well as counter-anion.

Several intersalation phases (e.g. Fe(phen) $_3^{2+}/\text{SO}_4^{2-}$  hectorite) have been tried for the desorption of complex salt from the interlayer, when they were equilibrated in aqueous solution as well as organic solvent. The results indicate that the binding of these ion pairs to the clay interlayers are quite strong. For example, the coefficient for desorption of Fe(phen) $_3^{2+}/\text{SO}_4^{2-}$  ion pairs from the two-CEC hectorite intersalate in water at 20°C is  $8.2 \times 10^{-10}$  mole<sup>2</sup> liter<sup>-2</sup>. Thus the intercalated salt is about as soluble as AgC1, which has a solubility product of  $1.56 \times 10^{-10}$  mole<sup>2</sup> liter<sup>-2</sup> at 25°C.

It is interesting that the intercalated anions in the hectorite intersalates can be readily exchanged at room temperature with a variety of anions. The adsorption isotherms were obtained for the exchange of  $\text{CrO}_4^{2-}$  anion in  $\text{Ni}(\text{phen})_3^{2+}/\text{CrO}_4^{2-}$ -hectorite by  $\text{MoO}_4^{2-}$ ,  $\text{WO}_4^{2-}$ ,  $\text{PO}_4^{3-}$ ,  $\text{Cr}(\text{OX})_3^{3-}$ ,  $\text{Cl}^-$ ,  $\text{CH}_3\text{CO}_2^-$  and  $\text{C}_6\text{H}_5\text{-COO}^-$  anions. For example, in the case of  $\text{MoO}_4^{2-}$ , essentially all of the intercalated  $\text{CrO}_4^{2-}$  (~43 meq/100 g of intersalate) is replaced at an equilibrium concentration of  $7 \times 10^{-4}$  M. However, among the exchange ions investigated, acetate has the lowest affinity for replacing intercalated  $\text{CrO}_4^{2-}$  anion.

X-ray diffraction measurements were used to study the swelling properties of Ni(phen) $_3^{2+}/\text{SO}_4^{2-}$ -hectorite system in two solvents used in the catalytic studies (toluene and water). Virtually no swelling occurred with toluene, but in the case of water an expansion of  $\sim 5$  Å was observed.

 ${\rm Zn}\,({\rm phen})_3^{2+}/{\rm SO}_4^{2-}$ -hectorite intersalate (2 equivalent CEC) was synthesized and a nitroxide spin probe [peroxylamine disulfonate (PADS)] was doped into the anion interlayers at about 2% level of exchange. The spin probe was used to estimate the interlamellar mobility at different relative humidity. For example, under fully wetted conditions the tumbling mobility of the intercalated 2-(PADS) was  $\tau_C \cong 3 \times 10^{-10}$  sec. Therefore, the interlayer takes on appreciable solution-like properties.

An indication of the retention of chemical and structural constitution of the complexes upon intercalation was observed by IR and electronic spectroscopy.

The ease with which  $\mathrm{XO}_4^{2^-}$  anions can be replaced in  $\mathrm{M}(\mathrm{chel})_3^{2^+}/\mathrm{XO}_4^{2^-}$ -hectorite intersalates suggested that these compounds may be effective catalysts in a triphase reaction system involving anionic nucleophiles. In this respect several types of layered silicate intersalates were synthesized and used for halogen exchange reactions on different alkyl halides as well as carboxylate and cyanide ion displacements. It was found that  $\mathrm{Ni}(\mathrm{phen})_3^{2^+}/\mathrm{SO}_4^{2^-}$ -hectorite is 140 times more selective for the reaction of 1-bromopropane than the largest substrate (1-bromo hexadecane) tried. The intersalation compounds were also examined for

# Kadkhodayan, Abbas

shape selectivity. However, despite the great size selectivity of the intersalates, no dramatic shape selectivity was observed. All catalysts except the cetylpridinium clay intersalate, exhibit a pseudo first-order dependency on the substrate concentration and the amount of catalyst.

THE SUCCESS OF THIS WORK IS DEDICATED TO MY GRANDMOTHER,

ANA, FOR WHOM NO ACKNOWLEDGMENT WOULD BE SUFFICIENT.

I HAVE ALWAYS WISHED THAT I COULD DO SOMETHING IN RETURN

FOR ALL SHE HAS DONE FOR ME...BUT NEVER COULD!

### **ACKNOWLEDGMENTS**

Credit must be extended primarily to mankind's development of the Scientific Method and, thereby, the only means we have of separating fictitious thought and fantasy from scientific realities of this universe. This method has and certainly will continue to change the world.

For one reason or another I never seriously worked hard on my Ph.D. until near the end. For Professor Thomas J. Pinnavaia, my research advisor, who was very patient and tolerant, I am very appreciative. I sincerely thank him for all that he has done for me.

Special thanks are also due Professor Carl H.

Brubaker, who served as my second reader and also to

Professor Max M. Mortland for providing special research
facilities and helpful discussions.

I also wish to thank Professors Ashraf M. El-Bayoumi and Richard Schwendeman, who also served on my guidance committee.

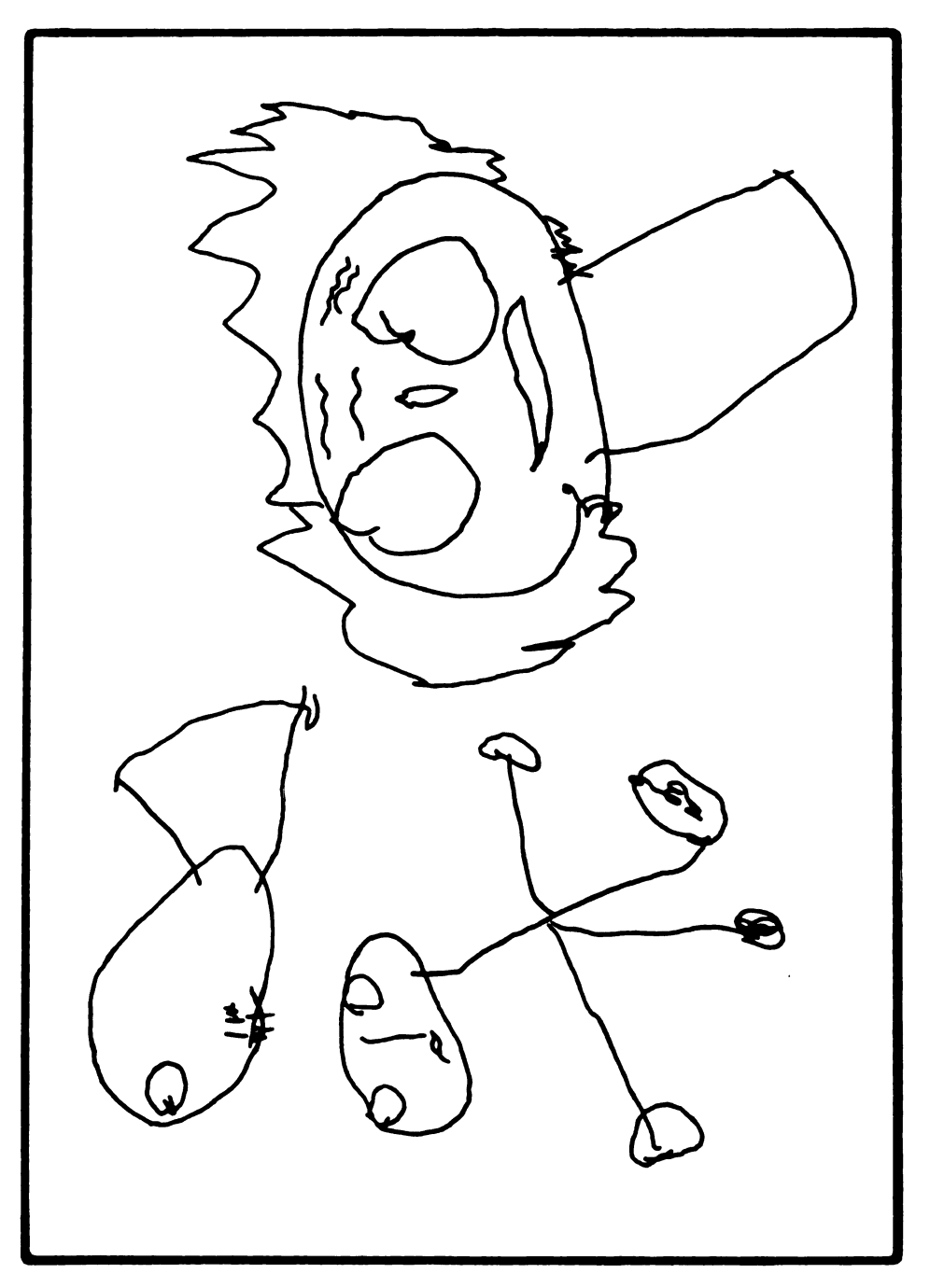
Special acknowledgment is due the members of the academic and technical staff of the Chemistry Department and also to colleagues of my research group whose cooperation and help has been invaluable.

Gratitude is expressed to Ms. Margy Lynch for her great assistance in typing this dissertation and help in many occasions.

Also, I would like to remember here Martin Rabb and Emmanuel Giannelis, who have become dear to me as friends.

Many thanks also go to all the people whose work has been administered in the following ways: a scholarship from the University of Teacher Education, Tehran, Iran; a Teaching Assistantship from the Department of Chemistry, Michigan State University; a Research Assistantship from the National Science Foundation, Michigan State University; a Sage Foundation Award from the Sage Foundation, Michigan State University.

Finally, I am deeply grateful to Nahid, with whom I share my life, for all her help, encouragement and friendship throughout the course of this study.



# Reproduced by permission from YASHA! Personal file, Spring, 1984

Yasha (as of now 3 years old), certainly did contribute to his father's work, did he not?

# TABLE OF CONTENTS

CHAPTER	PAGE
LIST OF	TABLES
LIST OF	FIGURES
LIST OF	SYMBOLS AND ABBREVIATIONS
CHAPTER	I INTRODUCTION
CHAPTER	II EXPERIMENTAL

CHAPTER PAGE

	3.	Fe(L) <sub>3</sub> SO <sub>4</sub> , [(L = 1,10-orthophen-
		anthroline) 3, 4, 7, 8-tetramethyl-
		1,10-phenanthroline, and 4-7-
		diphenyl-1,10-phenanthroline
		(Bathopheanthroline)]
	4.	$Fe(TPTZ)_2(ClO_4)_2$ , $4H_2O$ , $Fe(TPTZ)_2$ -
		so <sub>4</sub>
	5.	$Ni(en)_3SO_4$ and $Ni(NH_3)_6SO_4$ 56
	6.	$Fe(bP)_3(ClO_4)_2$ and $Fe(bP)_3SO_4$ 57
	7.	$K_3Cr(OX)_3 \cdot 3H_2O$
	8.	Elemental Analysis and Storage 57
		eparation of Intercalates
		eparation of Intersalates
		sorption Coefficient Measurement 59
		Exchange-Adsorption Isotherms 60
		on Exchange Adsorption Isotherm
		dies
	H. Kir	metics of Biphase and Triphase-
		alyzed Displacement Reactions 61
		ection of Benzyl Chloride With ts of the Acetate Ion 64
		lification of the Intersalate With
	211	ane Coupling Agent
	K. Phy	rsical Methods 65
	1.	
		ESR Studies 66
		UV-Visible Spectroscopy 67
		Gas Chromotography 67
	5.	Infrared Spectra 68
CHAPTER III	RESULTS	AND DISCUSSION 69
	A. Ads	sorption of Complex Salts on
	Sme	ectite-(Intersalation Reaction)69
	1.	Adsorption of Metal Complex
	_	Salts
	2.	X-ray Diffraction of M(chel) $\frac{2+}{3}$
	_	$XO_4^{2^-}$ -Hectorite 84
	3.	Anion Effects on M(chel) $_{\rm X}^{2+}$
		Adsorption 87
	4.	Effects of Ligand on M(chel) x+
		Adsorption 92
	5.	Electronic Spectra 95
	6.	Adsorption of Organic Salts 97
	7.	Desorption Coefficient Measure-
	_	ment
	8.	Anion Exchange Properties of
	_	Smectite Intersalate
	9.	Swelling of the Intersalation
		Phase 109
	10.	ESR Studies 111

CHAPTER		PAGE
	B. Ca	talytic Properties of the
	In	tersalates 120
	1.	Kinetics of the Haolgen
		Exchange
	2.	Substrate Size and Shape
		Selectivity
	3.	Structural Modification
	4.	Particle Size Effect 143
	5.	Carboxylate Ion Displacement 146
		Supported Cetyl Pridinium
		Bromide for TC 147
	7.	Halogen Exchange Using Organic
		Salt Intersalates
	8.	Kinetics of Cyanide Displace-
		ment on 1-Bromooctane
APPENDIX		
LIST OF REFE	RENCES.	

# LIST OF TABLES

TABLE		PAGE
1	X-ray Basal Spacing, d(001) of Na <sup>+</sup> -hectorite Exchanged with Different Complexes (Total Loading is 73 meq/100 gram clay)	71
2	X-ray Basal Spacing d(001) of Na <sup>+</sup> -Hectorite Exchanged with Different Complex Salts With Loading of 2 Equivalent CEC	. 74
3	Cation Exchange Capacity and X-ray Basal Spacing, d(001) of Different Clay Exchanged with Ni(phen) 3SO4	. 86
4	Effect of Ligand, Counteranion and Loading on the d(001) Spacing of Intersalated Hectorites	88
5	X-ray Basal Spacing, d(001) for Na <sup>+</sup> - Hectorite Exchanged with Different Organic Molecules (at 1 and 2 CEC Exchange Level)	. 98
6	Desorption Coefficient for 2 CEC Hectorite Intersalation Complexes	.105
7	Basal d(001) Spacing for (PADS) <sup>2-</sup> -Exchanged Hectorite Intersalates of Different Relative Humidity	.117
8	Calculated Rotational Correlation Times (nsec) of PADS <sup>2-</sup> Doped into Zn(phen) <sub>3</sub> SO <sub>4</sub> -Intersalate of Hectorite Clay	.119
9	Phase-Transfer Catalyzed Halide Displace- ment Reactions at 90°C with Ni(phen) $\frac{2^+}{3}$ /SO $\frac{2^-}{4}$ - Laponite Intersalates as Catalysts	. 125
10	Dependence of $k_{\mbox{\scriptsize obs}}$ on the Amount of Sodium Chloride Present	. 127
11	Phase Transfer Catalyzed Halogen Exchange Reactions	130

PAGE	TABLE
Kinetics Data for the Reaction of Butyl Bromide and Aqueous NaCl at 90°C	12
Pseudo First-Order Rate Constants $(10^2k_{\rm obs}~(hr^{-1}))$ for the Reaction of Aryl and Alkyl Bromides with NaCl at 90°C 138	13
Pseudo First-Order Rate Constants (10 <sup>2</sup> k <sub>Obs</sub> (hr <sup>-1</sup> )) for the Reaction of Alkyl Bromides with NaCl at 90°C	14
Effect of Particle Size on Pseudo First-Order Rate Constants (10 <sup>2</sup> k <sub>obs</sub> (hr <sup>-1</sup> )) for the Reaction of Alkyl Bromides with NaCl at 90°C	15
Reaction of Acetate Ion with Organic Substrate	16
Phase Transfer Catalyzed Halogen Exchange Reactions Using Cetyl Pyridinium Hectorite Complex (72 hr at 90°C)	17
Kinetics Data for the Reaction of Butyl and Octyl Bromide with Aqueous NaCl at 90°C	18

# LIST OF FIGURES

FIGURE	PAGE
1	Layer structure of smectite (hectorite) illustrating the intracrystalline space which contains the exchangeable cations.  oxygens Si <sup>4+</sup> , occasionally Al <sup>3+</sup> Al <sup>3+</sup> , Mg <sup>2+</sup> , Fe <sup>3+</sup> Hydroxyls
2	The conceptual structure of 2:1 layer silicate mineral. The trioctahedral structure of talc 4
3	The dioctahedral structure of pyrophyllite (2:1 layer silicate mineral). Both Figs. 2 and 3 adoped from Reference [8]5
4	Schematic representation of homoionic smectite containing 1 CEC equivalent of M(phen) $_3^{2+}$ ; the 18 Å intersalated phase which contains ca. 0.2 CEC equivalents of excess M(phen) $_3\overline{SO}_4$ salt; and the $\sim 30$ Å intersalate which contains ca. 1 CEC equivalents of excess M(bp) $_3\overline{SO}_4$ salt. $X^{2-}$ represents the $SO_4^{2-}$ ion
5	Schematic representation of a triphase system
6	Reaction flask used to minimize creeping of finely divided intersalated catalyst:  (A) Teflon-lined screw cap, (B) reaction chamber 4 (diameter) × 2 cm., (C) magnetic stirring bar
7	Schematic representation of ethylene diamine, phenanthroline and some of its derivatives and 2,4,6-tripyridyl-1,3,5-triazine ligands 72
8	001 X-ray reflections (Cu-ka) for an oriented film sample of Ni(phen) 3+/MoO4hectorite intersalate; d-spacings are given in Angstrom units

FIGURE

9	001 X-ray reflections (Cu- $k_{\alpha}$ ) for an oriented film sample of Ni(phen) $_{3}^{2+}/SO_{4}^{2-}$ -hectorite intersalate; d-spacings are given in Angstrom units
10	The crystal structure projected along the b axis. Complex ions drawn with heavy lines are lying relatively in a higher part of the unit cell than those drawn with light lines
11	Adsorption isotherms (25°C) for [Ni(phen) <sub>3</sub> ] SO <sub>4</sub> , [Ni(phen) <sub>3</sub> ]CrO <sub>4</sub> , and Nile Blue on hectorite in aqueous suspension
12	X-ray diffraction pattern of Fe(TPTZ) 2 / SO4 - hectorite prepared by addition of 15 equivalent CEC of the complex to Na - hectorite 90
13	X-ray diffraction patterns of 10,5,2, and 1 CEC equivalents of Ni(phen) 3+/Cl2-hectorite
14	Possible orientations of the Fe(TPTZ) <sup>2+</sup> ion on the surface of Na <sup>+</sup> -hectorite:  A) The complex cation oriented perpendicular to the silicate layers. B) Tilted orienta- tion. C) The complex cation oriented parallel to the silicate layers
15	UV-visible spectra of [Fe(phen) <sub>3</sub> ]SO, [Fe(3,4,7,8,-Me <sub>4</sub> -phen)]SO <sub>4</sub> , [Fe(4,7-diphenyl-phen) <sub>3</sub> ]SO <sub>4</sub> in solution and Na <sup>+</sup> -hectorite intercalated with these compounds
16	X-ray diffraction patterns of 2 CEC equivalents of Nile blue and 3,3-(4,4'-biphenylene)-bis-(2,5-diphenyl-2H-tetrazolium chloride)-hectorite
17	Anion exchange isotherms for Ni(phen) $_{4}^{2+}$ / CrO $_{4}^{2-}$ -hectorite intersalate at 25°C 108
18	X-ray diffraction pattern for Ni(phen) <sup>2+</sup> / SO <sup>2-</sup> -hectorite intersalate solvated by water
19	ESR spectrum at 20°C of the nitroxide spin probe, (PADS) <sup>2-</sup> , in DMSO solvent. The vertical line on this spectrum represents the position of q = 2.00

FIGURE	PAGE
20	Rigid-limit x-band ESR spectrum of PADS; the field increases to the right
21	ESR spectra at 20°C of the nitroxide spin probe, $(PADS)^{2-}$ doped at the 2% exchange level into $Zn(phen)^{2+}_3/SO^{2-}_4$ -hectorite at different relative humidity. A free electron signal at $g=2.0023$ is shown
22	Schematic representation of the three- phase system, using smectite intersalate as a solid phase
23	Experimental set-up for triphase catalytic reactions. Corning N° 9826 Culture tube $(20 \times 150 \text{ mm})$ containing organic, aqueous, and solid phase; a teflon coated magnetic stirring bar $(^{10}/_{16} \times ^{5}/_{16}  in. octagonal bar with pivot ring) is shown$
24	Plot of ln (unreacted) butyl bromide in the organic phase as a function of time for the reaction of 2 mL of 0.5 M n-butyl bromide in toluene with 3.0 mL of an aqueous 3.3 M NaCl catalyzed by 0.069 meq of Ni(phen) 2+/SO4 ion pair in Laponite at 90°C124
25	Plot of 10 <sup>2</sup> k <sub>Obs</sub> as a function of the amount of catalyst used. The catalyst and reaction conditions were similar to those described in Figure 24
26	Plot of ln(unreacted) 1,8-dibromooctane in the organic phase as a function of time for the reaction of 2 mL of 0.5 M 1,8-dibromooctane in toluene with 3.0 mL of an aqueous 3.3 M NaCl catalyzed by 0.069 meq of Ni(phen) 3+/SO <sub>4</sub> - ion pair in natural hectorite at 90°C
27	Selectivity induced by the hectorite intersalate catalyst on the pseudo first-order rate constants of Br-Cl exchange for normal and branched alkyl bromides with aqueous NaCl as a function of the number of carbon atoms in the alkyl chain. For the reaction conditions see Table 13, footnote $a140$
28	Schematic representation, showing edge view of the intersalated hectorite catalyst and the triphase catalyzed reaction zone.

FIGURE		PAGE
29	Plot of ln(unreacted) 1-bromooctane in the organic phase as a function of time for the reaction of 2 mL of 0.5 M 1-bromooctane in toluene with 10 mmol of sodium cyanide dissolved in 1 mL of water catalyzed by 0.069 meq of tricapryl methyl ammonium chloride ion pair in hectorite at 90°C	153
30	Plot of 2π/d (d is basal spacing) versus n (order of reflection), using least square fitting technique.	. 157

### LIST OF SYMBOLS AND ABBREVIATIONS

A Angstrom

acac acetylacetone

AEC anion exchange capacity

aq aqueous phase

Bathophenanthroline 4,7-diphenyl-1,10-

phenanthroline

bp 2,2'-bipyridyl

Bu Butyl

CEC cation exchange capacity

chel chelating ligand

clay mineral for catalyst

support

DMSO dimethylsulfoxide

Et ethyl group

en ethylene diammine

ESR electron spin resonance

Gauss

G.L.C. gas liquid chromotography

hr hour

IR infrared

intercalate a clay sample which has been

intercalated with a cation

intersalate a clay sample which has been

intercalated with a complex

salt.

intersalation

The term intersalation has been suggested for the intercalation of ionic salts in clays with neutral layer charge, e.g., kaolinite [41]. The term has been used in this dissertation to emphasize the presence of cationanion pairs in smectite-clay interlayers.

k<sub>obs</sub>

observed rate constant

L

ligand

M

general metal center

Me

methyl group

ML

milliliter

µm or µ

micron

mEq or meq

milliequivalent

mmol

millimoles

M

molar concentration

 $M(chel)_{3}^{2+}/XO_{4}^{2-}$ -hectorite

designation for a catalyst supported on hectorite

n-

normal

OEt

ethoxy group

-OH

hydroxyl group

org

organic phase

Ох

oxalate

P

polymer for catalyst support

(PADS)<sup>2-</sup>

peroxyl amine disulfonate

anion

PTC

phase transfer catalysis

phen

ortho-phenanthroline or

1,10-phenanthroline

phenyl group φ alkyl- or aryl-group R relative humidity r.h.  $0^+$  or Q(+)cationic complex as catalyst triphase catalysis TC 2,4,6-Tripyridyl-5-TPTZ Triazine τc rotational correlation (tumbling) time ultraviolet UV vacuum Vac. wt weight  $x, \overline{x}$  and  $y, \overline{y}$ general anion to be displaced in a triphase catalyzed reaction  $xo_4^{2-}$ any tetrahedral-ate anion (e.g.  $MoO_4^{2-}$ )

## **OBJECTIVES**

Layered silicate clays are ubiquitous constituents of the natural environment. These minerals are known to interact with numerous organic, inorganic and organometallic compounds to form complexes with a wide range of properties.

The intercalation properties of the layered silicates provide numerous opportunities to modify or enhance the selectivity of a catalytic species. Because of the crystalline nature of layered silicate clays, one might expect to make use of these materials in a phase transfer catalysis (PTC). PTC is a relatively new field. As in classical phase transfer catalysis, reactions are carried out in an aqueous-organic two-phase system, but a third, immiscible solid phase (triphase catalysis) is also present which may be recovered at the end of the catalytic reaction by simple filtration. Here lies the potential importance of such a technique in industry, since both discontinuous processes with dispersed catalyst and continuous processes on a fixed-bed catalyst are feasible.

Earlier studies have shown that intercalation compounds of hectorite, montmorillonite, and other smectite clay minerals can be tailored to function as selective liquid-solid phase transfer catalysts, particularly when the

spatial requirements of oriented reaction intermediates on the intracrystal surfaces differ for different substrates. Surface chemical equilibria can also be controlled and used to enhance the selectivity of intercalated clay catalysts. Since clay layers are negatively charged, the rational design of clays as phase transfer catalysts is generally restricted to intercalates in which the host structure is interlayered with catalytically active cations such as transition metal complexes. Anion intercalation is normally precluded on electrostatic grounds. Therefore, it could be of considerable interest to synthesize a new type of complex clay with anion intercalation that can then be used for triphase catalysis (TC).

In the present investigation, several catalyst systems based on intercalation compounds of smectite clays have been made. For example, intercalation of complex salts such as  $M(Phen)_3^{2+}SO_4^{2-}$ , where Phen = 1,10-Phenanthroline and M = Fe,Ni,Zn, produce well ordered systems in which the pore sizes can be adjusted to adsorb substrates in a limited size range. Therefore, catalytic selectivity based on the size or selective adsorption of the substrate can be anticipated.

### CHAPTER I

### INTRODUCTION

# A. Structure and Properties of Layer Silicates

The layered silicates, hectorite and montmorillonite described in this dissertation are smectite minerals, a class of naturally occurring clay minerals. The term "clay mineral" refers to a specific silicate with particle size less than 2  $\mu$  and with a definite stoichiometry and crystalline structure.

Smectites are composed of units made up of two silica tetrahedral sheets and a central octahedral sheet. All the tips of the tetrahedrons point in the same direction and toward the center of the unit. The tetrahedral and octahedral sheets are combined so that the tips of the tetrahedrons of each silica sheet and the hydroxyl groups of the octahedral sheet form a common layer. The layers are continuous in the a and b directions and are stacked one above the other in the c direction. In the stacking of the layer units, oxygen planes of each unit are adjacent to oxygen planes of the neighboring units, with the consequence that there is a very weak van der Waals interaction between them. The outstanding feature of

the smectite structure is that water and other polar molecules, such as certain organic molecules, can enter between the unit layers, causing the lattice to expand in the c direction. The c-axis dimension of smectite is, therefore, not fixed but varies from about 9.6 Å to substantially complete separation of the individual layers in some cases. Figure (1) is a diagrammatic sketch of the structure of smectite. In the 2:1 trimorphic or three sheet mineral of smectite there are two broadly divided structures: dioctahedral [aluminum silicate (Figure 2) and trioctahedral [magnesium silicate (Figure 3)] minerals. These can be subdivided into groups in which the layer charge arises predominantly from isomorphous substitution in the octahedral layer and those with charge arising from tetrahedral layer substitution. Further subdivisions can be made on the basis of layer charge density. Thus the different minerals of the smectite group form a continuous multidimensional series. tend to fall into discrete populations differentiated mainly by the source and density of their layer charge [1,2].

In the case of montmorillonite, isomorphous cation substitutions (commonly aluminum for silicon in the tetrahedral layer and magnesium and iron for aluminum in the octahedral layer) occur during formation and subsequent alteration. This leads to an imbalance of electrical charge which is compensated for by the presence

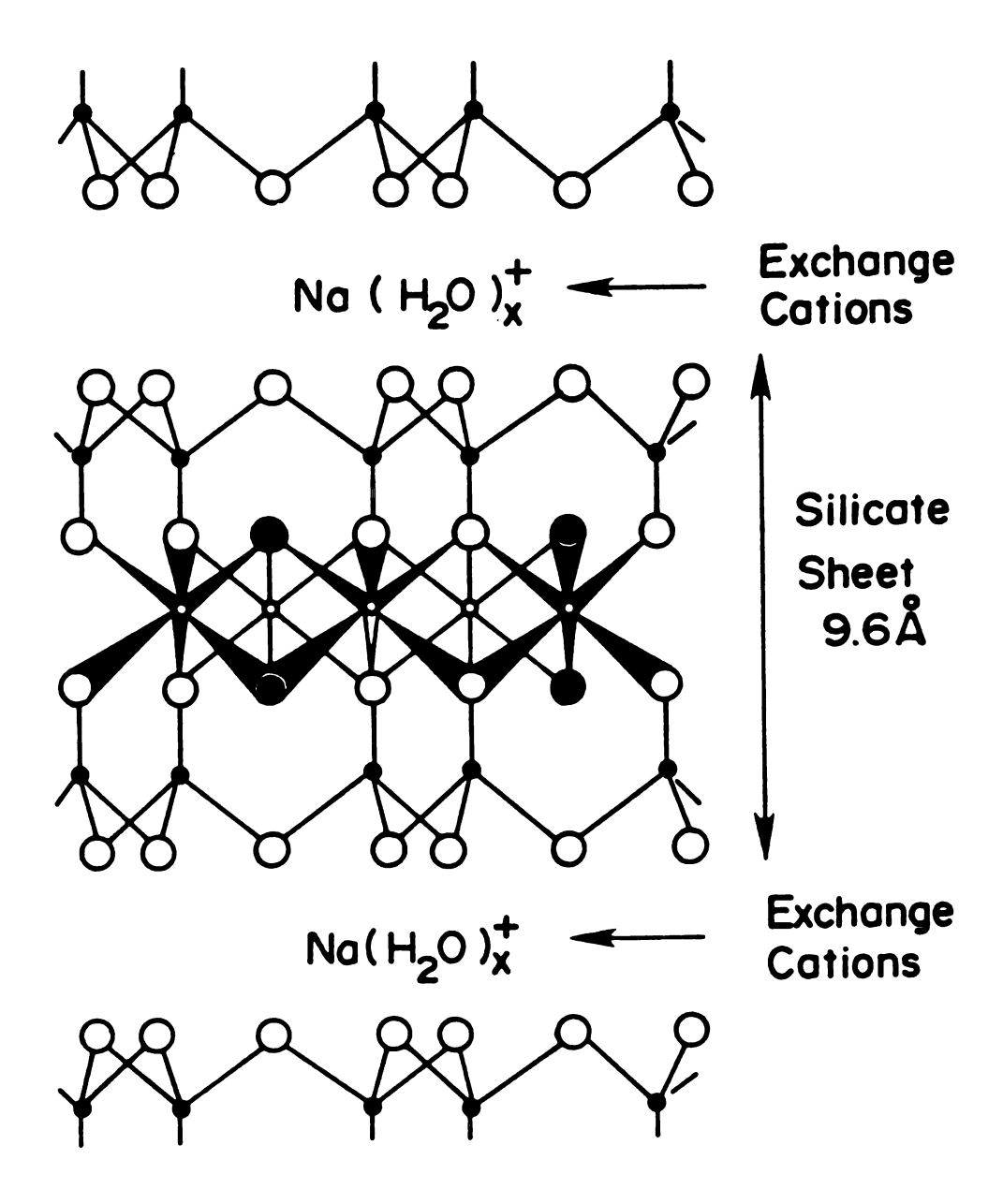


Figure 1 Layer structure of smectite (hectorite) illustrating the intracrystalline space which contains the exchangeable cations.

- O oxygens
- Si<sup>4+</sup>, occasionally Al<sup>3+</sup>
   Al<sup>3+</sup>, Mg<sup>2+</sup>, Fe<sup>3+</sup>
- Hydroxyls

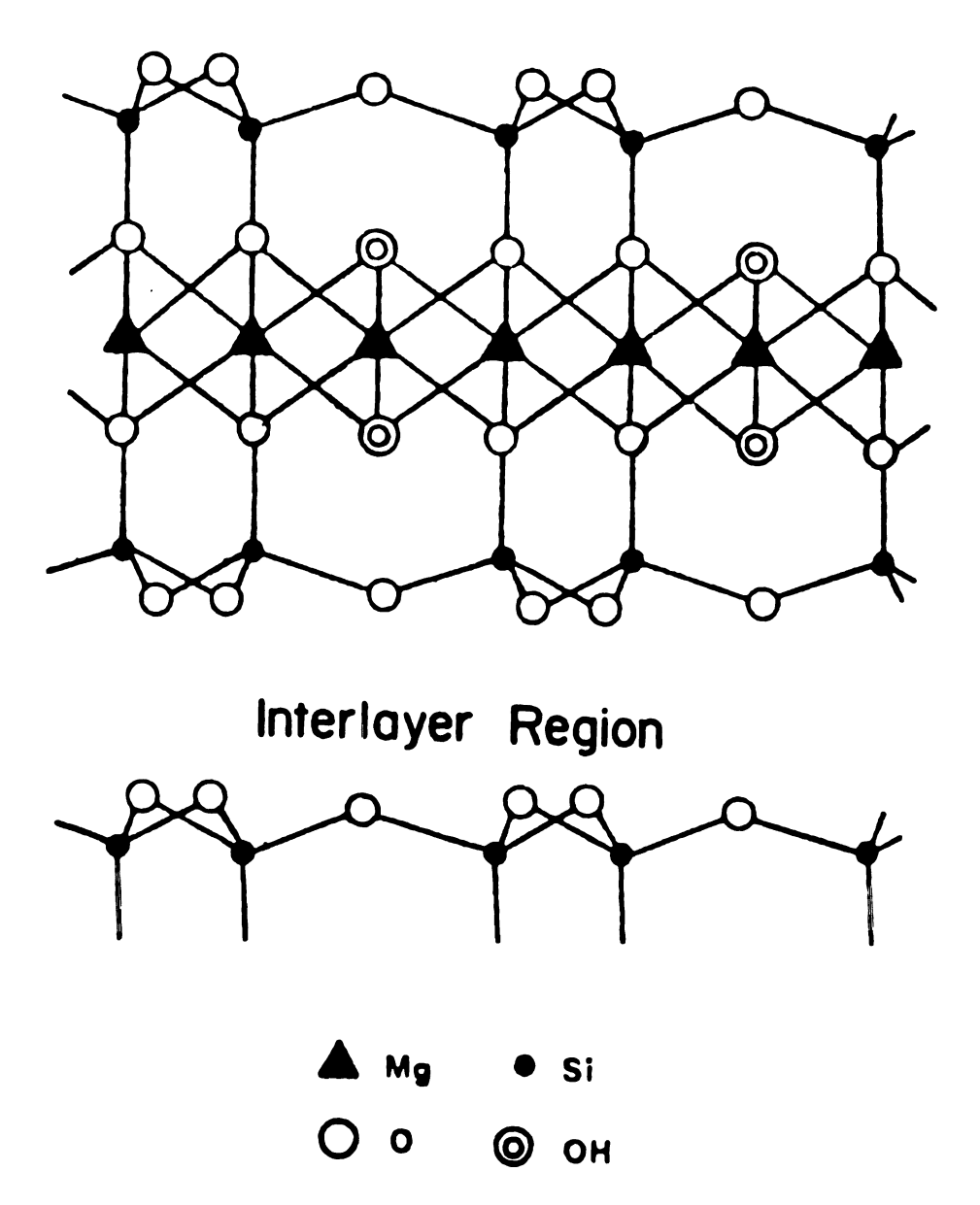
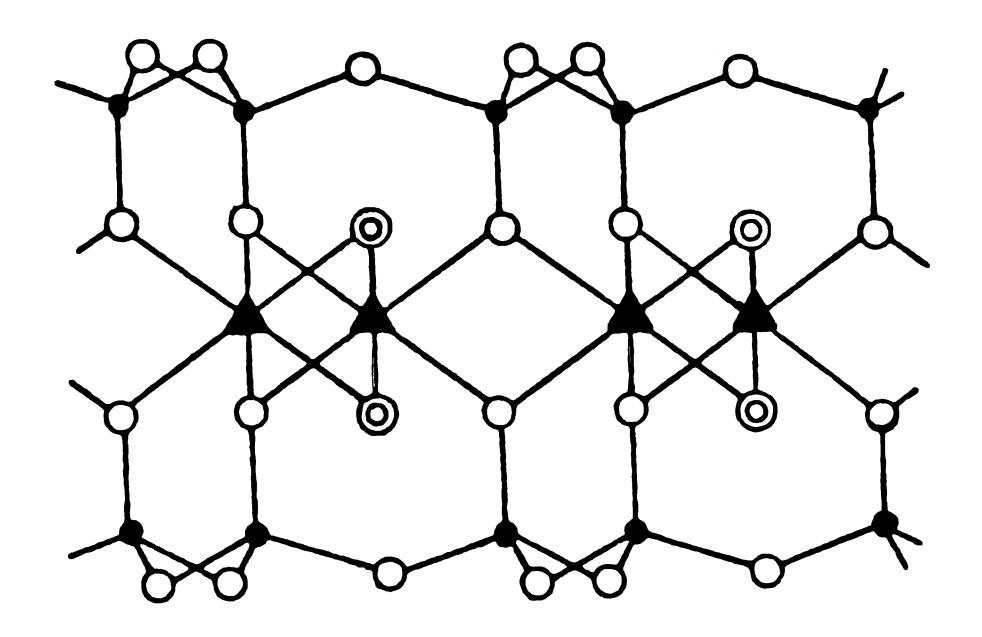


Figure 2 The conceptual structure of 2:1 layer silicate mineral. The trioctahedral structure of talc.



# Interlayer Region

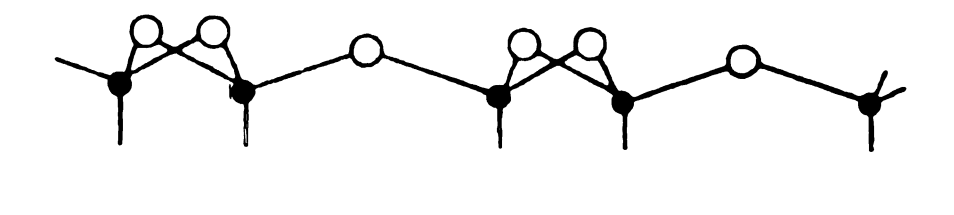




Figure 3 The dioctahedral structure of pyrophyllite (2:1 layer silicate mineral). Both Figs. 2 and 3 adopted from Reference [8].

of easily exchangeable cations on the mineral surface. A delicate balance exists between interlamellar attractive forces and the repulsive forces generated when the crystals are suspended in polar liquids. Often the repulsive forces are sufficient to cause separation of the individual sheets, exposing the entire surface to the liquid.

Interlamellar spacings in general depend upon the species of exchangeable cation present, the nature of the solvent, and whether or not any electrolytes are present. In aqueous suspensions interlamellar spacings as large as several hundred Angstroms have been observed. the silicate layers of Na<sup>+</sup>-montmorillonite in dilute aqueous suspension are completely dispersed (delaminated). As the concentration of the dispersion is increased, gelation occurs. The gelation phenomenon which occurs at concentration as low as 2 wt% clay, is believed to result from layer edge to face interactions which generate a "house-of-cards" structure [3]. An ideal montmorillonite may be defined as having the unit cell composition shown below [2] in which the superscripts (IV) and (VI) in the formula denote the respective tetrahedral and octahedral layer cations, and (M<sup>+</sup>) represents a univalent or equivalent compensating cation.

$$[(Si_8)^{IV}\cdot(Al_{3.33}Mg_{0.67})^{VI}\cdot O_{20}(OH)_4]0.67 M^+$$

The isomorphous substitution consists predominantly of Mg-for-Al in the octahedral layer, resulting in a net anionic charge of 0.67 units per unit cell. The Mg-for-Al substitution has been shown to result in incomplete neutralization of the negative charge on the apical oxygens and hydroxide groups coordinated to the magnesiums.

The anionic charge of the aluminosilicate layers is neutralized by the intercalation of compensating cations and their coordinated water molecules. The montmorillonite crystal structure thus consists of superimposed aluminosilicate layers, each of which is interleaved with a "layer" of hydrated, exchangeable compensating cations. These cations can alternatively be described as occupying the interlamellar spaces or the regions between the basal surfaces of opposing silicate layers. Although the compensating cations are normally located in the regions adjacent to the points of anionic charge on the basal surfaces, small anhydrous cations, principally Li or H ions, are capable of migrating through the basal surface oxygen sheet to the neighborhood of the isomorphous substitution sites. The protons appear to associate with the octahedral hydroxyl groups, instead of forming hydroxyl groups by reacting with the incompletely neutralized oxygens [4].

Hectorite is the trioctahedral analogue of montmorillonite and contains predominant octahedral Li-for-Mg substitution. In hectorite, which typically exhibits a layer charge of 0.67 e/Si $_8$ O $_{20}$ , the cation exchange capacity on an anhydrous basis is 87 meq/100 g., about one-fifth the exchange capacity of sulfonated styrene-divinylbenzene resins. Since the average distance between exchange equivalents in the mineral is ~8.3 Å [5], cations with cross sectional diameters greater than this value can saturate the interlamellar surfaces before 100% exchange is reached. Thus although the interlamellar surface is very large (~750 m $^2$ /g), the size of the exchanging ion can be a limiting factor in determining ion loading.

Hectorite: 
$$[(Si_8)^{IV} \cdot (Mg_{5.33}Li_{0.67})^{VI} \cdot O_{20}(OH)_4]0.67 M^{\dagger}$$

The commercial filler, Laponite<sup>®</sup> is a synthetic low-charge hectorite which, unlike the natural mineral, can be obtained with a negligible iron content. Another grade of Laponite<sup>®</sup> consists of a fluorohectorite in which the octahedral lattice hydroxyl groups have been replaced with fluoride ions.

Hectorite lacks the potentially acidic, exposed aluminum ions that are partly responsible for the acidic character of the surfaces of the montmorillonites. However, both hectorite and montmorillonite contain other acidic species adsorbed on the basal surfaces and in the interlamellar spaces.

Mortland et al. have reported [6] that residual water molecules remaining under vacuum in a base-saturated

montmorillonite are able to convert NH, into NH, The extent of the transformation suggests that these residual water molecules have a degree of dissociation higher than The NMR studies performed by D.E. Woessner and B.S. Snowder [7] also support the proposed dissociation mechanism and show that the dissociation of interlayer water is  $10^6 - 10^7$  times higher than in liquid water. The surface acidity of dried minerals may exceed that of concentrated sulfuric acid [8]. This can result in the catalysis of many desirable, undesirable, or unexpected reactions when these materials are incorporated in organic media. This acidity is related in origin, and is often similar in strength, to that of the acidic alumina-silica and zeolite cracking catalysts used in the petrochemical industry [9]. The surfaces of the silicate minerals may contain both Lewis and Bronsted acidic species, although the Bronsted acidity is probably the more significant in catalysis of reactions by the minerals.

The compensating cations of the montmorillonites, hectorites and related minerals can be exchanged with other hydrated inorganic cations, with metal complex cations (for example,  $Fe(Phen)_3^{2+}$ ), and with a wide variety of organic cations. Therefore a large active surface area (700-800 m<sup>2</sup>/g) allows an enormous range of guest molecules to be intercalated. In the intercalation processes several binding mechanisms may operate [9-11].

Due to the high negative surface charge (cation exchange capacity, CEC) and layer morphology, these minerals also serve as nature's own model for a Platy hydrophobic colloid of the "constant charge" type. The layer charge, indicated by a given structural formula, should only be regarded as an average over the whole crystal because this charge may vary (between certain limits) from layer to layer. The experimental evidence for this view and its implications for the colloid stability of montmorillonite suspensions have been described by Lagaly and co-workers [12,13]. Smectite clays possess a combination of cation exchange, intercalation and swelling properties which makes them unique. Their capacity as cation exchangers is fundamental to their intercalation and swelling properties. This distinguishes smectites from the micas and pyrophyllite/talc groups of minerals, which are not ion exchangers [14]. Because of the ability of the minerals to imbibe a variety of cations and neutral molecules, an almost limitless number of intercalates are possible. Because of the small particle size ( $<2 \mu$ ) of smectite clays and their unusual intercalation properties, they afford an appreciable surface area for the adsorption and catalysis of organic molecules. Recently, intercalated clay catalysts have been expertly reviewed by T.J. Pinnavaia [5]. Indeed, the probable catalytic role of smectites has been recognized in several "natural" processes [15], including petroleum forming reactions [16,17], chemical transformations in soils [10,18,19], and reactions related to chemical evolution [20-25].

Recent advances in the intercalation chemistry of smectite clays has rekindled interest in these minerals as catalysts or catalyst supports. By mediating the chemical and physical forces acting on interlayer reactants, one often can improve catalytic specificity relative to homogenous solution.

A second new class of smectite intercalation compounds makes use of robust cations as molecular props or pillars between the silicate layers. Recently it has been found that silicon could be introduced into the interlamellar regions by ion exchange of triacetylacetonato silicon (IV) cations (Si(acac)<sup>+</sup><sub>3</sub>) by in situ reaction of acetylacetone-solvated clays with SiCl<sub>4</sub>, or by formation of polychlorosiloxanes (-SiOCl<sub>2</sub>-)<sub>n</sub> [26].

The pillaring phenomenon leads to the formation of porous networks analogous to zeolites. Since pillared clays can have pore sizes larger than those of zeolites they offer a promising new means of facilitating the reactions of large molecules. By the intercalation of polynuclear hydroxy cations of some transition metals in smectite, new pillared clay catalysts with pore size larger than 10 Å have been synthesized [27].

As the smectite interlayers are swollen beyond the dimensions of the coordination sphere of the aquated metal ion, the complex becomes solvent-separated from

the surface and begins to tumble rapidly. Also, under multilayer solvation conditions only the first one or two layers adjacent to the silicate surface exhibit significantly restricted motions [28].

Complementary ESR and NMR experiments [29-32], along with quasi-elastic neutron scattering studies [33], have provided incisive information on the interlayer dynamics of clay intercalates. A general picture of the interlayer environment has emerged from these studies. At low degrees of interlayer solvation (e.g., 1-3 water layers) the solvated exchange cations adopt oriented positions on the interlamellar surfaces. Though oriented, the solvated cations are in a dynamic state and undergo anisotropic rotations about specific molecular axes. Uncoordinated water molecules between the solvated cations are capable of translational diffusion within and between the "cages" defined by the solvated cations and the silicate layers [33]. Restricted motions and preferred orientations also have been observed for intercalated organic species [30,34].

B. Intercalation of Transition Metal Complex Salts in Smectite ("INTERSALATION")

In contrast to the vast literature on clay-organic reactions [8,9,35], only a few references have been found describing interactions of chelated transition metal complexes on smectites.

Properties of the layered silicates change when different ions or chelated ions are adsorbed. Adsorption of ions or chelated metal ions by smectites may create changes in the chemical and physical properties of the clay. Adsorption of gases, surface area measurements, x-ray basal spacings, oxidation-reduction potentials as well as catalytic properties may be altered by exchange of complex metal ions onto the silicate surfaces. It was found [36] that related tris-ethylenediamine complexes  $Cr(en)_3^{2+}$ ,  $Co(en)_3^{3+}$ , and  $Cu(en)_3^{2+}$  afford appreciable surface areas when they occupy the exchange sites of montmorillonite. The metal complex clays showed promise as chromatographic supports for separation of light hydrocarbons and nitrogen oxides.

Mortland and Berkheiser [37] have demonstrated that  $\operatorname{Cu}(\operatorname{Phen})_3^{2+}$  and  $\operatorname{Fe}(\operatorname{Phen})_3^{2+}$  have marked affinity for exchange on to the  $\operatorname{Na}^+$ -hectorite surface and the homoionic exchange forms of the mineral have an  $\operatorname{N}_2$  surface area in the range 200-300 m<sup>2</sup>/g. This surface area is available for the adsorption of polar ( $\operatorname{H}_2\operatorname{O}$ ) and larger nonpolar (benzene) molecules. In addition to finding some unusual redox properties of the mineral bound ions, they also found that  $\operatorname{Fe}(\operatorname{bp})_3^{2+}$  and  $\operatorname{Cu}(\operatorname{bp})_3^{2+}$  hectorite are capable of binding metal complex in excess of two times the cation exchange capacity of the mineral through intercalation of the bromide or sulfate salts. Similar observation by Uylterhoeven et al. [38] showed that the

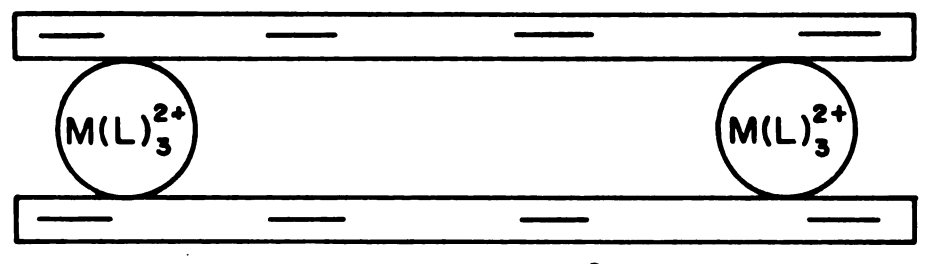
Cl uptake on hectorite is accompanied with the adsorption of an excess  $[Ru(2,2'-bipy)_3]^{2+}$  up to 1.55 meg/g.

Adsorption of  $M(chelate)^{n+}_{3}$  by ion exchange and intersalation mechanisms has been studied in considerable detail [39,40]. Recently Pinnavaia et al. [39] have shown that the binding of tris-bipyridyl metal complexes of the type  $M(bp)_3^{2+}$  (M = Fe<sup>2+</sup>, Cu<sup>2+</sup>, Ru<sup>2+</sup>) to hectorite surfaces to occur by two mechanisms: (1) replacement of Na<sup>+</sup> ions in the native mineral by cation exchange up to its cation exchange capacity and (2) binding of metal complex beyond the CEC of the mineral through "intersalation" of metal complex salt. (The term intersalation has been suggested for the intercalation of ionic salts in clays with neutral layer charge, e.g., Kaolinite [41]. The term will be used in this dissertation to emphasize the presence of cation-anion pairs in smectite-clay interlayers.) The binding of excess salt is believed to result from a screening of the electrostatic charge of the clay by the complex cation, permitting the penetration of more of the complex cation and its anion into the interlamellar regions of the layered silicate. In this case apparently the large ligands are responsible for this screening since simple inorganic salts do not behave in this fashion.

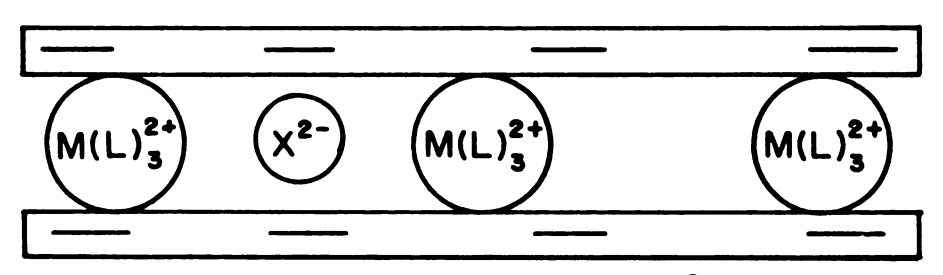
Complexes of the types  $M(bp)_3^{n+}$  or  $M(Phen)_3^{n+}$  are of special interest, in part, because they have a spherical shape and are among the more thermally stable complexes known. These complexes, due to their spherical shape,

should be capable of propping the interlayers of the mineral to a greater extent, therefore one now expects the regions between the exchange ions to be available for adsorption or surface catalyzed reactions. In fact several attempts have been made [37,39,40,42-44] to intercalate relatively large cations to act as molecular props to keep the layers The initial result by Mortland et al. [37] demonstrated that Fe(Phen)<sub>3</sub><sup>2+</sup> and Cu(Phen)<sub>3</sub><sup>2+</sup> do in fact act as ~8 Å molecular props in hectorite. They also concluded that van der Waals interactions appear to be responsible for the adsorption of the complex cations in excess of the exchange capacity. These van der Waals forces may also comprise an important driving force which causes a complete interlayer to be saturated before adsorption occurs in succeeding interlayers. intersalation reactions are very dependent on the nature of the counter-anion with the binding decreasing in the order  $SO_4^{2-}$ , Br  $\rightarrow ClO_4^{-} \rightarrow Cl$ . A complex cation like M(Phen)  $\frac{2+}{3}$ has a cross-sectional thickness of approximately 8 Å along the C3 axis [37] while its associated counter-anion of the type  $XO_A^{2-}$  ( $SO_A^{2-}$ ,  $MoO_A^{2-}$ ,  $CrO_A^{2-}$ , etc.) has a crosssectional diameter of approximately 4 Å. Thus, considering the thickness of the silicate layer (9.6  $\mbox{\normalfont\AA}$ ), the d(001) reflection of an air dried intersalated sample is expected to be ~30 Å. The size of the pockets created by the cations is large enough to accommodate the anions and still retain enough space for free rotation in a highly swelled

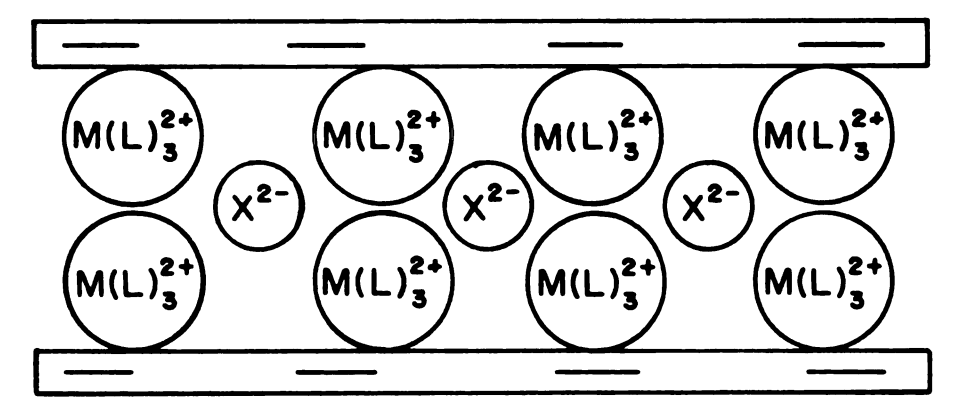
Figure 4 Schematic representation of homoionic smectite containing 1 CEC equivalent of  $M(phen)_3^{2+}$ ; the 18 Å intersalated phase which contains  $\underline{ca}$ . 0.2 CEC equivalents of excess  $M(phen)_3SO_4$  salt; and the ~30 Å intersalate which contains  $\underline{ca}$ . 1 CEC equivalents of excess  $M(phen)_3SO_4$  salt.  $X^{2-}$  represents the  $SO_4^{2-}$  ion and L represents the Phenanthroline ligand.



Homoionic, I8A°



Monolayer Intersalation, I8A°



Bilayer Intersalation,~30A°

system. In the present work peroxylamine disulfonate radical (PADS) spin probe is doped into the anion interlayers to estimate the interlamellar mobility. The result showed that PADS<sup>2-</sup> molecules have enough room to tumble fairly rapidly (i.e.,  $3 \times 10^{-10}$  sec), regarding the size of molecule, therefore, take on appreciable solution-like properties (see Chapter III).

The homoionic  $M(Phen)_3^{2-}$ -hectorites, which exhibit rational 18 Å x-ray reflections, have been characterized [37] with regard to surface area, H<sub>2</sub>O absorption, types of water present, and orientation of the complex ion in the interlayer regions. Two solid state phases have been isolated with 18 Å and ~30 Å spacings [40]. The 18 Å phase results from the presence of a monolayer of complex cation, whereas the ~30 Å phase contains two layers of complex cation. Schematic representations of the homoionic and intersalated phases are shown in Figure (4). In general, the surface areas of the new intersalated phases are low ( $\sim 30 \text{ m}^2/\text{g}$ ), because nearly all of the internal surface area is covered by complex cation. The homoionic and intersalated phases are thermally stable to ~350°C. Above this temperature the 18 Å homoionic and intersalated phases collapse to ~12 Å, due to loss of Phen or bp ligands, however, the ~30 Å intersalated phases behave quite differently. Thermolysis of a ~30 Å intersalate containing M(Phen) $_3^{2+}$  or M(bp) $_3^{2+}$ and  ${\rm SO}_{4}^{2-}$  ions affords a new high-temperature phase with an

(001) spacing near 18 Å. These high-temperature phases are thermally stable to at least  $550^{\circ}$ C, and they exhibit  $N_2$  surface areas up to  $360 \text{ m}^2/\text{g}$ . Chemical and spectroscopic studies indicate that the new high temperature phases consist of silicate sheets separated by two layers of carbon. Quantitative kinetics studies [45] have shown, rather remarkably, that these "graphitic clays" are so stable that the silicate layers can be dehydroxylated (640°C) without collapse of the interlayers. The rates of dehydroxylation are appreciably larger than those for ordinary smectite suggesting that the expanded interlayers are sufficiently porous to facilitate migration of water out of the structure.

#### C. The Principles of Phase Transfer Catalysis

Reaction between two substances located in different phases of a mixture is often inhibited because of the inability of reagents to come together. The classical solution to this problem, and by far the one most frequently used in the laboratory, is simply the use of a solvent which can dissolve both reagents. Use of solvents is not always convenient, and on an industrial scale it frequently is expensive. The technique of "phase transfer catalysis" provides a method which avoids the use of solvents [46-49]. Basically, all phase transfer catalyzed reactions involve at least two steps: (1) transfer of one reagent from its "normal" phase into the

second phase; and (2) reaction of the transferred reagent with the nontransferred reagent.

Jarrouse [50], as early as 1951, observed that the quaternary ammonium salt benzyltriethylammonium chloride markedly accelerated two-phase reaction of benzyl chloride with cyclohexanol (Reaction 1) and the two phase alkylation of phenylacetonitrile with benzyl chloride or ethyl chloride (Reaction 2).

$$C_6^{H_5-CH_2Cl} + Org.$$
+ NaOH  $C_6^{H_5CH_2N^+Et_3Cl^-(aq)} \longrightarrow O^{-CH_2-C}6^{H_5}$ 
+ NaCl + H<sub>2</sub>O (1)

$$\begin{array}{c}
CH_2CN \\
CH_2CN \\
CH_2CN
\\
+ C_2H_5C1 + NaOH
\end{array}$$

$$\begin{array}{c}
C_6H_5CH_2N^+Et_3C1^-(aq) \\
CH_2CN
\\
CH_2CN
\\
+ NaC1 + H_2O
\end{array}$$

$$\begin{array}{c}
C_2H_5 \\
CH_2CN
\\
+ NaC1 + H_2O
\end{array}$$

$$\begin{array}{c}
C_6H_5CH_2N^+Et_3C1^-(aq) \\
CH_2CN
\\
+ NaC1 + H_2O
\end{array}$$

In addition to this work, a number of other publications and patents appeared during the period 1950-1965 in which quaternary ammonium or phosphonium salts were used as catalysts for two-phase reactions [51-66], although in these instances either the general nature of phase transfer catalysis was apparently missed, or the catalytic activity was believed to involve only surfactant properties of the quaternary salts. Makosza and co-workers [67] later

reexamined the two-phase alkylation technique in great detail and published their findings in a number of papers, greatly expanding the understanding and utility of this alkylation method. Gibson [68] in two-phase permanganate oxidations, Makosza [67] with alkylation reactions, Hennis [69] with carboxylate displacement reactions, Brändström [70] with alkylation reactions, and Starks [47] with a variety of reactions, each recognized many of the elements of phase transfer catalysis by quaternary ammonium salts. The name "phase transfer catalysis" was first applied to the technique in patents [47] and in the journals [46], after which detailed evidence for the mechanistic pathway illustrated in (Scheme I) [48] was adduced. The recognition of crown ethers as phase transfer catalysts, in both liquid-liquid and liquid-solid reactions, was first published by Liotta and co-workers [71]. Since these earlier patents and papers, the literature on phase transfer catalysis has grown rapidly, so that now there are more than 1000 publications.

Phase transfer catalysts are onium salts, usually quaternary ammonium or phosphonium species, crown ethers, cryptands, or linear polyethers. The mechanism of catalysis is thought to vary to some extent with the type of system involved [72], but the simplest case arises with  $SN_2$  displacement reactions, typified by the reaction of a nucleophile,  $\overline{Y}$ , in an aqueous solution with an alkyl halide, RX, in an organic phase [46] (Scheme I).

#### (Scheme I)

MY is the alkali metal salt of the nucleophile and QX is the onium salt catalyst. The latter becomes involved the in a fast equilibrium in the aqueous phase to generate QY ion pairs and because of the relatively lipophilic character of Q, the anion, Y, is effectively 'ferried' into the organic phase. Here intimate contact with the alkyl halide is established and displacement readily occurs. Finally, the displaced anion, X, is 'ferried' back to the aqueous phase as the ion pair, QX, and the cyclic series of events is completed. The most common example for which a large amount of data are available is simple cyanide displacement on alkyl chlorides or bromides (Reaction 3)

$$R-C1 + NaCN \longrightarrow R-CN + NaC1$$
org. aq. org. aq. (3)

Simply heating and stirring a two-phase mixture of 1-chloroctane with aqueous sodium cyanide leads to essentially zero yield of 1-cyanooctane even after several days of reaction time. However, if a small amount of an appropriate quaternary ammonium salt is

added, then rapid formation of 1-cyanooctane is observed in essentially 100% yield after 1 or 2 hr. Quaternary cation,  $Q^+ = R_4 N^+$ , selected for its high compatibility with the organic phase, transfers cyanide ion into the organic phase as  $Q^+ CN^-$ , which then undergoes reaction with chlorooctane to produce cyanooctane. Coproduced  $Q^+ C1^-$  is rapidly reconverted to  $Q^+ CN^-$ , either in the aqueous phase or at the aqueous-organic interface, by anion exchange with sodium cyanide from the aqueous phase.

The concept of phase transfer catalysis is not limited to anion transfer systems, but is much more general, so that in principle one could also transfer cations, free radicals, whole molecules, or even energy (in a chemical form). Very little work has been reported on such systems, although we may certainly look forward to it in the future.

PTC is not only an academic curiosity. To date there exist about 20 processes which produce polymers, pharmaceuticals, and intermediates for dyestuffs and agrochemicals, and their outputs are 50-500 tons/y each.

Polycarbonates: In 1958, Bayer made polycarbonates by PTC—before PTC was "officially" discovered [73].

The reaction is between carbonyl chloride and the sodium salt of bisphenol

<u>Penicillin esterification</u>: The original commercial penicillin was benzylpenicillin:

with  $R = C_6H_5CH_2CO$ — chemically modified penicillins, developed in the 1960's, had different R side chains; in particular, Beecham developed the successful ampicillin  $(R = C_6H_5CH(NH_2)CO$ —). Penicillins are acids and are usually marketed as their salts.

Recently, two penicillins based on ampicillin in which the carboxyl group is esterified have been commercialized [74,75]. The idea is that the penicillin will no longer appear as a zwitterion when applied.

Instead, the new lipophilic form will diffuse into the tissues, penetrate pus, and will then hydrolyze to ampicillin at a wide range of sites. By use of a compound that hydrolyzes slowly, blood plasma levels of the antibiotic can be maintained with fewer doses per day.

To achieve these aims, a labile ester is required that will not hydrolyze too quickly but will be less stable than the  $\beta$ -lactam ring in penicillin.

Natural penicillins and the precursors of semisynthetic penicillins are manufactured by fermentation of a carbohydrate substrate with penicillium chrysogenum in the presence of phenylacetic acid (for penicillin G) or phenoxyacetic acid (for penicillin V) [76]. The penicillin is harvested by extraction with butyl acetate, but there are losses of at least 10% in waste streams. Further extractions with butyl acetate are uneconomic because unreacted phenylacetic acid or phenoxyacetic acid are simultaneously extracted at an unacceptable level. The penicillin can, however, be recovered by ion-pair extraction [77]. This is neither a chemical reaction nor a catalytic process, but it uses phase-transfer catalysts and the phase-transfer technique.

Additionally, phase transfer catalysis may function not only through liquid-liquid systems, but also with liquid-gas, liquid-solid, solid-gas, and presumably solid-solid systems. For example, in the liquid-gas combination, hydrogenation of olefins with the Wilkinson catalyst [78] is a system in which a gas phase reagent is transferred into the liquid phase and activated for reaction

$$R-CH \xrightarrow{\text{CH}_2} CH_2 + H_2 \xrightarrow{(\phi_3 P)_3 Ru(CO)} RCH_2-CH_3$$
 (5)

with the organic reagent.

Indeed, perhaps the oldest of all phase transfer reactions is the transfer and activation of oxygen by hemoglobin from the air in our lungs into the blood and throughout our bodies to where energy production is necessary. All phase transfer catalysts do not behave equally well for all kinds of reactions; some are often sensitive to such factors as: (i) the chain length and types of alkyl groups attached to the quaternary nitrogen or phosphorus atom; (ii) the presence of strong base or acid in the aqueous phase; (iii) the concentration of the inorganic reagent in the aqueous phase; and (iv) the presence of certain ions, such as iodide, perchlorate, or toluene sulfonate. Most anions prefer to reside in an aqueous phase rather than an organic phase, even a highly polar one, because of the favorable thermodynamic effect afforded by anion hydration. This effect results from spreading the electronic charge over the greater volume of the hydrated species, and is therefore dependent on the charge to volume ratio of the anion. To be highly effective as phase transfer catalysts for two-phase displacement reactions, the catalyst cation-anion pair needs to be strongly partitioned into the organic phase.

The optimum distribution of catalyst cation in anion transfer catalysis is that which allows the rate of the organic phase reaction to equal the rate of catalyst regeneration. For example, in the cyanide displacement reaction sequence:

$$R-C1+Q^+CN^- \xrightarrow{k_0} R-CN+Q^+C1^-$$
 organic phase reaction (6)

$$Q^{\dagger}Cl^{-} + NaCN \xrightarrow{k_{r}} Q^{\dagger}CN^{-} + NaCl$$
 catalyst regeneration (7)

Reactions (6) and (7) will have maximum rate when

$$k_{O}(RC1)(QCN) = k_{r}(QC1)(NaCN)$$
 (8)

If we assume that catalyst regeneration takes place only in the aqueous phase, then a definite aqueous phase concentration of the catalyst cation would be required (i.e., in contrast to the situation where all the catalyst cation is in the organic phase and catalyst regeneration occurs by anion transfer across the phase boundary). Values of  $k_{r}$  typical for anion exchange reactions in aqueous media are 5-10 orders of magnitude greater than k, so that even if catalyst regeneration occurred only in the aqueous phase, only a few hundredths of a percent of the catalyst need be in the aqueous phase to satisfy or exceed the criterion represented by equation (8). Thus, for most phase transfer catalyzed reactions involving anion transfer from aqueous to organic phases we wish to select a catalyst which will be soluble in the organic phase.

In fact, the distribution of catalyst cations between organic and aqueous phases depends not only on the organic structure of the cation, but also on the nature

of the anion associated with the cation, the polarity of the organic phase, the concentration of inorganic salt in the aqueous phase, the presence of solvating compounds, and possibly other factors.

The kind of anion associated with the catalyst cation has enormous influence on the extent to which a given cation-anion pair is extracted from the aqueous to the organic phase. This means, for example, that a catalyst cation which easily transfers iodide anions from the aqueous to the organic phase might be totally inadequate for the transfer of chloride ions.

Two principle characteristics of the anion most influence its tendency to increase or decrease the ability of a catalyst cation to transfer. First, anions are hydrated to different extents, depending mostly on the charge-to-volume ratio of the anion, and the more the anion is hydrated, the more strongly it will be attracted to the aqueous phase and the more difficult it will be to transfer. This water of hydration may or may not accompany the anion when it is transferred into the organic phase, although most measurements [48,79,80] indicate that the water is transferred.

Increasing the concentration of inorganic salts in the aqueous phase tends to salt out inorganic salts, pushing them into the organic phase. Increasing the inorganic salts concentration also ties up additional water of hydration, reducing the amount of water

available for anion hydration, providing in some cases for easier transfer of the anion into the organic phase.

Usually, the best phase transfer catalysis conditions are realized when the aqueous phase is saturated with the inorganic reagent. One also expects factors such as polarity of the organic phase and structure of the catalyst cation to influence selectivity of anion partitioning into the organic phase.

In reactions where the phase transfer step, rather than the organic phase reaction step, is rate limiting, the concentration of inorganic reagent in the aqueous phase not only affects the degree of anion hydration, as noted above, but will also directly affect the rate of the phase transfer step and therefore the rate of the overall catalysis sequence. This effect may be positive or negative, however, depending on the principal site of anion transfer for the particular system being used.

When the concentrations of anions are not maintained constant, or approximately so, then the rate equation must take these variations into account. We must first consider the mechanism by which the anion is transferred into the organic phase. The most obvious possibilities appear to be:

(a) Simple ion exchange across the interface (liquid ion exchange) [81]

$$(QC1) + CN = \frac{k_a}{} (QCN) + C1$$
org aq org aq
$$(QC1) + CN = \frac{k_a}{} (QCN) + C1$$

$$(9)$$

from which it may be shown that

$$[(QCN)_{org}] = \frac{k_a Q_o[(CN^-)_{aq}]}{k_a[(CN^-)_{aq}] + [(Cl^-)_{aq}]}$$
(10)

(b) Transfer of  $Q^+$  back and forth across the interface with anion exchange in the aqueous phase:

$$Q_{aq}^{+} + CN_{aq}^{-} \stackrel{k_{y}}{\longleftarrow} (QCN)_{aq}$$
 (11)

$$(QCN)_{aq} \stackrel{k_{\pi}}{\longleftarrow} (QCN)_{org}$$
 (12)

$$(QC1)_{aq} \stackrel{k_p}{\longleftarrow} (QC1)_{orq}$$
 (13)

$$Q_{aq}^{+} + Cl_{aq}^{-} \stackrel{k_{\chi}}{\longleftarrow} (QCl)_{aq}$$
 (14)

From this sequence of equilibria it may be shown that

$$[(QCN)_{org}] = \frac{\rho k_x k_{\pi} Q_o(CN^-)_{aq}}{k_x k_y + (1 + \rho k_p) k_y(C1^-) + (1 + \rho k_{\pi}) k_x(CN^-)_{aq}}$$
(15)

where  $\rho = V_O$  (volume of organic phase)/ $V_A$  (volume of the aqueous phase).

(c) Transfer of the inorganic salts into the organic phase for exchange:

$$(NaCN)_{aq} = (NaCN)_{org}$$
 (16)

$$(NaCN)_{org} + (QC1)_{org} = (QCN)_{org} + (NaC1)_{org}$$
 (17)

$$(NaCl)_{org} \neq (NaCl)_{aq}$$
 (18)

- (d) Transfer of anion at the organic-crystalline
  solid interface: (QCl)<sub>org</sub> + (NaCN)<sub>solid</sub> ≠ (QCN)<sub>org</sub>
  + (NaCl)<sub>solid</sub>.
- (e) Formation of micelles in the aqueous phase and transfer of anion across the micelle interface:

$$(QC1)_{\text{micelle}} + CN_{\text{aq}} = (QCN)_{\text{micelle}} + Cl_{\text{aq}}$$
 (19)

$$(QCN)_{micelle} \neq (QCN)_{org}$$
 (20)

Little is presently known about how important each of these mechanisms is to anion transfer, but it is likely that each will be favored in particular experimental circumstances. Mechanism (a) would be expected to be favored by using a very large catalyst cation so that essentially none of it is partitioned into the aqueous phase. Mechanism (b) would be favored by use of a catalyst cation that partitioned into both phases.

Tetrabutylammonium salts are a common example. Mechanism (c) will be favored by use of an organic solvent in which the inorganic salt has appreciable solubility, such

as methanol or acetonitrile, along with an aqueous phase saturated with the inorganic salt (or even dry inorganic salt). An anion having appreciable organic structure will also facilitate this route to anion exchange. Mechanism (d) will be expected when the catalyst can interact directly on the surface of the solid, such as with crown ethers or cryptates, which can exchange not only anions, but also entire salt molecules. Mechanism (e) will be favored by use of catalyst cations that are good micelle-forming agents, such as RN (CH<sub>2</sub>)<sub>2</sub> salts where R is a long chain such as C<sub>16</sub>H<sub>33</sub>-, and by the use of dilute inorganic solutions. Mechanism (e) represents a transition zone between true phase transfer catalysis and reactions that are catalyzed by micelles [82]. Most reported work deals with kinetics that probably have either mechanism (a) or (b) as the predominant mode of anion transfer, and the kinetics equations to be developed are based on these. Kinetics for situations in which mechanisms (c)-(e) are likely to predominate have not been well studied at this time and therefore will be left for the future.

- D. Development of Supported Phase Transfer Catalysts
  - 1. Concept of triphase catalysis (TC)

Triphase catalysis (TC) has recently been introduced [83] as a unique form of heterogeneous catalysis in which

the catalyst and each of a pair of reactants are located in separate phases. Based on this concept, new synthetic methods have been developed for aqueous phase-organic phase reactions using a solid phase catalyst. Although it is only at an early stage of development, TC shows considerable potential for practical use.

Regen has shown [84] that the development of a technique which used insoluble catalysts to accelerate aqueous-organic phase reactions would not only be an interesting possibility but could also provide the basis for synthetic methods competitive with or even superior to existing ones. Furthermore, recently he critically reviewed the triphase catalysis. Figure (5) illustrates the general features of a triphase catalyst system.

Two immediate advantages would be (1) simplified product work-up and (2) easy and quantitative catalyst recovery. From the standpoint of industrial applications, this concept is a very attractive one due to low energy and capital requirements for processing. In addition, such a technique would be ideally suited for continuous flow methods.

# 2. Relationship of triphase to phase-transfer catalysis

The term, "phase-transfer catalysis", was originally introduced by Starks to characterize a process in which: "reaction is brought about by the use of small quantities of an agent which transfers one reactant across the

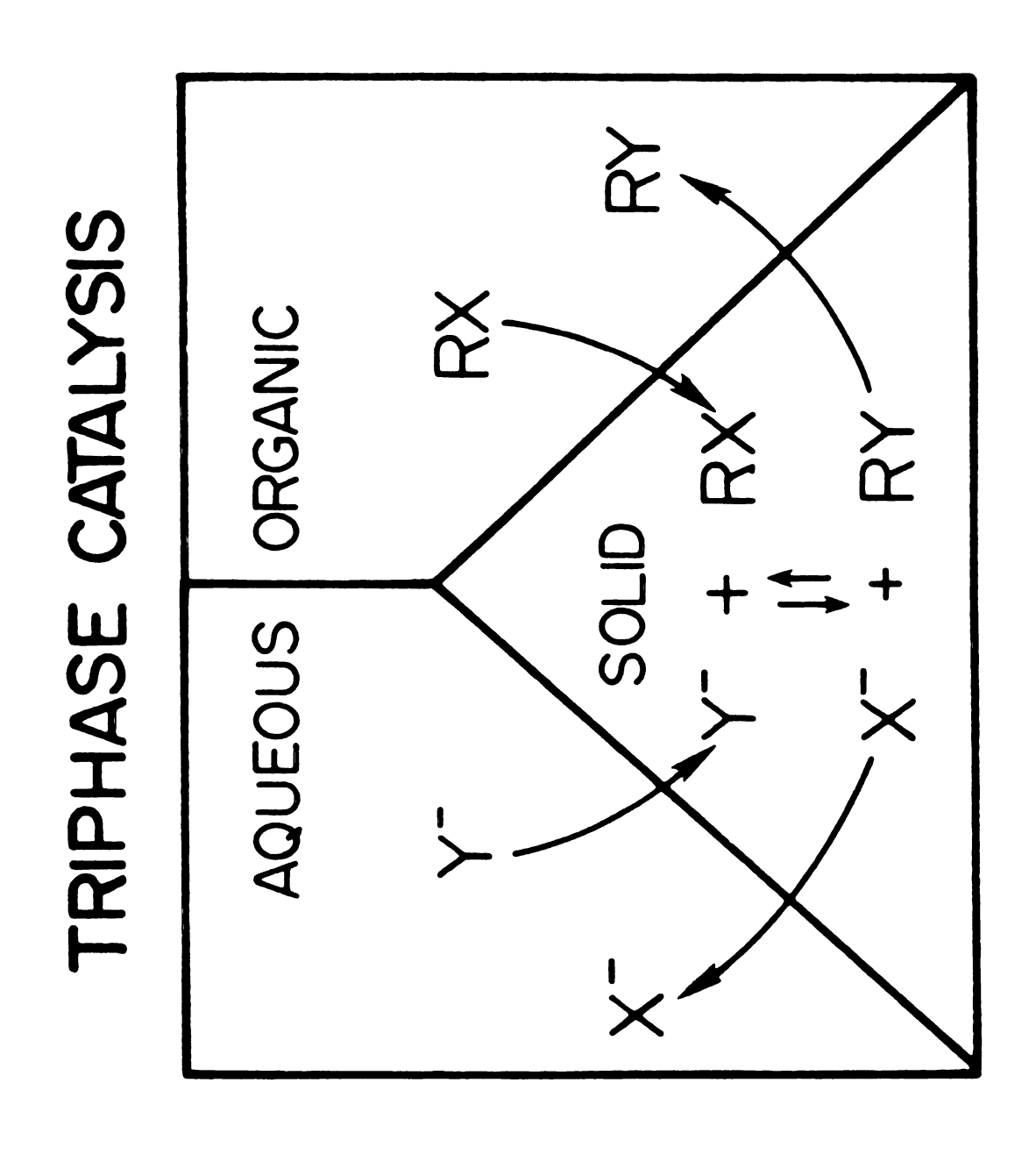


Figure 5 Schematic representation of triphase system.

interface into the other phase so that reaction can proceed" [46]. It is an attractive phrase, but one which carries with it clear mechanistic implications. Work by Starks et al., [48] and Landini et al., [85] provide very strong support for this concept. Recently, however, there has been some concern over its appropriateness in describing certain aqueous organic phase reactions using a soluble catalyst [86] (e.g., evidence is beginning to appear in support of an interfacial process for dihalocarbene reactions [87]. Reference to the solid phase catalysts discussed here as heterogeneous or immobilized phase-transfer catalysts is unwarrantable on the basis of the limited data available and their classification as such should be avoided. All of these systems will require detailed examination before their relationship to phase transfer [88], micellar [89,90,82] and interfacial [87,91] catalysis becomes clear. term triphase catalysis transmits no mechanistic information, yet it serves as an adequate description of the technique.

Triphase catalysis has been established as a synthetic technique for accelerating aqueous organic phase reactions. The inherent complexity associated with three phase catalytic systems makes this a particularly challenging and intriguing new area for the mechanistic chemist who is interested in testing his ingenuity for designing meaningful experiments in unconventional

systems. Moreover, the practical potential of this technique for laboratory as well as industrial applications is great. In brief, it appears highly probable that TC will expand significantly over the next few years along synthetic and mechanistic lines.

## 3. Polymer-supported phase transfer catalysts

One disadvantage of phase transfer catalysis is that it involves the addition to reaction mixtures of material which must be removed again at some later stage. Also some of the catalysts which are particularly useful, crown ethers, cryptands, and chiral onium salts are expensive and certainly worth some effort expended in their recovery. Consequently the attachment of these species to a crosslinked polymer support, with all the usual advantages of retention, isolation, and recovery, is a highly attractive property.

Probably the first use of a polymer-supported phase transfer catalyst was that reported by Regen [83] using bound benzyl trialkylammonium salts. Related approaches were reported by Brown using similar species [92], and by Montanari, using supported phosphonium salts, crown ethers, and cryptands in addition [93].

If a mechanism similar to the one proposed for unbound catalyst operates in supported systems, then it is necessary to imagine the phase boundary existing at the catalytic sites as depicted in Scheme (II). The

(Scheme II)

process of transporting anions back and forth across the boundary can then occur via local backbone and side-chain motion of the catalyst support. This model would predict the efficiency of catalysis to be improved by increasing the length and hence the flexibility of the linkage between the catalyst and the polymeric backbone by introducing a "spacer arm", and this seems to be so in practice [92,94,95]. Brown [92] has examined the catalytic effect of three bound ammonium salts, (21-23), in the alkylation of 2-naphthol and found the "spacer arms" provide a significant improvement.

$$CH_{2}OC(CH_{2})_{x}N^{+}Me_{3}C1^{-}$$

$$x = 5, (21)$$

$$x = 11, (22)$$

$$CH_{2}N^{+}Me_{3}C1^{-}$$

$$(23)$$

Similarly Montanari and his coworkers [94] examined the catalysts (23)-(29) in iodide and thiophenate ion displacement reactions on 1-bromooctane. In this instance the half-lives of reactions are reduced by

P CH<sub>2</sub> = NHCO (CH<sub>2</sub>)<sub>10</sub> = 
$$p^+Bu_3Br^-$$
  
(24)-(27), n = 0-3

factors up to ~10 by increasing the length of the spacer arm. Other workers have demonstrated the catalytic action of bound crown ethers in displacement reactions [96] and also the effectiveness of supported pyridinium residues [97]. The importance of the mobility of a bound catalyst has been reinforced by the use of 'macronet' type supports [95]. These are prepared by crosslinking a linear polymeric species and generally yield highly flexible, three-dimensional networks capable of absorbing large volumes of solvent.

In general, bound phosphonium salts, crown ethers, and cryptands appear to be better phase transfer catalysts than supported ammonium salts [93] and possess higher thermal stability [93,98]. This parallels the known behavior of the analogous unbound species [88]. Though little is known in detail about the kinetics of these systems rates appear to depend linearly on both substrate concentrations [83b,94,99], and the amount of catalyst used [83b,99]. However, the effect of support loading or frequency of catalytic sites on the polymeric skeleton

is not yet understood [83b,92]. Whereas one system appears to function with considerable efficiency when the backbone is virtually totally substituted [92], a closely related one [83b] shows a dramatic drop in activity when the loading is increased from ~20 percent to the range 46-76 percent. In the latter case the phase transfer catalyst is bound close to the backbone of the macromolecular support, whereas the former involves the use of a "spacer arm" and this may account for the difference. Generally the overall amount of catalyst employed varies considerably, but quantities as low as 1 mol percent based on the substrate can be effective, and quantities up to ~100 mol percent have also been used. This illustrates very nicely the advantage of bound species, because even with such large amounts of additives, no additional separation and purification factors are introduced since the bound species can be readily filtered off and washed.

Supported catalysts usually compare favorably with their unbound counterparts, but in some instances the activity is somewhat reduced. Most work has been carried out by using styrene/divinylbenzene resins of the gel type (1-4 percent crosslinked) as the support. In the case of bound ammonium salts commercial anion-exchange resins have proved to be convenient sources.

Macroporous resins [92,83b,96] 'popcorn' polymer [83b], and silica [99] also have been successfully employed.

However, the last-mentioned material has the disadvantage of dissolving in strongly alkaline media.

Smid and his coworkers [100,101] have examined in some detail the cation-binding properties of linear poly (vinylbenzo crown ethers) and have also employed these as catalysts in decarboxylation reactions. Though this is not a true phase transfer catalyst system, there is a close relationship between these areas.

Polymer-supported phase transfer catalysts are being used in a growing number of synthetic applications. Simple halogen exchange reactions [93,83c,95] and nucleophilic displacements on organic halides [92,93,83,97,102] have been particularly successful. In the case of iodide ion [93,83c,95], cyanide ion [93,83c,95], and thiophenate ion [93,95] displacement, concentrated aqueous solutions of the alkali metal salts have been employed. In reactions involving phenoxide and alkoxide ions [83c], concentrated aqueous sodium hydroxide has been used.

Toluene is the most commonly chosen organic solvent and the mole ratio of supported catalyst/substrate is typically ~10<sup>-1</sup>. In the case of catalysts attached by a long 'spacer arm' a number of non-polar organic solvents have been shown to be equally satisfactory, although the catalytic activity of species without a 'spacer arm' is very low in n-heptane [94], and is consistent with the known behavior of this solvent with polystyrene. More recently, o-dichlorobenzene has been reported to be a

useful solvent [97]. The C-alkylation of nitriles has also received some attention [104-106] [Reaction (31)].

 $C_6^{H_5CH_2CN/RBr + NaOH (aq)}$   $C_6^{H_5CH_2CN/RBr + NaOH (aq)}$   $C_6^{H_5CHCN + NaBr + H_2O}$  (31)

The organic phase in this instance usually consists of the reactants alone, and although some reactions have produced high yields [105], others have given variable results [104]. In the latter case commercial ion-exchange resins were used as the catalysts, with a crosslink ratio generally of ~8 percent, and it is possible that diffusional limitations may have arisen in this instance.

Other transformations successfully catalyzed by polymer-supported phase transfer species include the dehalogenation of vicinal dibromides by sodium iodide/sodium thiosulphate to yield alkenes [83c], the oxidation of alcohols to aldehydes using sodium hypochlorite [83c], alcohol chlorinations by dichlorocarbene [83c], and the reaction of carbonyl compounds, in the presence of strong base, with alkyl halides [95] and with chloromethyl p-tolyl sulphones or chlorophenylacetonitrile [107] to afford substituted

ketones [95] and oxiranes [107] respectively (Reaction (33)).

$$C_{6}^{H_{5}CH_{2}CCH_{3}} + RBr \xrightarrow{NaOH (aq)} C_{6}^{H_{5}CHCCH_{3}} + NaBr + H_{2}O$$
(32)

$$\begin{array}{c}
\text{CH}_{3} \\
\text{CH}_{3} \\
\text{CH}_{2}
\end{array}$$

$$\begin{array}{c}
\text{CH}_{3} \\
\text{CH}_{2} \\
\text{CH}_{2} \\
\text{CH}_{2}
\end{array}$$

$$\begin{array}{c}
\text{CH}_{3} \\
\text{CH}_{3} \\
\text{CH}_{3} \\
\text{CH}_{3} \\
\text{CH}_{2}
\end{array}$$

$$\begin{array}{c}
\text{CH}_{3} \\
\text{CH}_{3} \\
\text{CH}_{2}
\end{array}$$

$$\begin{array}{c}
\text{CH}_{3} \\
\text{CH}_{3} \\
\text{CH}_{3} \\
\text{CH}_{3}
\end{array}$$

$$\begin{array}{c}
\text{CH}_{3} \\
\text{CH}_{3} \\
\text{CH}_{3} \\
\text{CH}_{3}
\end{array}$$

$$\begin{array}{c}
\text{CH}_{3} \\
\text{CH}_{4} \\
\text{CH}_{4} \\
\text{CH}_{4} \\
\text{CH}_{4} \\
\text{CH}_{5} \\
\text$$

Polymer-supported chiral catalysts have also been investigated recently. A number of optically active linear polymeric tertiary amines have been used purely as base catalysts in various homogeneous reactions [108-111]. Particularly, the use of supported chiral catalysts provides a possible major step forward in the synthesis of useful materials, and is yet a further example of the sophistication in chemical transformation being achieved today in many research laboratories. Colonna et al. [107], have reported an ephedrinium-based chiral triphase catalyst I and used it to perform Darzens

condensations. Asymmetric induction was achieved with optical yields as high as 23%. Although the products obtained in the triphase catalyst system I were of lower optical rotation than those from the analogous biphase system II, the polymer-supported catalyst had the advantage of being easily and completely removed from the product mixture by filtration.

## 4. Polymer-supported 'solvents' and 'cosolvents'

Regen has coined the expression "polymer-supported cosolvent" [112,113] in describing a resin-bound, linear oligoethylene oxide chain (34). A similarly supported analogue of hexamethylphosphoramide (HMPA) (35)  $(R = CH_3)$  also has been reported [114], which employed

a linear polystyrene backbone. Dipolar aprotic solvents like HMPA are known to be excellent alkali metal ion solvators, and hence readily promote nucleophile displacement [115,116] and carbanion-forming reactions [115]. Not surprisingly, therefore, the bound phosphoramide (35) (R = -CH<sub>3</sub>) does indeed function as a phase transfer catalyst in the displacement reactions of aqueous iodide and acetate ions on n-octyl bromide in toluene [114]

presumambly functioning by specifically solvating the potassium counterion and increasing its lipophilicity.

### 5. Inorganic-based catalysts

Only a few reports have appeared thus far describing inorganic-based triphase catalysts [99,117]. Phasetransfer (PT) catalysts, namely phosphonium salts, have been immobilized on silica gel. Good organofunctionalization are obtained with silica gel. The surface of silica contains silanol-OH groups mainly responsible for adsorption. Also,-O-strained siloxane linkages [118] can be transformed into -OH by reflux with 35% hydrochloric acid [119]. Silica gel activated in this manner gives good linking reactions with the alkyltrialkoxysilanes to afford the alkyl-functionalized silica gel [119].

Activated silica + Br (CH<sub>2</sub>)<sub>3</sub>Si(oEt)<sub>3</sub> 
$$\xrightarrow{\text{Toluene}}$$
  $\xrightarrow{\text{reflux}}$   $\xrightarrow{\text{O}}$  Si(CH<sub>2</sub>)<sub>3</sub>Br  $\xrightarrow{\text{PBu}_3}$   $\xrightarrow{\text{O}}$  Si(CH<sub>2</sub>)<sub>3</sub>P<sup>+</sup>Bu<sub>3</sub>Br<sup>-</sup> (36)

The most likely structure for the chemical linkage is shown in (37). It is also the most stable to hydrolysis.

Bridge formation with one or two oxygen atoms between the polymer support and the organosilicic function is also possible, although bridging with one atom occurs less frequently and is of minor importance [120,121].

Recently Tundo et al. have shown that the activity of phase-transfer catalysis immobilized on polystyrene matrices increases if there is a chain between the active center and the matrix [94]. In the case of immobilization on silica gel, however, the length of the hydrophobic chain strictly determines the adsorption capacity of the polar support, which then controls the rate of the reaction.

It is thus correct to speak of three-phase catalysis: two reagents, each derived from a distinct phase, come into close contact on a third phase and react. A similar situation is also observed on nonfunctionalized silica gel [122], which adsorbs organic compounds by transporting them into the cavities of the polymer matrix where they react with the second reagent, which has also been adsorbed. However, it may be difficult for the anionic species to migrate up to support. This will depend on the hydrophilic nature of the salt, since both the anion and the cation must be dissociated and solvated by the less polar silica gel [122,123]. If the gel itself contains positive centers, the local concentration of anions involved in the catalysis will be greater than that of the immobilized onium salt for the same adsorption

capacity of the gel. Furthermore, adsorption of the substrate by the gel is dependent on the solvent. When catalyst supported on silica gel are used, the best solvent will undoubtedly be that which gives the lowest R<sub>f</sub> in silica gel TLC. Aliphatic hydrocarbons are always the best solvent for PT reactions catalyzed by phosphonium salts supported on silica gel.

Swelling dialets the mesh size of organic resins which, in turn, allows a greater accessibility of the reagents to the catalytic sites [124]. However, the lack of uniformity precludes selectivity toward organic substrates of different dimension. In contrast, inorganic supports are not swollen by organic solvents. The catalytic activity of silica gel in apolar solvents is two-fold. First, the reactions rates are higher in apolar media, and second, the substrate is more strongly adsorbed on the insoluble support. Moreover, since the three-dimensional structure does not vary with the solvent and is well defined [125], there are greater possibilities of studying and applying the selectivity phenomena [126].

In case of alumina the active sites are both Brönsted and Lewis acids, it can catalyze a large and varied number of organic reactions [127]. Alumina differs from silica gel in its adsorption and ion interaction properties since it promotes nucleophilic replacements to a greater extent than silica gel. In the absence of water, alumina offers an aprotic polar environment favoring nucleophilic substitution [128-130].

The degree of functionalization of alumina is less than that of silica gel, consistent with the fact that the surface concentration of hydroxyl groups is lower in alumina than in silica gel  $(0.1-2.5 \text{ OH/nm}^2 \text{ and } 4-10 \text{ OH/nm}^2 \text{ respectively})$ .

Appreciable selectivity has been observed by Tundo et al. [126], in the nucleophilic substitution reaction with aqueous potassium iodide toward halide of different sizes (1-bromobutane, 1-bromooctane, and 1-bromohexadecane) using the phase-transfer catalysts of the type shown in reaction (38).

Al<sub>2</sub>O<sub>3</sub> 
$$= \frac{\text{OH}}{\text{OH}} \frac{\text{H}_2\text{N}(\text{CH}_2)_3\text{Si}(\text{OC}_2\text{H}_5)_3}{\text{toluene, reflux}} = \text{Al}_2\text{O}_3$$
  $= \frac{\text{O}}{\text{O}} \text{Si}(\text{CH}_2)_3\text{NH}_2$   $= \frac{\text{Br}(\text{CH}_2)_{10}\text{COCl}}{\text{benzene, pyridine}} = \text{Al}_2\text{O}_3$   $= \frac{\text{O}}{\text{O}} \text{Si}(\text{CH}_2)_3\text{NHCO}(\text{CH}_2)_{10}\text{Br}$   $= \frac{\text{NBu}_3, 80^{\circ}\text{C}}{\text{PBu}_3, 65^{\circ}\text{C}} = \text{Al}_2\text{O}_3$   $= \frac{\text{O}}{\text{O}} \text{Si}(\text{CH}_2)_3\text{NHCO}(\text{CH}_2)_{10}\text{P}^{+}\text{Bu}_3\text{Br}^{-}}$ 

or

$$Al_{2}O_{3}$$
  $si(Ch_{2})_{3}NHCO(Ch_{2})_{10}N^{+}Bu_{3}Br^{-}$  (38)

Earlier studies have shown that intercalation compounds of hectorite, montmorillonite, and other smectite clay minerals can be tailored to function as

selective liquid-solid phase transfer catalysts, particularly when the spatial requirements of oriented reaction intermediates on the intracrystal surfaces differ for different substrates [131]. Surface chemical equilibria also can be controlled and used to enhance the selectivity of intercalated clay catalysts [132]. Since clay layers are negatively charged, the rational design of clays as phase transfer catalysts is generally restricted to intercalates in which the host structure is interlayered with catalytically active cations such as transition metal complexes [5,133]. Anion intercalation is normally precluded on electrostatic grounds. Most recently the use of montmorillonite supported phase transfer catalysts such as the benzyltri-n-butyl ammonium ion have been studied [134]. The present study demonstrates that the well ordered intersalation offers new possibilities for selective triphase catalysis of displacement reactions involving anionic nucleophiles.

E. Anion Exchange and Catalytic Properties of Smectite
Intersalates

Anion exchange in smectites generally is <5 meq/100 g. Anions of the appropriate size may replace structural hydroxyls only at the edges of smectite crystals [135], and in general the only factor preventing complete substitution is the fact that many OH ions are within the lattice and,

therefore, not accessible. Hendricks [136] suggested that another factor in anion exchange is the geometry of the anion in relation to the geometry of the claymineral structure units. Anions such as phosphate, arsenate, borate, etc., which have about the same size and geometry as the silica tetrahedron, may be adsorbed by fitting on to the edges of the silica tetrahedral sheets (see Section A) and growing as extensions of these sheets. Other anions such as sulfate, chloride, nitrate, etc., because their geometry does not fit that of the silica tetrahedral sheets, cannot be so adsorbed.

In the case of polyanion adsorption Theng et al., [35] have concluded that, if polyanion adsorption were largely restricted to the crystal edges of clays, we might also expect that those minerals which show interlayer swelling in water to take up more of the polymer as compared with their non-swelling counterparts. This is so because, unlike the adsorption of small, simple anionic species, steric and accessibility factors come into play during the interaction of polyanions and clay minerals. In accord with this expectation, Ahlrichs [137] and De and Jain [138] have observed that the adsorption of krilium-type polymers by 2:1 type layer silicates decreased in the order of montmorillonite > vermiculite > biotite > pyrophyllite. This observation further argues for the reactivity of the edge surface towards polyanions since such minerals as biotite and pyrophyllite have few,

if any, exchangeable cations with which the functional groups of the polymer may interact.

The failure of synthetic polyanions to form interlayer complexes with expanding 2:1 type layer silicates has led to the widely accepted view that the active sites on clay surfaces, in general, are mainly located at the crystal edges and identifiable with Al·OH or its protonated form, Al·OH<sub>2</sub>. Although such sites clearly play an important part in the adsorption by kaolinite-type minerals they may not be of great significance to polyanion uptake by 2:1 type layer silicates.

In the present work, an attempt is made to demonstrate some of the unique properties of anion intercalation within the interlamellar regions of smectite clay minerals. As previously described in Section B, a novel class of intercalates in which two layers of  $M(\text{chelate})_{\mathbf{x}}^{\mathbf{n}+}$  and a layer of counteranions are bound in the interlamellar region of the layered silicate. The anions present between interlayers can actually be replaced by other anions, in fact this is a first indication that layered silicates can act as anion exchangers with anion exchange capacity (AEC)  $\sim 50$  meq/100 g of intersalate (see Chapter III for detail).

The anion exchange takes place without significant loss of the complex cation, which remains immobilized on the surface. It is expected that layered silicate

intersalates to be of considerable importance in part, because they convert a mineral which is normally a cation exchanger into an anion exchanger which might be utilized as sinks for the deactivation of hazardous and pollutants anion. In addition, they provide an opportunity to investigate the effects of intercalation on the catalytic activity and selectivity of anions.

The positioning of the anions between two layers of metal complex cations can influence their solvation properties, therefore the interlayers may be sufficiently lipophilic to allow penetration of the interlayers by organic reagents while at the same time allowing the anions to be replaced by exchange with salt from an aqueous phase. Therefore one of the objectives of this research is to elucidate the catalytic properties of intersalates, particularly application of the intersalates in a triphase catalyst system.

#### CHAPTER II

#### **EXPERIMENTAL**

#### A. Materials

Unless stated otherwise, all reagents were obtained commercially and used without further purification.

#### 1. Natural Hectorite

Naturally occurring sodium hectorite (B1-26) with a particle size <2  $\mu$ m was obtained from the Baroid Division of NL Industries in the precentrifuged and spray-dried form. The idealized anhydrous unit-cell formula of hectorite is Na<sub>0.66</sub>[Li<sub>0.66</sub>Mg<sub>5.34</sub>](Si<sub>8.00</sub>)O<sub>20</sub>(OH,F)<sub>4</sub>, and the experimentally determined cation-exchange capacity is 73 meg/100 g of air-dried clay [138].

# 2. Sodium Montmorrillonite (Wyoming)

This mineral was obtained from the Source Clay Mineral Repository. The mineral was allowed to sediment and then was saturated with  $\mathrm{Na}^+$  ions by adding an excess of sodium chloride. The clay was centrifuged and dialyzed until free of excess sodium chloride and then freeze dried. Ion exchange of  $\mathrm{Na}^+$  in the native mineral with  $1.0~\mathrm{M}$  Cu( $\mathrm{NO}_3$ ) and subsequent analysis of the minerals

for copper indicated the cation exchange capacity (CEC) of 80 meg/100 g.

## 3. Synthetic Hectorite (Laponite-RD)

A synthetic hectorite with the structural formula of  $Na_{0.22}Li_{0.14}[Mg_{5.64}Li_{0.36}](Si_{8.00})O_{20}(OH)_4$  was obtained in powder form from Laporte Company. The cation exchange capacity of this hectorite is 55 meq/100 g and the size of average particle is ~10 Å thick, with an average diameter of 200 Å.

#### 4. Fluoro-hectorite

This synthetic clay was donated by Corning Glass Works. The compound was provided in (11.2 g of fluorohectorite/100 ml suspension). The structural formula was given as  $\text{Li}_{1.4}^{\text{[Mg}}_{3.4}^{\text{Li}}_{1.6}^{\text{]}}^{\text{(Si}}_{8.00}^{\text{)O}}_{20}^{\text{(F)}}_{4}^{\text{.}}$  The particle size is >>2  $\mu$ m and the CEC is 193 meq/100 g.

All of the hectorites and montmorillonite were freeze dried and stored in a desiccator over anhydrous CaCl<sub>2</sub>.

#### 5. Reagents and Solvents

Ethylenediamine (en); 2,2'-bipyridyl(bP);1,10phenanthroline monohydrate (Phen); 4,7-diphenyl-1,10phenanthroline or Bathophenanthroline (BathPhen);
3,4,7,8-tetramethyl-1,10-phenanthroline (TM-Phen),
2,4,6-tri-(2-pyridyl-s-triazine (TPTZ) were purchased
from Aldrich Chemical Company and G. Fredrick Smith
Chemical Company, respectively. TPTZ was purified by
recrystallization from petroleum ether.

All alkyl and aryl halides as well as internal standards and solvents used in this study were purchased from Aldrich Chemical Company except 1-bromo-3,5,5-trimethylhexane which was obtained from K & K Laboratories. Tricaprylmethyl-ammonium chloride (poly Sciences), nile blue (MCB Manufacturing Chemists, Inc.), 3,3-(4,4'-biphenylene)-bis-[2,5-diphenyl-2H-tetrazolium chloride] (Morton Thiokol, Inc., Alfa) cetylpyridinium chloride and polybrene

$$\left[\left[-\frac{\text{CH}_{3}}{\text{N}^{+}}\right] \left(\text{CH}_{2}\right)_{6} - \frac{\text{CH}_{3}}{\text{CH}_{3}} \left(\text{CH}_{2}\right)_{3} - \left[\text{2Br}\right]_{x}\right]$$

(Aldrich Chemical Co.) were stored in a vacuum dry desiccator over CaCl<sub>2</sub>.

Dowex exchange resin  $2 \times 3$ , 100-200 mesh, Cl-form was a gift from the Dow Chemical Company. Silane coupling agent Z-6076 [ClCH<sub>2</sub>CH<sub>2</sub>CH<sub>2</sub>Si(OCH<sub>3</sub>)<sub>3</sub>] was purchased from Dow Corning Corporation. The spin probe peroxylamine disulfonate, potasium salt, (PADS) (Aldrich Chemical Company) was kept under N<sub>2</sub> atmosphere to prevent possible decomposition. All solvents and inorganic reagents used were ACS reagent grade.

#### B. Synthesis

1.  $\underline{M(Phen)}_{3}\underline{SO_{4}}$  and  $\underline{M(bP)}_{3}\underline{SO_{4}}$  Complexes (M = Ni, Fe, Zn)

Metal tris(1,10-phenanthroline) and tris(2,2'-bipyridyl) complexes were prepared as sulfate salts by reaction of the free ligand and an aqueous solution of the metal sulfate according to literature methods [139, 140]. The crystals were extracted with hot benzene to remove any adsorbed free ligand.

# 2. Ni (Phen) $_{3}XO_{4}$ (XO<sub>4</sub> = MoO<sub>4</sub>, CrO<sub>4</sub>, WO<sub>4</sub>)

An anion exchange method was adopted for the preparation of these salts from the chloride salt. amount of anion exchange resin (Dowex 2 × 3, 100-200 mesh, Cl-form) was saturated by diluted HCl solution and then washed several times with deionized water. After filtration the resin was transferred to a chromatographic column where the chlorine was exchanged for  $SO_4^{2-}$  by treatment with concentrated (1  $\underline{\text{M}}$ ) Na<sub>2</sub>SO<sub>4</sub> solution. The eluants were checked with silver nitrate for the absence of Cl. The direct exchange between the Cl -form of the resin and  $MoO_4^{2-}$ ,  $CrO_4^{2-}$  or  $WO_4^{2-}$  anions was not practical; because the exchange process is slow and requires a large excess of  $XO_4^{2-}$ . However, the  $SO_4^{2-}$ -form of the resin could be readily exchanged with the appropriate  $xo_a^{2-}$ anion. BaCl, was used to check for the absence of sulfate. A 0.05 M solution of tris-(1,10-phenanthroline)-nickel (II) chloride heptahydrate prepared by literature method [140] was passed through the exchange column. The flow rate was about 1 mL/min and the ratio of resin to salt was 2:1 (meq:meq). The  $XO_4^{2-}$  complex salts were

recrystallized from hot deionized water. Despite the tediousness of this process the yield was almost quantitative.

3. Fe(L)<sub>3</sub>SO<sub>4</sub>, [L = 1,10-orthophenanthroline; 3,4,7,8tetramethyl-1,10-phenanthroline, and 4-7-diphenyl-1,10-phenanthroline (Bathopheanthroline)]

Fe(L) $_3$ SO $_4$  complexes were prepared according to previously reported procedures [141-144]. The absorption spectra of the complexes were in agreement with those reported in the literature.

4. Fe (TPTZ) 2 (ClO<sub>4</sub>) 2,4H<sub>2</sub>O,Fe (TPTZ) 2SO<sub>4</sub>

Bis 2,4,6-tri(2-pyridyl)-s-triazine) iron (II)

perchlorate tetrahydrate and sulfate were synthesized by the method of Watton et al. without modification

[145-146].

Care must be taken in handling perchlorate complex salts as these salts are potentially <u>explosive</u>! The electronic spectra agreed well with literature values [141].

5.  $\underline{\text{Ni(en)}_{3}\text{SO}_{4}}$  and  $\underline{\text{Ni(NH}_{3})_{6}\text{SO}_{4}}$ 

The tris(ethylenediamine) nickel (II) sulfate, was synthesized according to the procedure of George and Wendlandt [147]. Hexammine nickel (II) sulfate was prepared by the addition of an excess of concentrated aqueous NH<sub>3</sub> to a saturated solution of NiSO<sub>4</sub>·xH<sub>2</sub>O

The precipitation of small violet-colored crystals was accomplished by the addition of 95 percent ethanol. The

hexammine complex was washed with ethanol and ether and then air dried.

# 6. $\underline{\text{Fe (bP)}}_3 \underline{\text{(ClO}}_4)_2 \underline{\text{and Fe (bP)}}_3 \underline{\text{SO}}_4 \underline{\text{-}}$

Fe (bP)  $_3$  (ClO $_4$ )  $_2$  was prepared according to the methods of Burstall and Nyholm [148]. Tris(2,2'-bipyridyl) iron (II) sulfate heptahydrate, Fe (bP)  $_3$ SO $_4$ ·7H $_2$ O was prepared by adding an excess of the amine to a solution of FeSO $_4$ ·7H $_2$ O. The solution was heated one hour at 90°C. The solution was evaporated to a low volume and the dark red paste extracted several times with hot benzene. The remaining material was dissolved in water and crystallized from aqueous solution. Crystals were collected in a büchner funnel and dried over  $P_4O_{10}$ .

# 7. $\underline{K_3Cr(OX)_3 \cdot 3H_2O}$

Potassium trioxalatochrominate (III) trihydrate was synthesized by a known procedure [149].

# 8. Elemental Analysis and Storage

Elemental analyses were performed either by Gailbraith Laboratories, Inc., Knoxville, TN or Spang Microanalytical Laboratory, Eagle Harbor, MI. All complexes and catalysts were stored in a desiccator over anhydrous  $CaCl_2$  or  $P_4O_{10}$ .

#### C. Preparation of Intercalates

Intercalation reaction of all complex cations were performed under similar conditions, since all complexes

were quite stable and also soluble in water.

In a typical experiment a 1.0 wt% aqueous suspension (e.g. 0.1 g of the mineral in 10 ml H<sub>2</sub>O) was added to a vigorously stirred aqueous solution of the complex cation containing ~1.2 meq/meq of clay. The reaction mixture was stirred over an hour. After an equilibration time of 24 h the clay was repeatedly washed with deionized water and then collected by centrifugation. The resulting homoionic metal-complex exchange forms of the minerals were either air-dried or freeze-dried, as desired, and stored in a desiccator over anhydrous CaCl<sub>2</sub>.

## D. Preparation of Intersalates

Identical procedures were used for the intersalation reaction of all  $M(Chel)_{X}^{2+}$  (x = 2,3) and organic salts. In a typical intersalation reaction 0.10 g of freeze-dried hectorite with a CEC of 73 meq/100 g was slurried overnight in 10 mL deionized water (1.0 wt%) and sonified for about half a minute before being added to a vigorously stirred aqueous solution of the complex salt (0.146 meq) at room temperature. Typically, the concentration of the salt solution was 2 mg/mL ( $\sim$ 0.002 M).

After an equilibration time of 24 hours, the products were collected by centrifugation and washed with a minimum amount of deionized water. The

intersalates then were either freeze dried or spread on a glass surface for air drying. Air dried samples are more convenient for weighing and transferring to a reaction flask. (For film sample preparation see Section 2 of Physical Methods.)

The intersalation of the complex salts in smectite is highly dependent on the initial state of dispersion of the clay. To ensure optimum dispersion of the platelets, the 1.0 wt% mineral suspension was sonified by use of a cell disruptor model W185 from Ultrasonic Inc. immediately prior to its addition to the aqueous complex salt solution.

## E. Desorption Coefficient Measurement

Procedures similar to that described for the  $Fe\,(Phen)\,_3^{2+}/SO_4^{2-}-hectorite\ intersalate\ were\ followed\ for\ all\ desorption\ coefficient\ measurements.\ A\ 0.04\ g\ sample\ of\ Fe\,(Phen)\,_3^{2+}/SO_4^{2-}-hectorite\ containing\ one\ cation\ exchange\ equivalent\ of\ Fe\,(Phen)\,_3^{2+}\ and\ one\ equivalent\ of\ Fe\,(Phen)\,_3^{2+}/SO_4^{2-}\ ion\ pairs\ was\ stirred\ in\ 10.00\ mL\ of\ an\ appropriate\ solvent\ (ethanol\ or\ water)\ at\ 20^{\circ}C\ in\ a\ thermostat.\ After\ 48\ hours\ of\ equilibration\ time\ the\ suspensions\ were\ filtered\ by\ use\ of\ a\ milipour\ filter\ (0.02\ \mu)\ and\ the\ filtrates\ were\ analyzed\ by\ atomic\ absorption\ (Perkin\ Elmer\ Atomic\ Absorption\ Spectrometer\ 560)\ .$  The instrument was calibrated\ against Fisher\ standards.

#### F. Ion Exchange-Adsorption Isotherms

Ion exchange isotherms were developed for the adsorption of Ni(Phen)  $_3^{2+}$ SO<sub>4</sub>, Ni(Phen)  $_3$ CrO<sub>4</sub> and Nile blue on Na-hectorite by adding the appropriate amount of complex salts aqueous standard solution to a known weight (0.04 g) of Na-hectorite and bringing the suspensions volume to 25.00 ml. The suspensions were allowed to equilibrate for 48 hours and then centrifuged. The supernatant solution was analyzed for the concentration of complex salts by UV-VIS spectrophotometery. Standard curve of absorbance versus concentration was constructed with a known concentration of the complex salts. The absorption maximum was obtained at 520, 369, and 633 nm for Ni(Phen)  $_3$ SO<sub>4</sub>, Ni(Phen)  $_3$ CrO<sub>4</sub> and Nile blue respectively. Adsorption isotherms were reproducible within experimental error as determined by checking certain points on the isotherms.

#### G. Anion Exchange Adsorption Isotherm Studies

Anion exchange isotherms were developed for the adsorption of  $PO_4^{3-}$ ,  $MOO_4^{2-}$ ,  $Cr(OX)_3^{3-}$ ,  $WO_4^{2-}$ ,  $\phi COO$ ,  $C\overline{I}$  and MeCOO on Ni(Phen) $_3^{2+}/SO_4^{2-}$ -hectorite. An appropriate amount of salt solution was added to a known weight (400 mg) of complex-hectorite and the suspension was diluted to a volume of 50.00 mL. The suspensions were allowed to equilibrate for 48 hours and then centrifuged. The supernatant was analyzed for the concentration of  $CrO_4^{2-}$ 

anion by spectrophotometry. The adsorption maximum was obtained at 369 nm for  $\text{CrO}_4^{2-}$  anion and the amount of anion adsorbed by the complex-hectorite was determined by  $\text{CrO}_4^{2-}$  desorption from the intersalates. Selected points on the isotherms were checked for reproducibility. In general, the results were reproduced to within  $\pm 10\%$ .

H. Kinetics of Biphase and Triphase-Catalyzed Displacement Reactions

Procedures similar to that described for the conversion of alkyl bromides to alkyl chlorides were followed for all displacement reactions described in this dissertation. The reactions of alkyl bromides with NaCl under triphase conditions were carried out as follows. Air dried Ni (Phen)  $_{3}^{2+}/SO_{4}^{2-}$  -hectorite (0.1566 g 0.069 meg of Ni(Phen) 3SO, as catalyst) was dispersed in 3.0 mL aqueous 3.3 M NaCl in a 15 × 150 mm Pyrex culture tube fitted with a teflon-lined screw cap and magnetic stirring bar. A specially designed flat-bottomed reaction flask (see Fig. 6) was sometimes substituted for the culture tube. This design was especially effective in minimizing "creeping" of the finely divided mineral-supported catalyst up the walls fo the flask during the course of the reaction. The mixture was stirred for a few hours until a homogeneous suspension was obtained. suspension was added 1.0 mmol of the appropriate alkyl bromide in 2 mL toluene. The tubes were sealed with a

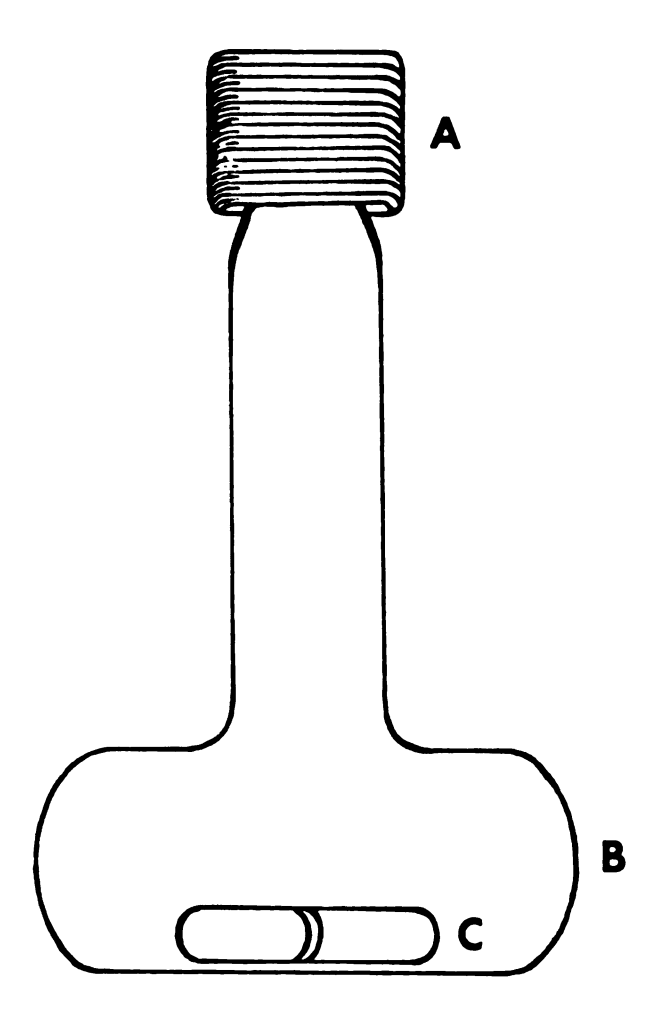


Figure 6 Reaction flask used to minimize creeping of finely divided intersalated catalyst: (A)
Teflon-lined screw cap, (B) reaction chamber
4 (diameter) × 2 cm., (C) magnetic stirring bar.

teflon-lined screw cap and vigorously shaken for a minute. The kinetics experiment was then started by placing the tube in an oil bath maintained at the desired temperature. The reaction was followed by withdrawing l-µL samples of the organic phase at different times (no less than 30 minute intervals) and monitoring the disappearance of the reactant by GLC. For sampling, the tube was removed from the oil bath, shaken, quickly cooled to nearly room temperature, opened, resealed and returned to the bath. The overall process took less than 1 min. The temperature of the oil bath used for the kinetic experiments was controlled to ±0.5°C with the aid of a temperature controller (4831 automatic temperature controller, model 4831, Parr Instrument Co.) attached to an Iron-Constantan thermocouple. Product mixtures were analyzed by GLC on a Hewlett-Packard model 5880A with a flame ionization detector and a capillary 12.5 M  $\times$  0.2 mm crosslinked dimethyl silicone column. First-order rate constants were determined by fitting the experimental data to the best linear curve by a least-squares method. Similar methodology was utilized in studying the reaction under biphase (liquid-liquid) conditions except that appropriate amounts of complex salts were used in place of the hectorite intersalates.

I. Reaction of Benzyl Chloride with Salts of the Acetate
Ion

Benzyl chloride was purified by distillation under reduced pressure before use. Air dried Ni(Phen)  $\frac{2+}{3}/SO_4^{2-}$  hectorite (0.1566 g, 0.069 meq) was carefully placed in the bottom of a 50-mL culture table. Sodium acetate (1.1 mmol) in 3 mL deionized water was slowly added to the tube, and then 2.0 mL toluene was added. A sample of benzyl chloride (1 mmol) was then added to the organic layer via syringe. The tube was then sealed with a screw cap, shaken vigorously for a minute, immersed in an oil bath maintained at 90°C for 48 hr, withdrawn, and cooled to room temperature. The concentrations ratios were measured by GLC analysis. The product benzylacetate was characterized by GLC retention time. Only two peaks (benzyl chloride and benzylacetate) were detected.

J. Modification of the Intersalate with Silane Coupling
Agent

A 1 mL sample of chloropropyltrimethoxysilane (Z6076, Dow Corning) was shaken vigorously with 100 mL deionized water in a 250 ml Erlenmayer flask, until the solution became clear with no haze. The pH of the solution was adjusted to 3.0 with HCl and 10 mL of this solution was then added to a paste of Ni(Phen) $^{2+}$ /SO $_4^{2-}$ -hectorite intersalate (~0.2 g). The mixture was stirred for a few hours and then centrifuged. The clay was

washed with a very small amount of water, spread on a glass slide, and stored in a desiccator upon drying.

#### K. Physical Methods

### 1. X-ray Diffraction Studies

All d(001) basal spacings were determined with a Philips X-ray diffractometer or Siemens crystalloflex-4, both equipped with Ni filtered Cu k, radiation. The film samples were prepared by allowing an aqueous suspension of the mineral to evaporate on a microscope glass slide and monitoring the diffraction over a range of 20 values (2-40°). In some cases the self-supported films were supported on a glass slide by the aid of double surface tape. Highly ordered self-supporting oriented films samples of intercalates or intersalates were obtained by allowing a ~1% water suspension of the complex mineral to evaporate at room temperature on a flat polyethylene surface and then peeling the dried films away. Basal spacings of fully solvated and swelled samples were obtained by first forming a thin film of the mineral on a 1 × 1", porous ceramic tile in place of microscope slide. This sample was then suspended under solvent and allowed to equilibrate for 30 min. solvent adsorbed in the pores of refactory material, allowing the tile to function as a solvent reservoir and prevented the film from drying during the X-ray

diffraction measurements. This is a quite convenient method for determining the basal spacings of minerals wetted with a solvent which is very volatile. In a blank experiment, no diffraction patterns from the microscope slide or the ceramic tile was observed in the scanning range of interest. The peak positions in the angle 20 were converted to d basal spacing with a standard chart, (Cu  $K_{\alpha}$ ,  $\lambda = 1.5405$  Å).

#### 2. ESR Studies

Electron spin resonance (ESR) spectra were recorded at x-band frequency with a Varian E-4 ESR spectrometer, using quartz tubes containing thin films of the doped hectorite intersalates. Highly ordered self-supporting films of  $Zn(phen)_3^{2+}/SO_4^{2-}$ -hectorite intersalates containing PADS<sup>2-</sup> as a spin probe at the 2% exchange level were prepared by evaporating at room temperature an aqueous suspension of the intersalate on a flat polyethylene or teflon surface and then peeling the films away. The self-supported film samples of the intersalates were placed in chambers of 52% or 98% relative humidity (r.h.) or vacuum dried for a few days before the measurements were made. Since the crystallites are oriented with their silicate layers parallel to the film surface, narrow strips of film (ca. 3 × 12 mm) placed vertically in a quartz glass ESR tube (I.D. 4 mm) or on a teflon holder could be positioned in the cavity of an

ESR spectrometer with the silicate layers at a known angle to the external magnetic field.

In the case of fully wetted samples, a suspension of the clay sample was centrifuged, and a glass capillary tube was immersed into the paste. Then approximately 1 cm of the tip of the capillary which was filled with the paste was cut and placed in a quartz glass ESR tube for the measurement.

Standard pitch served as a standard for which q = 2.0023.

## 3. UV-Visible Spectroscopy

Electronic spectra were recorded on a Varian

Associates Cary Model-17 spectrophotometer. Absorption

spectra of complex solutions were obtained using matched

1 cm path-length quartz cells. In the case of clay
complexes, the samples were prepared by mulling in mineral

oil and placing the mull between silica disks. A mull

sample of native clay was placed in the reference beam

to reduce the effect of scattering.

## 4. Gas Chromatography

All product mixtures along with solvent and internal standards were analyzed by gas-liquid chromatography (GLC) on a Varian Associates Model 920 single-column chromatograph equipped with a thermal conductivity detector. The column was a 5' × 0.25" 5% SE-30 on chromosorb W. Also, a Hewlett-Packard Model 5880A gas chromatograph system with flame ionization detector

(minimum detectable level:  $5 \times 10^{-12}$  g/sec. of carbon) was used in some studies. The output of the detector was recorded on 5880A high speed printer/plotter with key stroke programming for data handling system.

The triphase catalytic products were separated on a high speed metal capillary column (12.5 M × 0.2 mm cross-linked dimethyl silicone) and were identified by comparison of GLC retention times with those of an authentic sample. The percentage of products was determined by integration of the chromatographic peaks. Integrations were carried out by the dual channel integration and computation, cartridge tape units, and BASIC programming.

## 5. Infrared Spectra

Infrared spectra were recorded by use of, or with a Perkin-Elmer Model 457 grating spectrophotometer.

The samples were prepared by using a KBr matrix or mulling the sample in fluorolube (Hooker Chemical Company) and placing the mulls between CsI disks. A wire mesh screen served as an attenuator in the reference beam of the spectrometer.

#### CHAPTER III

#### RESULTS AND DISCUSSION

- A. Adsorption of Complex Salts on Smectite (Intersalation Reaction)
- 1. Adsorption of Metal Complex Salts

Metal tris chelates of the type  $M(\text{chel})_X^{2+}$  (X = 2,3), where M = Fe, Ni, Zn and chel = phen and its derivative, bipy, TPTZ, en, rapidly displace the surface Na<sup>+</sup> ions from aqueous dispersions of hectorite. The exchange reaction may be schmatically represented by Equation (39), wherein the heavy lines represent the negatively charged silicate layers with a thickness of ~9.6 Å:

$$\frac{\text{M(chel)}_{3}^{2+}}{\text{No}^{+}} \qquad \frac{\text{M(chel)}_{3}^{2+}}{\text{(M(chel)}_{3}^{2+})} \sim 8\text{ Å}$$

$$\frac{\text{M(chel)}_{3}^{2+}}{\text{M(chel)}_{3}^{2+}} \sim 8\text{ Å}$$

$$\frac{\text{M(chel)}_{3}^{2+}}{\text{M(chel)}_{3}^{2+}} \sim 8\text{ Å}$$

$$\frac{\text{M(chel)}_{3}^{2+}}{\text{M(chel)}_{3}^{2+}} \sim 8\text{ Å}$$

$$\frac{\text{M(chel)}_{3}^{2+}}{\text{M(chel)}_{3}^{2+}} \sim 8\text{ Å}$$

The exchange reaction, which is quantitative up to the cation exchange capacity (CEC) of the clay and independent of the

counter-anion affords homoionic clay intercalates (Table 1). The values given in the Table are in good agreement with the value expected for a monolayer of intercalated complex. A schematic representation of the ligands used are also given in Fig. (7). Analogous reactions can be observed with other smectite clays such as montmorillonite [40].

The sulfate salts of  $M(\text{chel})_X^{2+}$  complexes will also react with  $Na^+$ -hectorite according to Equation (39), provided that the amount of salt initially present does not exceed the CEC of the mineral. However, if the sulfate salts are present in excess of the CEC, then some of the metal complex will bind to the clay interlayers as  $M(\text{chel})_X^{2+}/SO_4^{2-}$  ion pairs. The intersalation process may be represented schematically by Equation (40).

Analogous intersalates were obtained using other  $XO_4^{2-}$  salts, specifically,  $CrO_4^{2-}$ ,  $MoO_4^{2-}$ ,  $WO_4^{2-}$ , in place of  $SO_4^{2-}$ . Chemical analysis of Ni(phen) $_3^{2+}/SO_4^{2-}$  and  $MoO_4^{2-}$  hectorite indicates the presence of one equivalent of Ni(phen) $_3^{2+}$  to balance the layer charge of the clay and one equivalent as Ni(phen) $_3^{2+}/XO_4^{2-}$  ion pairs. The basal

X-ray Basal Spacing, d(001) of Na<sup>+</sup>-hectorite Exchanged with Different 73 meg/100 gram clay). Complexes (Total Loading is Table 1.

	A princes leses	
Type of Complex	d (001), A	$\Delta d(001)$ , (Å) $b$
$[ni(nH_3)_6]^{2+}$	13.0	3.4
[Ni (en) <sub>3</sub> ] <sup>2+</sup>	13.5	4.9
$[\text{Fe}(\text{TPTZ})_2]^{2+}$	20.0	10.4
[Fe(phen) <sub>3</sub> ] <sup>2+</sup>	17.7	8.1
$[Fe(3,4,7,8-Me_4-phen)_3]^{2+}$	19.0	4.6
[Fe(4,7-diphenyl-phen) $_3$ ] <sup>2+</sup>	20.1	10.5

 $^b$ The Van der Waals thickness for the silicate layers is  $\sim\!\!9.6~\rm{\AA};~\Delta d\,(001)$  is the difference between d(001) for the collapse layers and the intercalate.  $^{\it a}$ The d-spacings are for samples dried at room temperature.

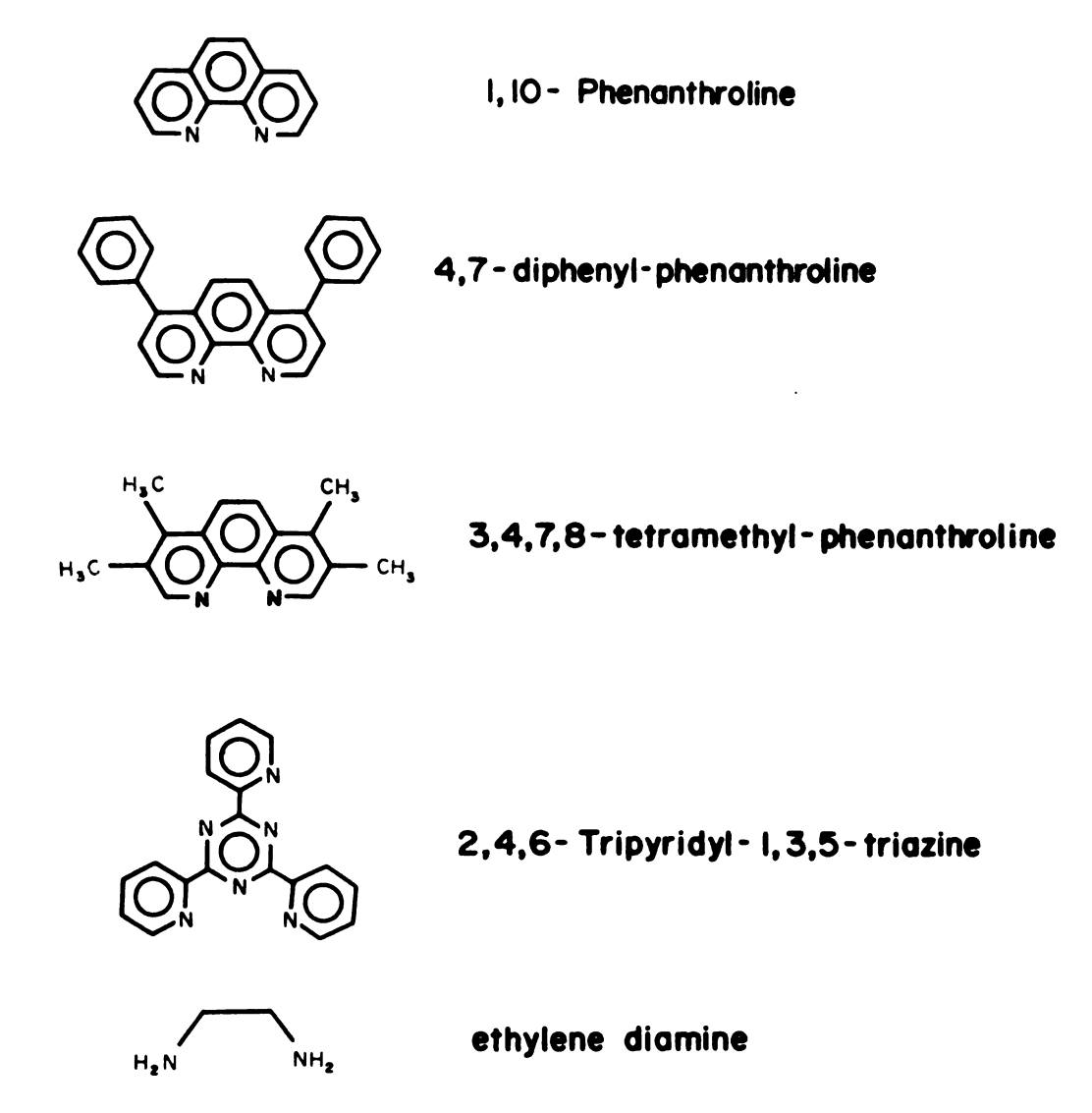


Figure 7 Schematic representation of ethylene diamine, phenanthroline and some of its derivatives and 2,4,6-tripyridyl-1,3,5-triazine ligands.

spacing of these intersalates (Table 2) also suggests the presence of two molecular layers of metal complex cation. Figures (8) and (9) illustrate the 001 X-ray reflections of an oriented film sample of Ni(phen)  $_3^{2+}/xo_4^{2-}$  hectorite. These results are in accordance with the findings of Berkheiser and Mortland [37,40], and Pinnavaia et al. [39,151] where several complexes with different chelated ligands and counter-anions were studied.

The results for M(chel) 3SO intersalates suggest that the stacking of complex cation and  $SO_4^{2-}$  ions in the interlayers is similar to stacking patterns of hydrated  $\text{M(chel)}_{3}\text{SO}_{4}$  salts in the crystalline state, wherein layers of complex cation are separated by layers of hydrated  $SO_4^{2-}$  ions [152,153]. Tanaka et al. [152], in their crystal structure determination of tris-(2,2'-bipyridyl) nickel(II) sulfate hydrate, have shown that the complex cations and hydrated sulfate anions crystallize in alternating sheets. The arrangement of complex ions, sulfate and water of crystallization are shown in Fig. (10). They concluded that the pseudo three-fold axis of the complex is nearly vertical to the (001) plane and each optical isomer ( $\Lambda$  and  $\Delta$ ) is arranged along the a axis in a separate layer occupying almost all the half-cell. In the study of crystal structure of tris-(o-phenanthroline)iron(III) perchlorate hydrate White et al. [153], also concluded that the disposition of the perchlorate anions and tris(o-phenanthroline)iron(III)

Table 2. X-ray Basal Spacing d(001) of Na<sup>+</sup>-Hectorite Exchanged with Different Complex Salts With Loading of 2 Equivalent CEC.

Basal Spacing <sup>a</sup> d(001), (Å)	Δd(001), (Å) <sup>b</sup>
29.1	19.5
29.4	19.8
26.0	16.4
28.5	18.9
28.0	18.4
27.5	17.9
28.5	18.9
29.4	19.8
	29.1 29.4 26.0 28.5 28.0 27.5 28.5

The d-spacings are for air dried samples at room temperature.

<sup>&</sup>lt;sup>b</sup>The van der Waals thickness for the silicate layers is  $\sim 9.6 \text{ A}$ ;  $\Delta d (001)$  is the difference between d (001) for the collapse layers and the intercalate.

Figure 8 001 X-ray reflections (Cu- $k_{\alpha}$ ) for an oriented film sample of Ni(phen) $_3^{2+}/\text{MoO}_4^{2-}$ -hectorite intersalate; d-spacings are given in Angstrom units.

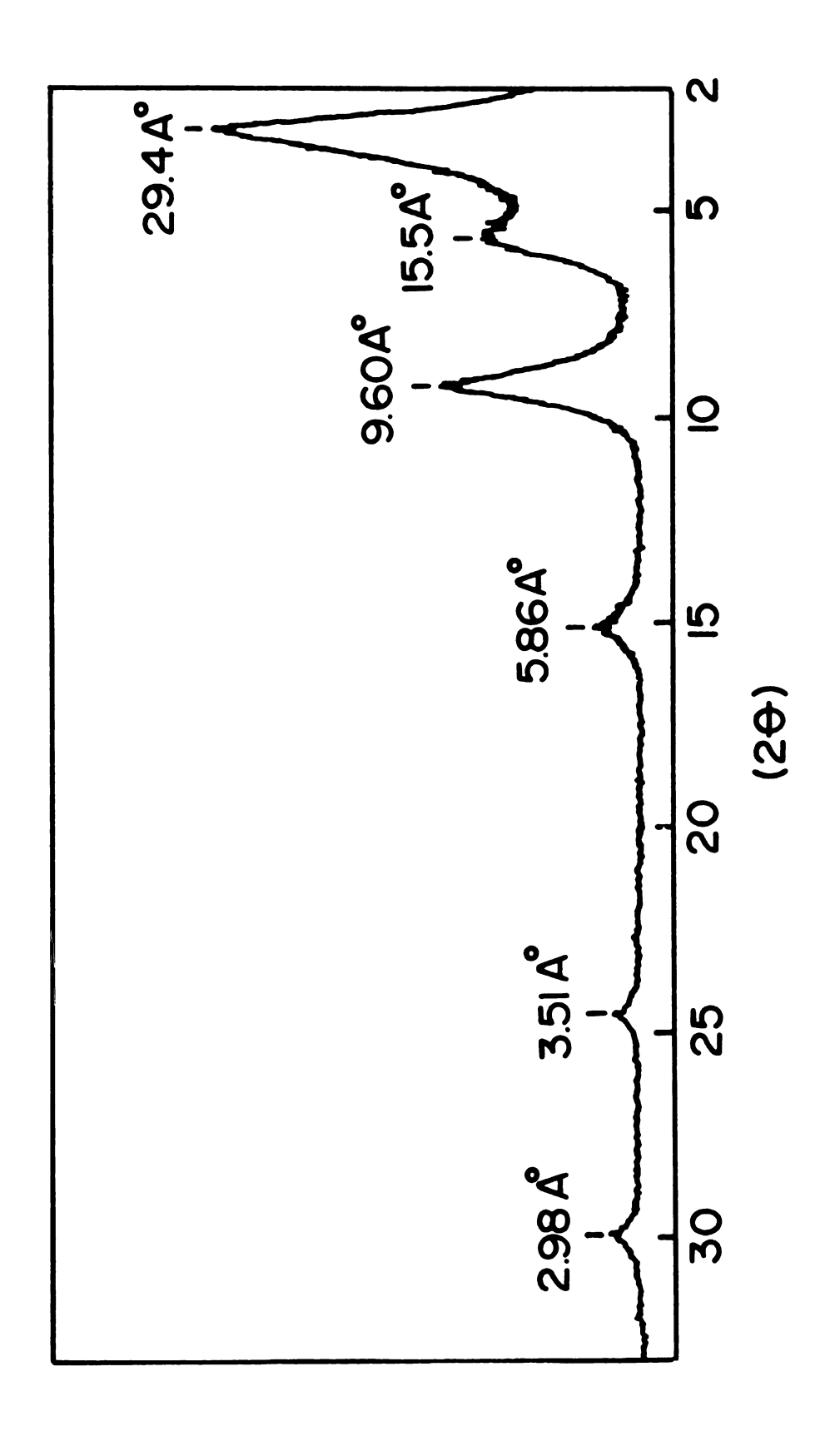
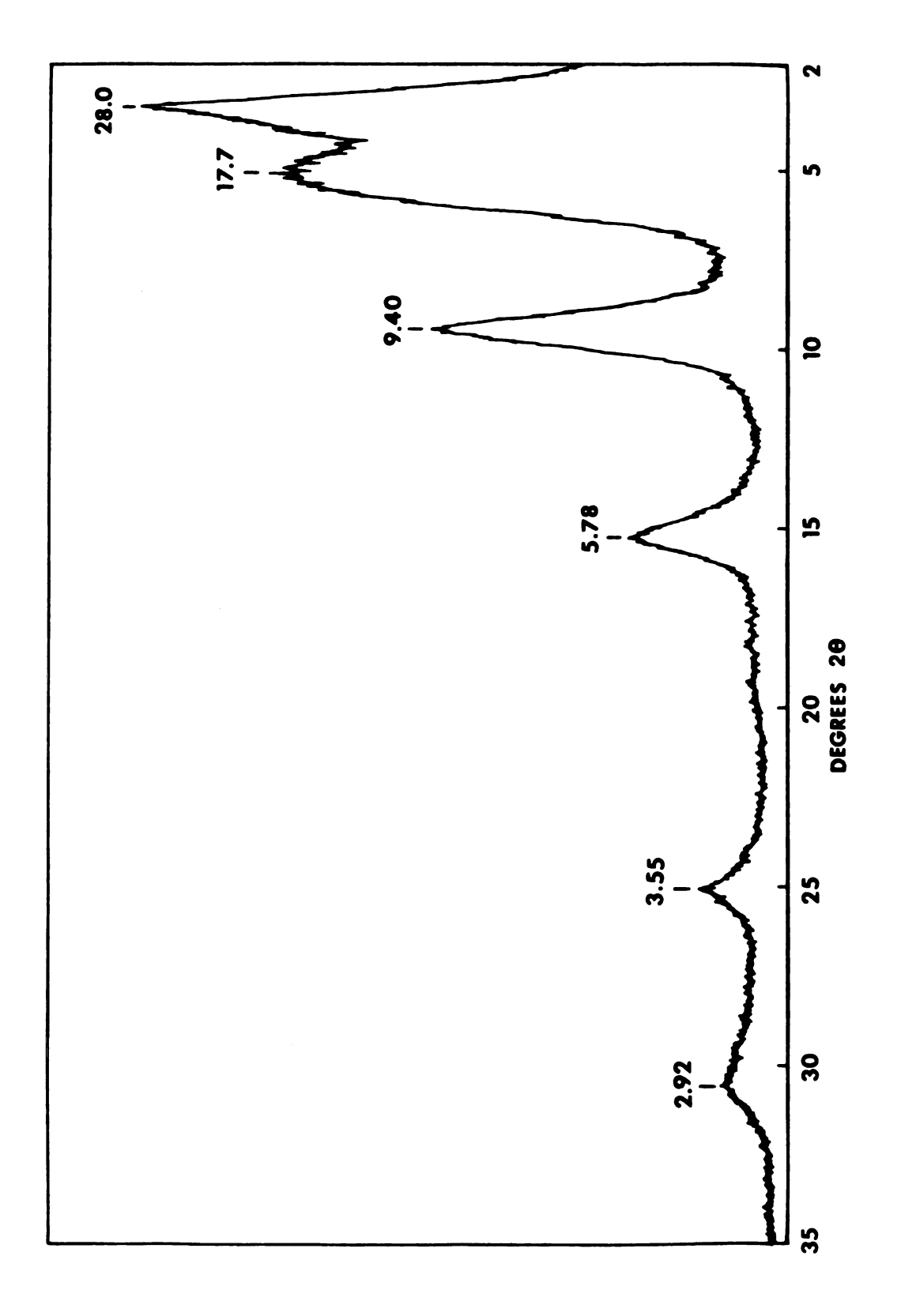
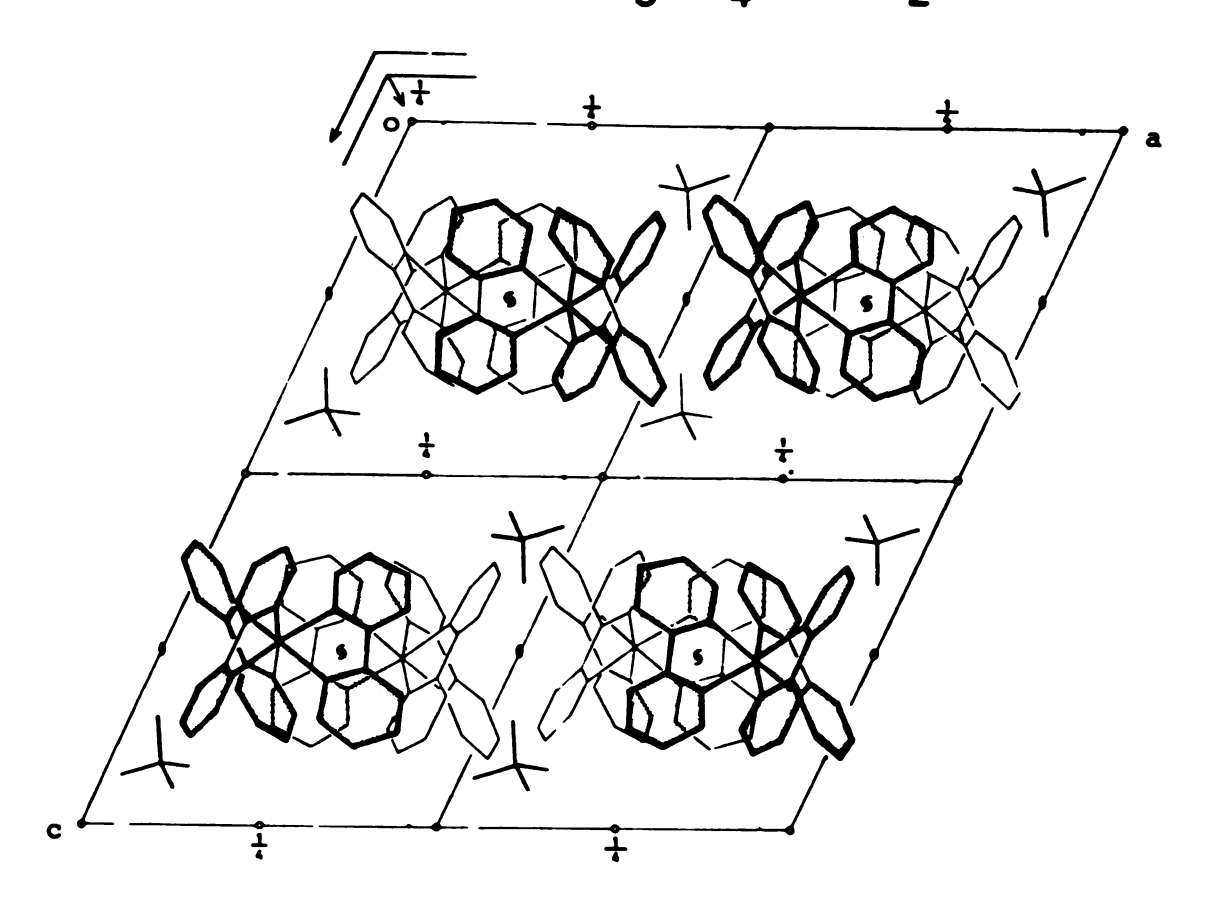


Figure 9 001 X-ray reflections (Cu- $k_{\alpha}$ ) for an oriented film sample of Ni(phen) $_3^{2+}/SO_4^{2-}$ -hectorite intersalate; d-spacings are given in Angstrom units.



# $Ni(bp)_3 SO_4 \cdot 7.5 H_2O$



Wada, Sakabe, Tanaka (1976).

Figure 10 The crystal structure projected along the b axis. Complex ions drawn with heavy lines are lying relatively in a higher part of the unit cell than those drawn with light lines.

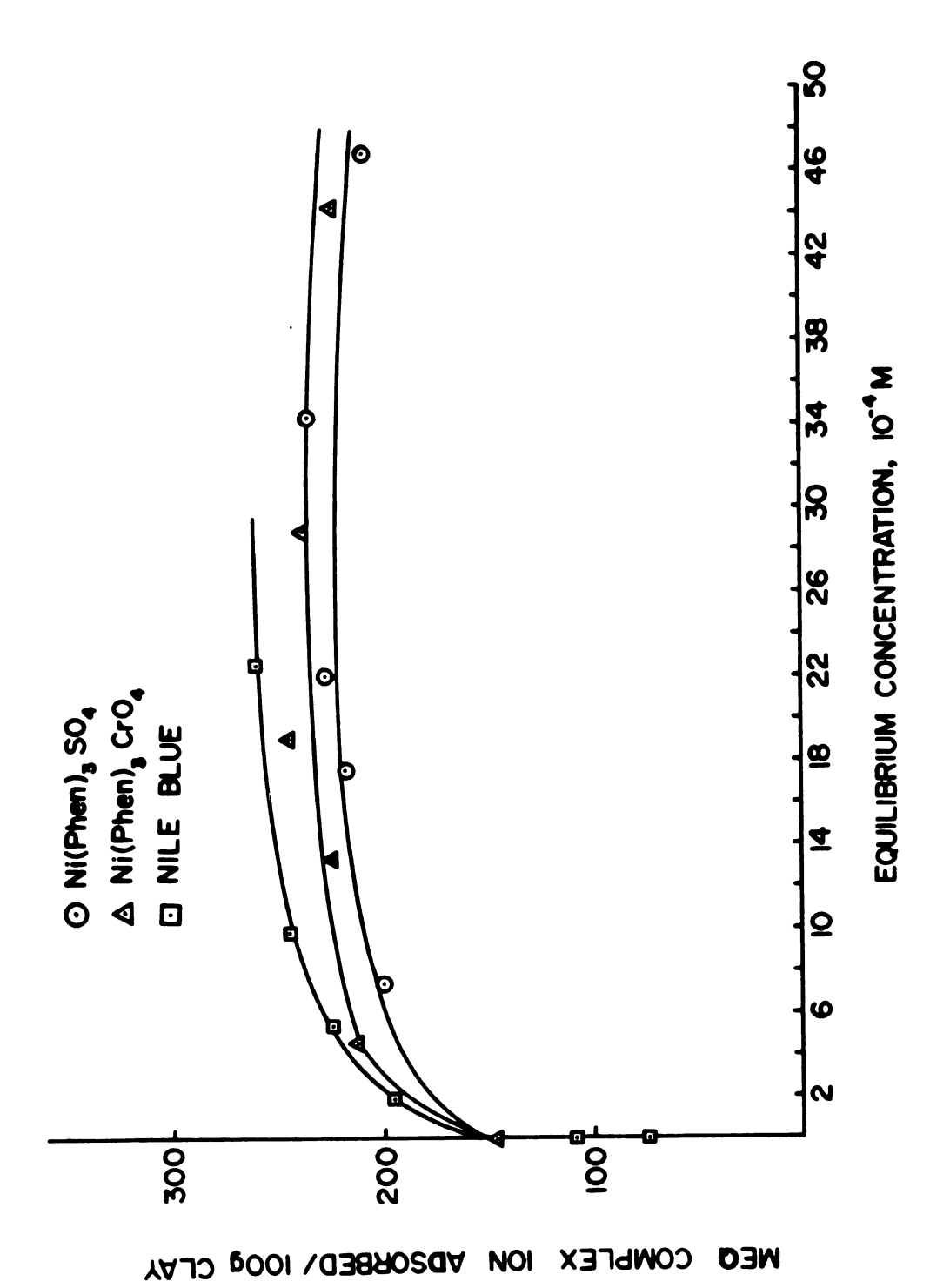
cations within the cell is generally in the form of alternating sheets parallel to the a,b plane. However, unlike the pure salts, the interlayer of the intersalates can be swelled by solvent, and the anions are exchangeable (vide infra).

The adsorption isotherms in Figure (11) demonstrate that Ni(phen)  $_3$ XO $_4$  (XO $_4$ =SO $_4^{2-}$ , CrO $_4^{2-}$ ) have a marked affinity for the surfaces of Na<sup>+</sup>-hectorite in aqueous suspensions. It can be seen that the amount of the metal complex adsorbed exceeds the cation exchange capacity of the mineral (73 meq/100 g). In order to maintain electrical neutrality, the complex ions bound in excess of the exchange capacity must be accompanied by intercalated counterions. The isotherms show several interesting features. In the region between 0 and 146 meq of bound complex per 100 g of hectorite, the slope is vertical, indicating the exchange equilibrium

$$Na^{+}$$
-hectorite + Ni (phen)  $\frac{2+}{3}$   $\rightleftharpoons$  Ni (phen)  $\frac{2+}{3}$ -hectorite + Na<sup>+</sup>
(41)

lies 100% to the right. X-ray diffraction of air dried samples with loadings of 73 meq/100 g (1 CEC) gives  $\sim$ 18 Å basal spacing independent of drying temperature over the range 20-150°C. Space filled models of the complexes show that the cations are approximately 8 Å thick along the  $C_2$  symmetry axis. This observed spacing is consistent

Figure 11 Adsorption isotherms (25°) for [Ni(phen)<sub>3</sub>]SO<sub>4</sub>, [Ni(phen)<sub>3</sub>]CrO<sub>4</sub>, and Nile blue on hectorite in aqueous suspension.



with the value ~8 Å expected for monolyers of complex ions oriented on the surface with their three-fold axis perpendicular to the silicate sheets [39].

In the region between 73 and ~240 meq/100 g, excess salt begins to penetrate the interlayer regions. However, complete double layer intersalation should form at 146 meq/100 g, since the samples with loading of 146 meq/100 g and beyond give ~30 Å basal spacings Fig. (9) due to excess complex salt accommodation in an ordered phase of intersalation.

Additional complex salt is also intersalated at loadings beyond 146 meq/100 g (2 CEC) and this excess complex salt may be accommodated in the surface regions between the coulombically bound monolayers of exchange cations. This extra adsorption (beyond 2 CEC) is dependent on the size of complex and perhaps preferential ion pairing in solution at high concentration of complex salt as well as the solvation properties of the complex. The adsorption isotherm for Nile Blue (Fig. 11) showed results similar to that obtained for Ni (phen)  $_3$ XO $_4$ , except that the amount of complex capable of being intersalated beyond the CEC is slightly more than for the Ni (phen)  $_3$ XO $_4$  systems.

The adsorption isotherms were reproducible within experimental error and the complexes were stable over the course of the investigation with no observable change in the molar absorptivities of the complexes in solution.

Moreover, the intersalates exhibited no diffraction lines

corresponding to the free salt. Therefore all of the bound salt is intersalated.

Despite the highly ordered intersalated phases obtained by adsorption of Ni(phen) 3XO4, the X-ray diffraction patterns of all Ni(phen) 2+/XO4--hectorite [see Figs. (8 and 9)] indicate that the interlayers are interstratified. That is, some layers have spacings which are larger or smaller than the value indicated by the first order reflection. The interstratification can be caused by a nonuniform charge distribution in the silicate sheets or by the irregular distribution of complex salts within the interlamellar space of the smectite. Although the charge heterogeneity was not determined independently in this study, such inhomogeneous charge distribution has been observed previously in smectites [12].

It was observed that the intercalation of excess complex salt was highly dependent on the exchange cation, conditions of solvation, and the swelling of the clay at the time of addition of excess salt [40]. In addition, large quantities of the complex salt were intercalated into a second layer in the interlamellar region of the clay only in the highly expanded smectite, like Na<sup>+</sup>-hectorite or montmorillonite.

# 2. <u>X-ray Diffraction of M(chel)</u> $\frac{2+}{3}$ /XO $\frac{2-}{4}$ -Hectorite

The effects of the complex salt on the d(001) spacings of  $Na^+$ -hectorite are shown in Table (2). One CEC equivalent complex of Ni (phen)  ${}_3XO_A$  resulted in  ${}^\sim18$  Å basal

spacing, while a ~30 Å basal spacing is found for two equivalent CEC of the complex. Intermediate loadings (between 1.4-2 CEC) often resulted in randomly interstratified systems with d(001) values between 18 and 30 Å. Considering the size of  $M(phen)_3^{2+}$  complexes, one may approximate 102 milliequivalents of complex cation per 100 g of clay for a complete monolayer in the interlayer of an expanding clay. Since the cation exchange capacities of Baroid hectorite (73 meg/100 g) and Laponite (55 meg/100 g) are less than the concentration of complex cation needed for monolayer coverage, the 18 Å spacing is sufficient to accommodate all the exchanged complex cations. However, the cation exchange capacity of fluoro-hectorite (193 meg/100 g) exceeds the concentration of cation needed for monolayer coverage; therefore, we would expect at least a partial two-layer coverage, resulting in higher spacings, if all the exchange sites are occupied by complex cation.

X-ray diffraction analysis of Ni(phen) $_3^{2+}/SO_4^{2-}$ -clay with loading of 1 CEC does show a one-layer interlamellar complex, d(001)  $\cong$  18 Å, in natural hectorite and Laponite, but a two-layer complex in fluoro-hectorite, Table (3). At a loadings higher than 2 CEC of the complex salt the basal spacings of clays dried in air at room temperature did not exceed  $\sim$ 30 Å, which is indicative of a two-layer interlamellar complex made up of the exchanged complex cations and excess complex salt. Therefore, quantities

Cation Exchange Capacity and X-ray Basal Spacing, d(001) of Different Clay Exchanged with Ni (phen) $_3$ SO $_4$ . Table 3.

Basal Spacing, d(001), (Å)	18.3	17.9	27.6	18.0
Cation Exchange Capacity of Clay meq/100 g	73	55	193	80
Type of Clay	Natural hectorite (Baroid)	Synthetic hectorite (Laponite)	Synthetic hectorite (fluoro-hectorite)	Natural montmorillonite (Wyoming)

 $^{a}{
m l}$  equivalent of cation exchange capacity of the complex was added to all clays.

of complex salt in excess of that required to produce the two-layer complex was evidently expelled from the interlayers of Na<sup>+</sup>-hectorite upon air drying. Presumably, the excess salt coated the external surfaces of the clay particles. Also, any unintercalated salt used in preparation of the clay complex would exist on the external surfaces of the clay particles upon air drying.

## 3. Anion Effects on $M(chel)_{X}^{2+}$ Adsorption

The differences in the basal spacing between  $Fe(TPTZ)_2(ClO_4)_2$ ,  $Fe(TPTZ)_2SO_4$  and between Ni(phen)<sub>3</sub>Cl<sub>2</sub>, Ni(phen) 3SO<sub>4</sub> shown in Table (4) prompted an examination of anion effects on the intersalation of  $Fe(TPTZ)^{2+}_{2}$  and Ni(phen) $_{3}^{2+}$  salts. The results of Table (4) suggest that the additional binding of a complex cation through the intercalation of salt, is dramatically dependent on the nature of the anion. At all loadings beyond the cation exchange capacity, the Fe(TPTZ) $_{2}^{2+}/(Clo_{4}^{-})_{2}$ -hectorite system exhibits monolayer spacings of 20 Å. Presumably, all of the free salt is expelled from the interlayers upon drying the  $Fe(TPTZ)_2(ClO_4)_2$  system at high loadings. Considering the size of  $Fe(TPTZ)_{2}^{2+}$  complex (longitudinally almost twice as large as  $Fe(phen)_3^{2+}$  complex), one expects that even at loading of 1 equivalent CEC the concentration of the complex cation would exceed the monolayer coverage. Therefore, partial two-layer coverage, with a higher d(001) spacing would be expected. Fe(TPTZ) $_{2}^{2+}$  shows no tendency towards intersalation with hectorite clay when  $Clo_4^-$  was

Table 4. Effect of Ligand, Counteranion and Loading on the d(001) Spacing of Intersalated Hectorites.

Type of Complex	Equivalents of Complex a Salt/Equivalents of Clay	Basal Spacing <sup>b</sup>
Fe(TPTZ) <sub>2</sub> (ClO <sub>4</sub> ) <sub>2</sub>	0.5	20.0
Fe(TPTZ) <sub>2</sub> (ClO <sub>4</sub> ) <sub>2</sub>	1	20.0
Fe(TPTZ) <sub>2</sub> (ClO <sub>4</sub> ) <sub>2</sub>	2	20.0
Fe (TPTZ) $_2$ (ClO $_4$ ) $_2$	15	20.0
Fe(TPTZ) <sub>2</sub> SO <sub>4</sub>	1	20.0
Fe(TPTZ) <sub>2</sub> SO <sub>4</sub>	2	20.0
Fe(TPTZ) <sub>2</sub> SO <sub>4</sub>	15	29.4
Ni(phen) <sub>3</sub> Cl <sub>2</sub>	1	18.0
Ni(phen) <sub>3</sub> Cl <sub>2</sub>	2	20.0
Ni(phen) <sub>3</sub> Cl <sub>2</sub>	5	23.2
Ni(phen) <sub>3</sub> Cl <sub>2</sub>	10	27.6
Ni (phen) 3SO4	1	18.0
Ni(phen) <sub>3</sub> SO <sub>4</sub>	2	29.1
Ni(phen) <sub>3</sub> SO <sub>4</sub>	5	29.3
Ni (phen) 3SO4	10	29.2

Concentration of the salts for reaction with 1 equivalent  $M(chel)_3$  salt is  $1.5 \times 10^{-3} \frac{M}{M}$  (e.g. 0.5 equivalent of  $M(chel)_3$  salt is  $0.75 \times 10^{-3} \frac{M}{M}$  and so on).

ball samples were air dried oriented films.

the counterion. However, when the SO<sub>4</sub><sup>2-</sup> salt was used, the tendency toward intersalation improved and finally at 15 equivalent CEC of the salt a higher d spacing of 29.4 was detected. Nevertheless, the degree of intersalation still was low since very high amounts of salt (15 equivalent CEC and beyond) were needed to detect any change in the d spacing. It is to be noted that Fe(TPTZ)<sub>2</sub>SO<sub>4</sub> at complete two-layer coverage of complex cation should give a d spacing of 34 Å. Therefore, the observed interstratified broad peaks at the highest loading of 15 equivalent CEC would be indicative of partial two-layer coverage with poor ordering (see Fig. 12).

The diffraction pattern for the Ni(phen) $_3^{2+}$  complex show interesting features. When the Cl salt was used the d spacing gradually increased as the amount of salt was increased and, eventually, at 10 equivalent CEC two molecular layers of the complex cation were obtained (Fig. (13)). In contrast, the  $\mathrm{SO}_4^{2-}$  anion is much more effective in ordering two molecular layers of the complex cation. The Ni(phen) $_3\mathrm{SO}_4$  intersalate exhibits 10 orders of reflection with  $\mathrm{d}(001)\cong 30$  Å, at a reaction stoichiometry of only 2 equivalent CEC. Similar results were obtained when  $\mathrm{MoO}_4^{2-}$ ,  $\mathrm{WO}_4^{2-}$  and  $\mathrm{CrO}_4^{2-}$  was used in place of  $\mathrm{SO}_4^{2-}$  counterion.

The qualitative order for intercalation of the anions correlates well with the anion binding selectivity reported by Pinnavaia et al. [39].

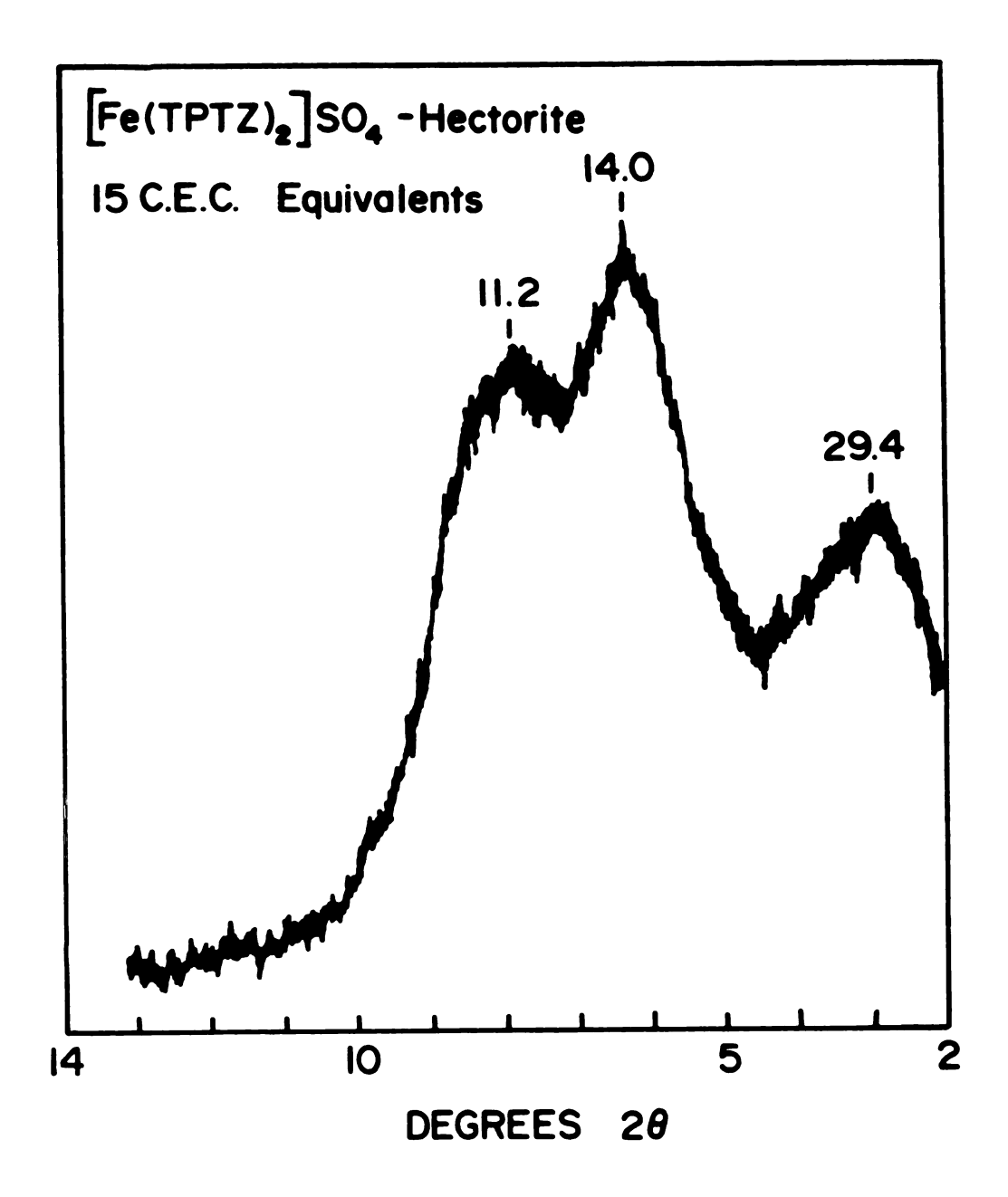


Figure 12 X-ray diffraction pattern of Fe(TPTZ) $_2^{2+}/SO_4^{2-}$  hectorite prepared by addition of 15 equivalent CEC of the complex to Na<sup>+</sup>-hectorite.

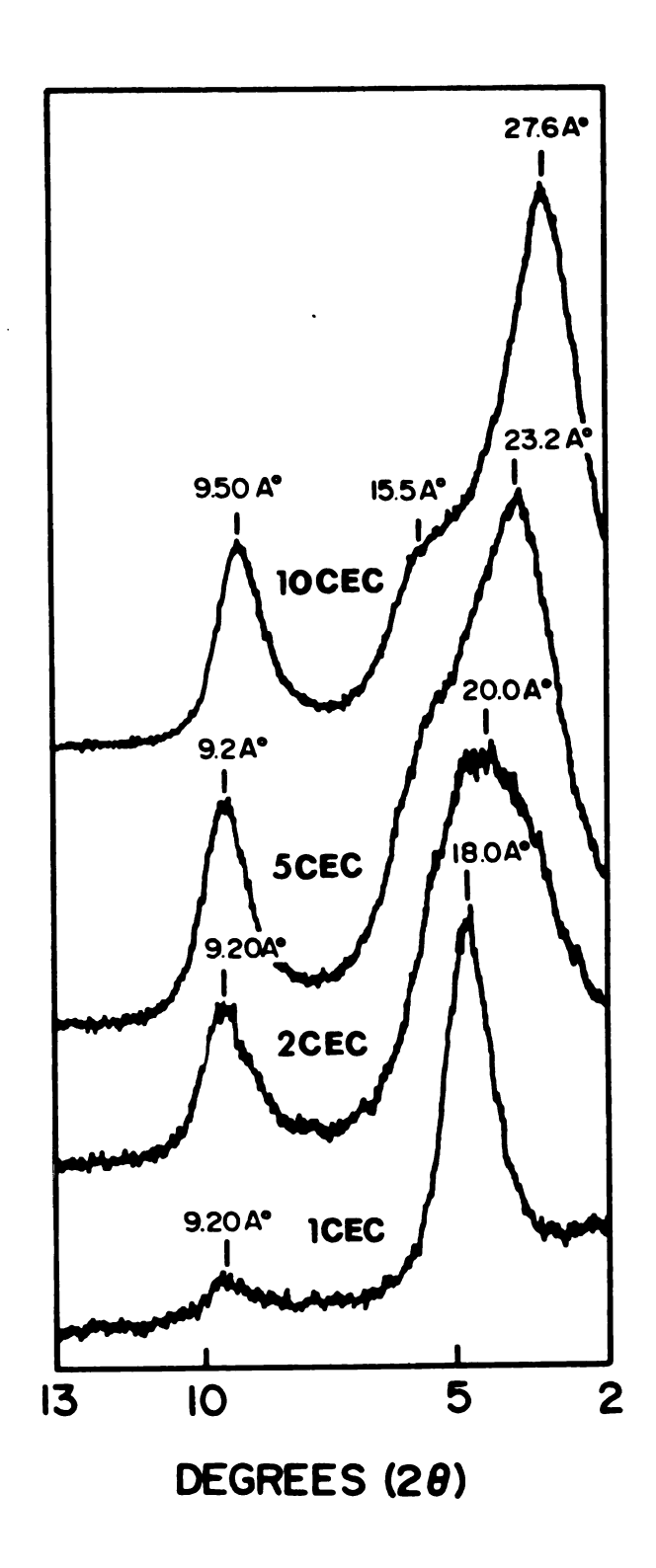


Figure 13 X-ray diffraction patterns of 10,5,2, and 1 CEC equivalents of Ni(phen) $\frac{2+}{3}/Cl_2^-$  hectorite.

# 4. Effects of Ligand on M(chel) 2+ Adsorption

Complex cations of different size and shape were prepared by using various ligands. Basal spacings of the homoionic intercalated complexes were determined. results are shown in Table (1). The dependence of the basal spacing on the size of the complex cation indicates that the intercalation of larger cations gives rise to a higher basal spacing. Hence it is possible to monitor the basal spacing by selection of an appropriate ligand in a given complex. Fe(TPTZ) $_{2}^{2+}$  is a large cation due to the size of ligand. The intercalation of this iron complex in hectorite does not produce the expected 001 basal spacing, since the longer dimension of the complex (estimated by space filling models) is approximately 18 Å, it is possible that the complex is oriented parallel to the silicate layers. Attempts at explaining the basal spacings by rearrangement of the cations are qualitatively illustrated in Fig. (14).

In addition, Fe(TPTZ)<sub>2</sub>SO<sub>4</sub> and Fe(phen)<sub>3</sub>SO<sub>4</sub> are different only in the type of ligand. Due to the larger size of TPTZ, a more efficient layer screening effect is expected. However, the experimental data show that the Fe(TPTZ)<sub>2</sub>SO<sub>4</sub> complex has little tendency toward intersalation. Very poor ordering is observed when Fe(TPTZ)<sub>2</sub>SO<sub>4</sub> is intercalated in hectorite (see Table 4 and Fig. 12), while Fe(phen)<sub>3</sub>SO<sub>4</sub> readily forms a well-ordered intersalation (see Fig. 9). Perhaps the dominant factor here is

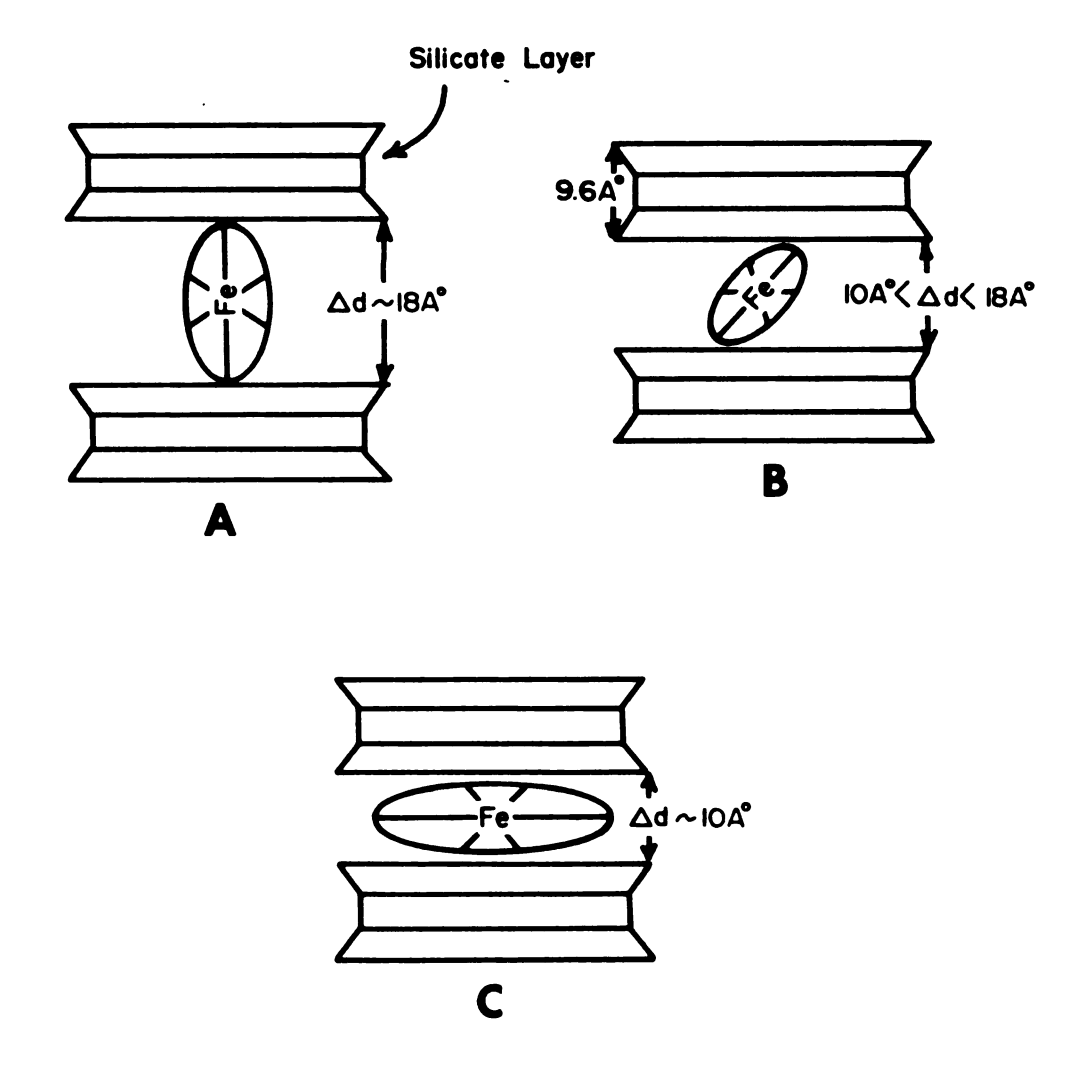


Figure 14 Possible orientations of the Fe(TPTZ)<sup>2+</sup> ion on the surface of Na<sup>+</sup>-hectorite: A) The complex cation oriented perpendicular to the silicate layers. B) Tilted orientation.

C) The complex cation oriented parallel to the silicate layers.

the effective cationic charge. In the case of  $Fe(TPTZ)_{2}^{2+}$  the positive charge is spread over a larger molecule in comparison with  $Fe(phen)_{3}^{2+}$ .

These results show that the intersalation process depends upon not only the nature of the anion but also on the type of the chelating ligand. As previously mentioned, it is believed that the screening of the electrostatic charge of the clay by the complex cation permits the penetration of more complex cation and its anion into the interlamellar regions. However, the screening of the electrostatic charge of the silicate layer seems to be very much dependent upon the size, shape and the charge of the cationic complex. Therefore ligands play an important role in the intersalation reaction, as they are responsible for this screening effect. Simple inorganic salts or a complex like Ni(NH<sub>3</sub>)<sub>6</sub>SO<sub>4</sub> do not behave in this manner.

Phenanthroline derivatives 3,4,7,8-tetramethyl phenanthroline and 4,7-diphenylphenanthroline both are larger than the phenanthroline molecule. Basal spacings for the homoionic intercalation compounds are 19.0 and 20.1 Å respectively (see Table 1). In most cases the 2 CEC intersalation complexes of the sulfate salts give more or less the same basal spacings as the Fe(phen)<sub>3</sub>SO<sub>4</sub> intersalate (~30 Å). The reason may be explained by the charge distribution over a bigger molecule which may

lower the interlayer ordering and therefore lowers the d spacings.

#### 5. Electronic Spectra

An indication of the retention of chemical and structural constitution of all chelated complexes used in triphase catalysis (see Section B) upon intercalation were provided by an electronic spectral study. The spectrum of  $Ni(phen)\frac{2+}{3}/SO_4^{2-}$ -hectorite could not be obtained because of low absorption.

From the extensive investigations [154-157] of the spectra of the ortho-phenanthroline complexes formed by iron, it has been concluded that the intense absorption bands of these compounds in the visible region (Fig. 15) are due to the transfer of electronic charge between the d-orbitals of the metal ion and the  $\pi$ -orbitals of the ligands. The intensity of the visible absorptions implies that charge-transfer configurations make an important contribution to the electronic ground state of these complexes [158,159]. That is, there is appreciable  $\pi$ electron exchange between the cubic t2g metal d-orbitals and the  $\pi$ -orbitals of the ligands. The small shift toward lower energy for  $\boldsymbol{\lambda}_{\text{max}}$  between the pure complex in aqueous solution and the intercalated complexes can be attributed to the change in the silicate layer environment. Thus, the spectral studies indicate that the chelated complexes retain their constitution in the intercalated state.

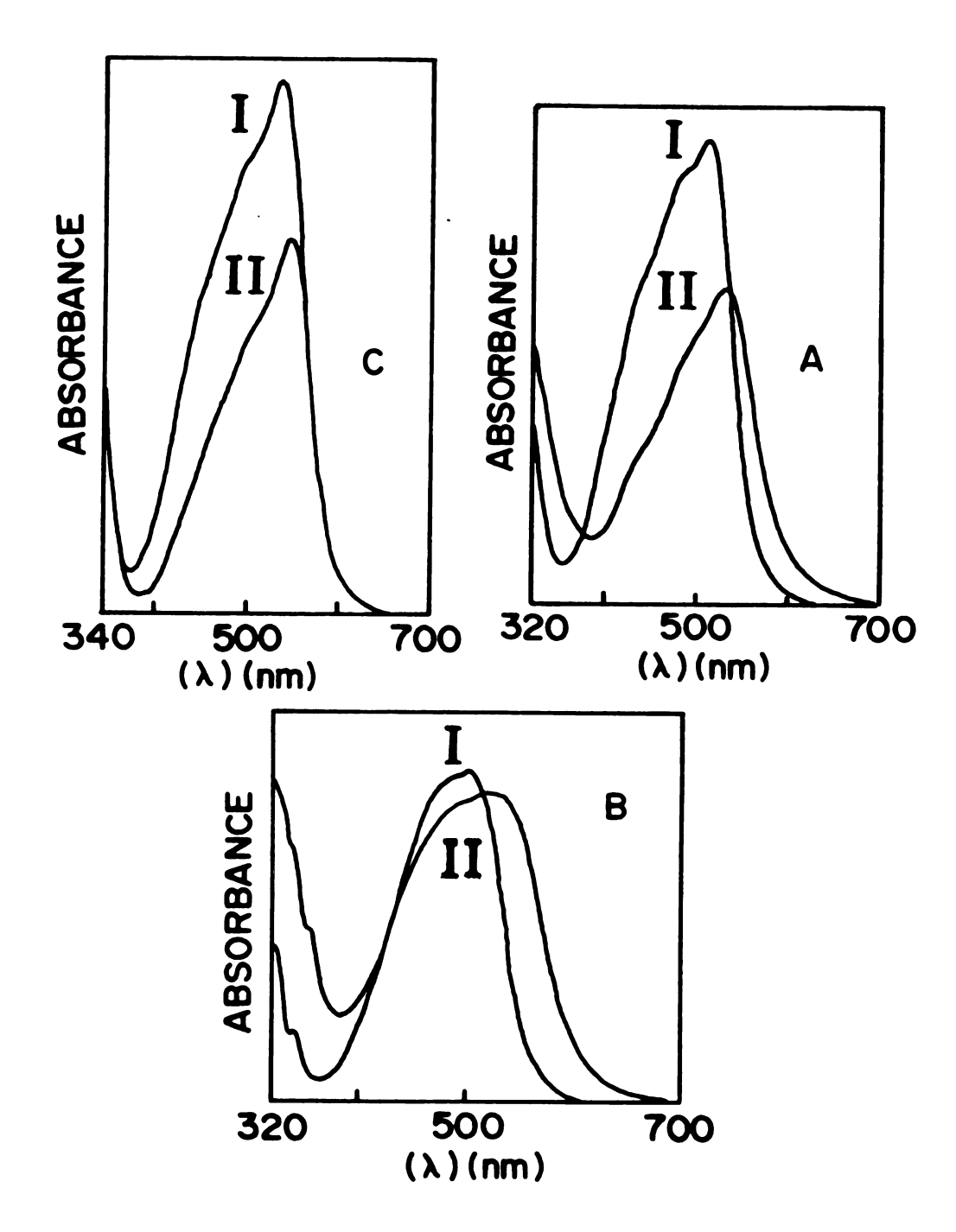


Figure 15 UV-visible spectra of A) [Fe(phen)<sub>3</sub>]SO<sub>4</sub>,
B) [Fe(3,4,7,8-Me<sub>4</sub>-phen)]SO<sub>4</sub>, and C) [Fe(4,7-diphenyl-phen)<sub>3</sub>]SO<sub>4</sub>· in I—aqueous solution and II—Na<sup>+</sup>-hectorite intercalated with these complexes.

#### 6. Adsorption of Organic Salts

Compounds 1-5 were studied with the aim of elucidating the behavior of intercalated organic salts in smectite as triphase catalysis.

$$\begin{bmatrix} \begin{bmatrix} - & \text{CH}_3 & \text{CH}_2 \\ & & \text{CH}_3 \end{bmatrix} & \begin{bmatrix} \text{CH}_2 & \text{CH}_2 \\ & & \text{CH}_3 \end{bmatrix} & \text{CH}_2 & \text{CH}_2 \end{bmatrix} = \begin{bmatrix} \text{CH}_3 & \text{CH}_2 \\ & & \text{CH}_3 \end{bmatrix}$$
(2)

$$\begin{bmatrix} (c_{2}n_{3})^{\frac{1}{2}} & \cdots & \cdots \\ (5) \end{bmatrix}$$

The above organic salts were intercalated at the 1 and 2 equivalent CEC level. For compounds 1-3 X-ray diffraction patterns showed one strong (001) peak, presumably first order, but the higher order reflections were very weak. Moreover, increasing the loading from 1 CEC to 2 CEC organic salts resulted in small change in d spacings (Table 5). In the case of compounds 4 and 5,  $\Delta d$  was increased two-fold and higher order of diffraction

X-ray Basal Spacing, d(001) for Na +-Hectorite Exchanged with Different Table 5.

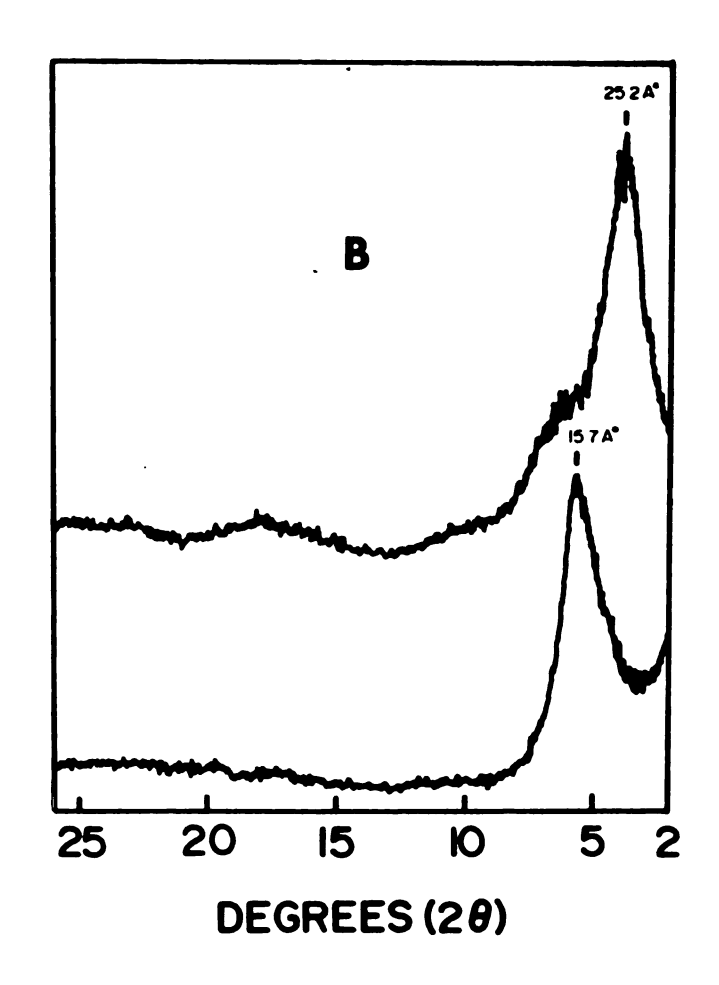
Exchanged with Different $a$	d(001) for 2 CEC (Å)	20.6	23.2	16.9	25.0	27.6	
Organic Molecules (at 1 and 2 CEC Exchange Level). $^a$	d(001) for 1 CEC (Å)	20.6	20.1	14.2	15.7	16.7	
Organic Molecul	Compound Number	1	2	3	4	ហ	

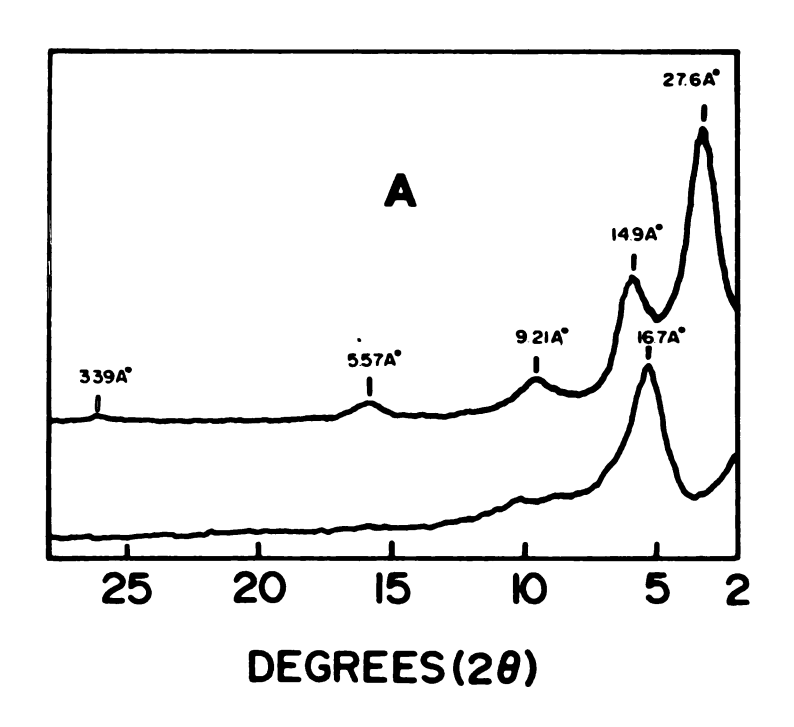
 $^{\it a}$ All samples were in the form of films on a glass slide and air dried at room temperature before the measurements.

were pronounced. In fact, these organic salts in smectite clays, when intercalated behave much like the chelated metal complexes discussed earlier. Although no information was obtained about the orientation of the organic molecules in the clay, the two-fold increase in Ad may be indicative of an ordered double layer of cation/anion pairs. For example, Fig. (16) illustrates the basal spacing for 1 and 2 equivalents CEC intercalation of compound 4 and 5. The X-ray diffraction pattern of compound 5 at 2 CEC loading is well ordered, while compound 4 shows less ordering. The ordering was not improved when the intersalation reaction of compound 4 was repeated in the presence of excess sulfate anion. Perhaps the charges cannot be adjusted to the surface charge patterns in the hectorite, as with 5, when  $SO_A^{2-}$ anion is introduced.

The basal spacings of 1 CEC and 2 CEC hectorite cetylpyridinium complex (1) were determined and in both cases a value of 20.6 Å was observed, [see Table (5)]. It is difficult to interpret these spacings in terms of the orientation of the molecule at the surface. For example, for monolayer coverage of compound 1, the molecule should give d(001) = 14 Å, as suggested by Greenland et al. [160]. These workers also concluded that higher spacings like 21 Å for 1 CEC intercalates perhaps is due to interstratified systems containing varying

Figure 16 X-ray diffraction patterns of 1 and 2 CEC equivalents of A) Nile bue and B) 3,3-(4-4'-biphenylene-bis-(2,5-diphenyl-2H-tetrazolium chloride)-hectorite.





proportions of the one layer (d(001) = 14 Å), two layer (d(001) = 18 Å) and three layer (d(001) = 22 Å) complexes. The basal spacing of 20.6 Å corresponds to an interlamellar separation of 11.0 Å and an interlamellar volume of approximately  $8.2 \times 10^{25} \text{ Å}^3$  per 100 g (the surface area of Na<sup>+</sup>-hectorite = 750 m<sup>2</sup>/g). This volume can accommodate approximately 286 meq of cetylpyridinium ions (volume of one cetylpyridinium ion taken to be  $470 \text{ Å}^3$ ). It is to be expected, therefore, that complexes containing less than this quantity of the cetylpyridinium compound should show no change in d spacing.

Intercalation of compound 2 also showed no significant change in basal spacing at loading of 73 and 146 meg /100 g (see Table 5). Also, the organic salt was intercalated in the presence of excess  $SO_4^{2-}$  anion, to examine the effect of counter-anion. No change was observed in the d spacing, suggesting that perhaps the adsorption here is due primarily to van der Waals forces. Therefore, the intersalation reaction is not dependent on the nature of the counter-anion. The high spacing observed for this organic molecule may be indicative of a more or less vertical orientation of the molecule in the interlayer surfaces, which is not uncommon in molecules with aliphatic chain.

In an attempt to minimize the desorption of salt from the clay interlayers, the intercalation of a chain-like macromolecule (polybrene) was examined. Since the

intersalates are used for catalytic reactions, desorption of the catalyst from the interlayer is undesirable (see Sections A-5 and B-1).

When polybrene (3) was intercalated at a loading of 1 and 2 CEC level, a difference of 2.7 Å in 001 spacing was observed (see Table 5). It is interesting to note that when 2 CEC phase was equilibrated in de-ionized water for several hours no changes in d spacing was detected.

Lagaly et al. [161] concluded that the ionene  $[-N^-](CH_2)_x]_n$  chains are adsorbed in the interlayers completely in trains. The rate of desorption should be very low and the probability that all of the adsorbed segments can be simultaneously detached from the surface is small. In addition, the translational entropy gained by the system provides the driving force for the strong attachment of the polymer to the surface. However, due to the complexity of the system more study is required to explore the details of anion adsorption.

All organic salts (1-5) were checked by IR spectroscopy for retention of structural constitution after intercalation with hectorite clay. The spectra showed absorption bands characteristic of the authentic molecules.

### 7. Desorption Coefficient Measurement

Several intersalated phases have been examined for the desorption of complex salt from the interlayer when they were equilibrated in ethanol and water as a solvent. After equilibration for 48 hours no significant loss of the complex salts was observed. The desorption coefficient (Table 6) shows that the binding of  $M(chel)_3^{2+}/XO_4^{2-}$  ion pairs to the clay interlayers is quite strong. For example, the coefficient for desorption of  $Fe(phen)_3^{2+}/SO_4^{2-}$  from the two-CEC hectorite intersalate in water at  $20^{\circ}C$  is  $8.2 \times 10^{-10}$  moles $^2/liter^2$ . The desorption coefficients for  $Fe(phen)_3SO_4$  and  $Fe(3,4,7,8-Me_4-phen)_3SO_4$  are even smaller in nonaqueous media (see Table 6).

Fe(4,7-diphenyl-phen)<sub>3</sub>SO<sub>A</sub> has a higher desorption coefficient in ethanol and this is because the complex is more soluble in ethanol than water. However, a very low coefficient for desorption of this complex was observed in aqueous media, i.e.,  $5.2 \times 10^{-13}$  moles<sup>2</sup>/liter<sup>2</sup>, at 25°C. Thus intercalated complex salts are about as soluble as barium sulfate, silver chloride, or calcium carbonate which they have solubility product of  $1.08 \times 10^{-10}$ ,  $1.56 \times 10^{-10}$ , and  $8.7 \times 10^{-9}$  moles<sup>2</sup>/liter<sup>2</sup> at 25°C respectively. This result is somewhat misleading, however, because the desorption coefficient depends strongly on the M(chel) $_{3}^{2+}/XO_{4}^{2-}$  loading of the intersalate. As the loading decreases, the desorption coefficient increases. Consequently, the intersalate can be converted to homoionic  $M(chel)_3^{2+}$ -hectorite by washing the compound a finite number of times with water.

Desorption Coefficient for 2 CEC Hectorite Intersalation Complexes. Desorption Coefficient Moles<sup>2</sup>/liter<sup>2</sup>  $6.0 \times 10^{-10}$  $4.2 \times 10^{-10}$  $8.2 \times 10^{-10}$  $5.2 \times 10^{-13}$  $7.1 \times 10^{-10}$ 5.7 × 10<sup>-11</sup> Solvent Etoh Eton Etoh  $H_2^0$ H<sub>2</sub>0 H<sub>2</sub>0 Fe (4,7-diphenyl-phen) $_3$ SO $_4$ Fe  $(3,4,7,8,-Me_4-phen)_3SO_4$ Fe (4,7-diphenyl-phen) $_3$ SO $_4$ Fe(3,4,7,8-Me<sub>4</sub>-phen) $_3$ SO<sub>4</sub> Type of Complex Fe (phen)  $_3$ SO $_4$ Fe (phen)  $_3^{SO}_4$ Table 6.

### 8. Anion Exchange Properties of Smectite Intersalates

Significantly, the intercalated  $XO_A^{2-}$  ions in the smectite intersalates can be readily exchanged at room temperature with a variety of other  $XO_4^{2-}$  ions and, in part, with singly charged anions such as halide and some organic anions. The adsorption isotherms were obtained for the exchange of  $Cro_A^{2-}$  in the parent intercalation compounds by inorganic, organic, and complex anions of differing size, shape and symmetry. Figure (17) illustrates the exchange isotherms for replacement of  $CrO_A^{2-}$  in Ni (phen)  $_{3}^{2+}/\text{CrO}_{4}^{2-}$ -hectorite by  $\text{MoO}_{4}^{2-}$ ,  $\text{WO}_{4}^{2-}$ ,  $\text{PO}_{4}^{3-}$ ,  $\text{Cr}(\text{OX})_{3}^{3-}$ ,  $Cl^{-}$ ,  $CH_3CO_2^{-}$  and  $C_6H_5-COO^{-}$  ions. The adsorption isotherms were measured by quantitative analysis of  $Cro_4^{2-}$  ion replaced by the incoming anion. Almost all of the intercalated  $CrO_4^{2-}$  (~43 meq/100 g of intersalate) is replaced by anions with a charge greater than unity at an equilibrium concentration of  $6 \times 10^{-4}$  M. PO<sub>A</sub><sup>3</sup> anion replaces  $CrO_4^{2-}$  almost entirely perhaps due to the higher charge of the phosphate anion, however,  $Cr(OX)_3^{3-}$  anion replaces  $CrO_4^{2-}$  at a lower level, maybe due to its larger size. The difference between  $MoO_4^{2-}$  and  $WO_4^{2-}$  ion in the isotherm is not understood, since both have the same charge and the size difference is negligible. Though the binding of  $CrO_A^{2-}$  is favored over chloride and benzoate, a significant fraction of the  $\operatorname{CrO}_4^{2-}$  can be replaced by these latter ions at relatively low equilibrium concentrations. Among the exchange ions investigated, acetate

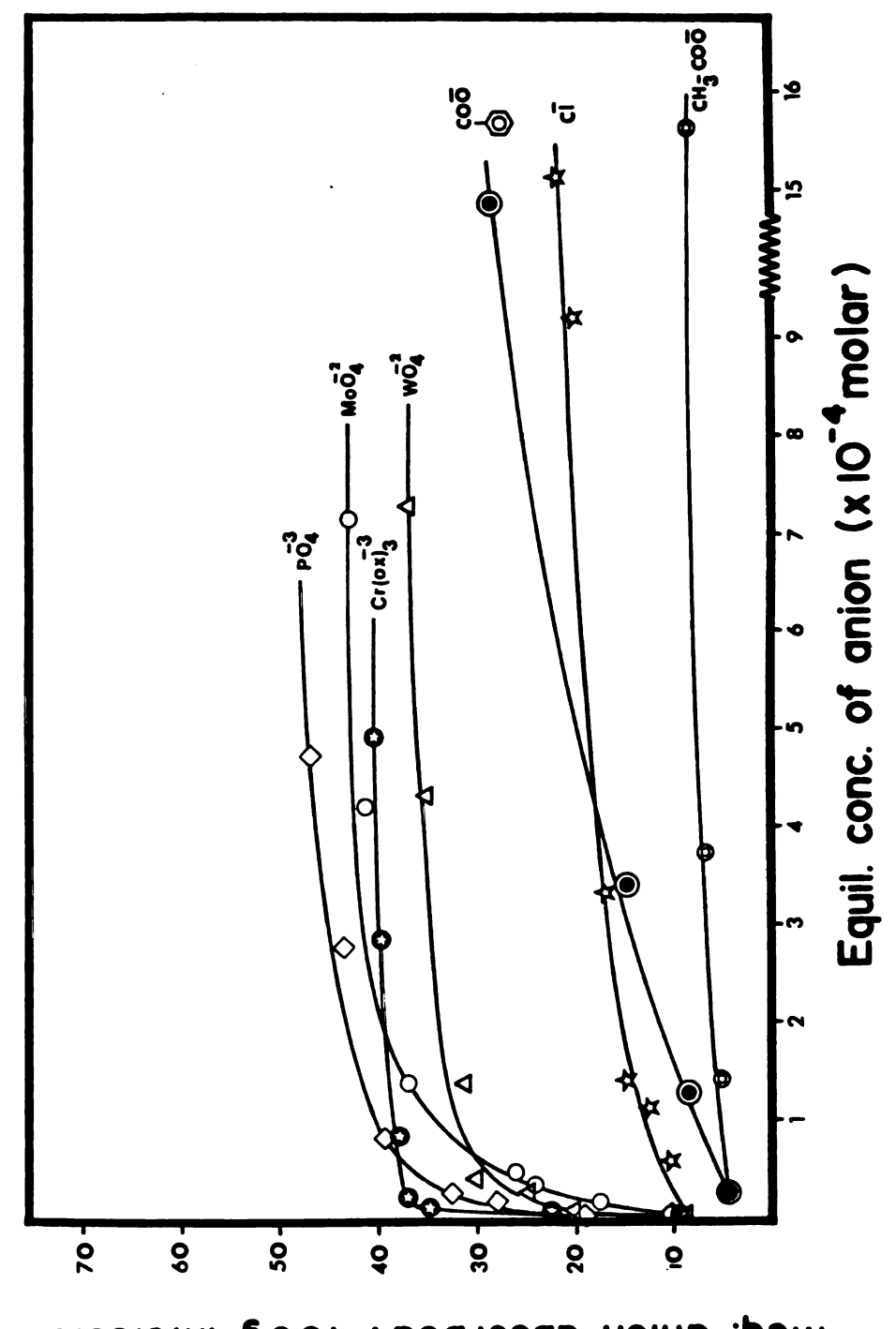
has the lowest affinity for replacing intercalated  $\text{CrO}_4^{2-}$ . The adsorption isotherms [see Fig. (17)] demonstrate that hectorite intersalates in fact do act as anion exchangers and in many cases the amounts of anion replaced is very close to the calculated value for the anion exchange capacity (AEC) of the clay intersalates.

As can be seen from the isotherms, the greatest tendency for anion exchange reactions occurs for anions with higher charge. The adsorption isotherms for anions with charges of -2 and -3 indicate that in the region between zero and 45 meq of adsorbed anion per 100 g of complex-clay the slope is very steep. A steep slope is indicative of an equilibrium displaced far to the right.

$$[M(chel)_{3}^{2+}/Y^{2-}]$$
-hectorite +  $X^{2-} \neq [M(chel)_{3}^{2-}/X^{2-}]$ -hectorite +  $Y^{2-}$ . (42)

X-ray diffraction patterns and d(001) basal spacings are almost unchanged after the anion exchange reaction, indicating that the intersalated phase remains intact during the anion exchange process.

As described earlier, the anion exchange takes place without significant loss of the complex cation, which remains immobilized on the surface. This is important, since the negligible desorption, over long periods of time, is a desirable property, for catalytic activity of the layered silicate intersalates.



Meq. anion absorbed / 100g intersalate

Figure 17 Anion exchange isotherms for Ni(phen) $_3^{2+}/\text{CrO}_4^{2-}$ hectorite intersalate at 25°C.

#### 9. Swelling of the Intersalation Phase

To obtain an indication of the swelling properties of  $M(chel)_{3}^{2+}/SO_{4}^{2-}$ -hectorite, X-ray powder diffraction measurements were carried out under conditions where the interlayers were solvated by the two solvents used in the catalytic studies (see Chapter III). The observed reflections [Fig. (18)] provide a qualitative indication of the extent of interlayer swelling. The position of the first order reflections were as follows: 33 Å (water), 28 Å (toluene). Virtually no swelling occurs with toluene, because the same reflection is observed when no solvent occupies the interlayer regions. Water, however, swells the interlayer region. It can be seen from the figure that the interlayers are interstratified. That is, some layers have spacings which are larger or smaller than the value indicated by the first order reflection. The interstratification can be caused by nonuniform charge distribution among silicate sheets and by the partial segregation of the complex salt. Nevertheless, the observed reflections provide a qualitative indication of the extent of interlayer swelling. In triphase catalysis, one of the liquid phases is water. Since no organic solvent can compete with water in swelling of the clays, the role of substrate in a possible swelling is not significant (see Chapter III-B).

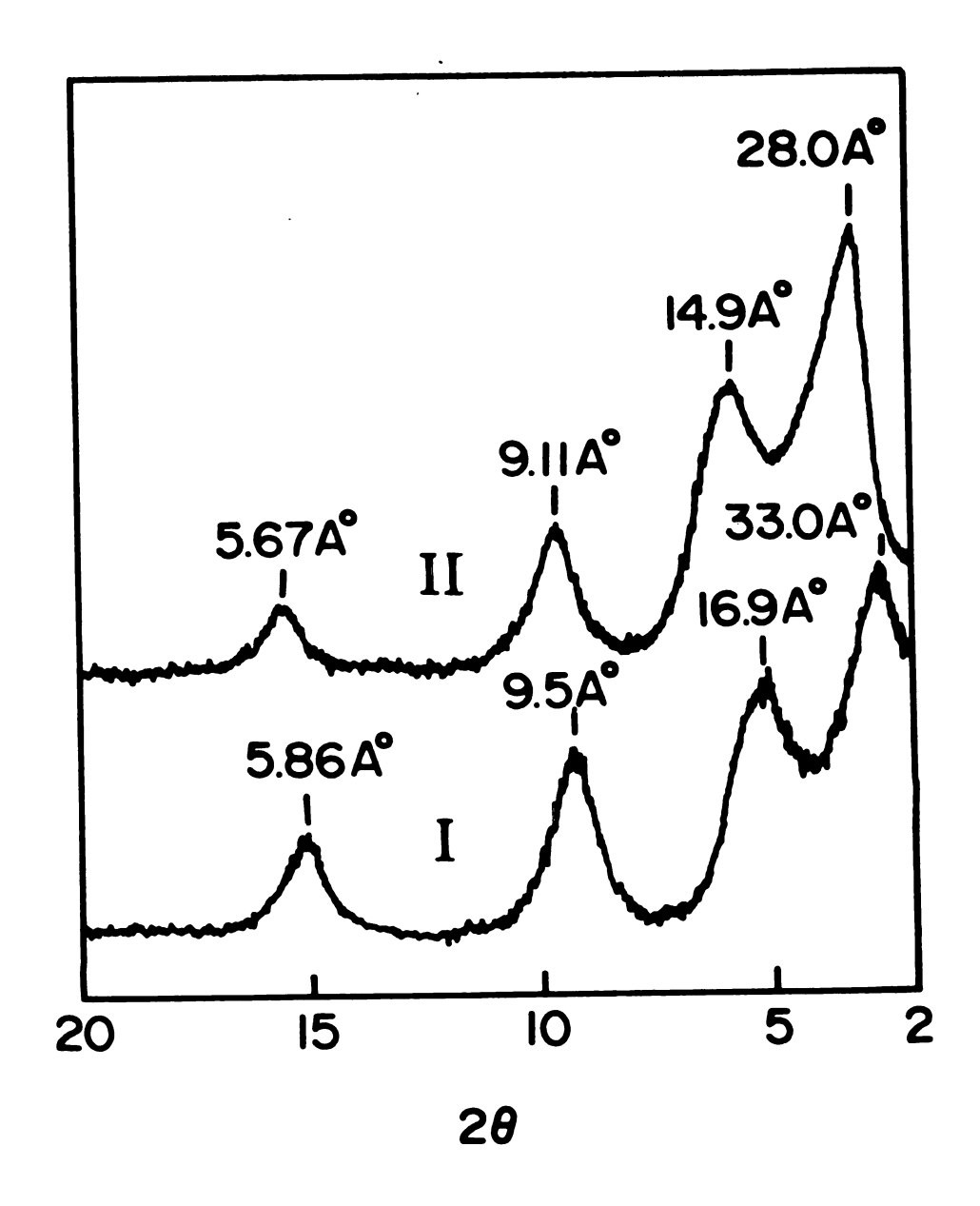


Figure 18 X-ray diffraction pattern for Ni (phen)  $_3^{2+}/SO_4^{2-}$  hectorite intersalates solvated by (I) water and (II) air-dried film.

#### 10. ESR Studies

Paramagnetic cations such as Mn<sup>2+</sup> and Cu<sup>2+</sup> have been utilized as spin probes to characterize the environment of exchangeable cations adsorbed on smectite surfaces [162,163]. A nonrigid, solution like interlayer was observed under certain conditions. This observation led to the supporting of homogeneous rhodium phosphine complexes in the intercrystal environment, with retention of catalytic activity [131,164].

Also, attempts have been made to relate [165] the mobility of organic exchange cations such as protonated 4-amino-2,2,6,6-tetramethyl piperidine N-oxide on smectites to the extent of dehydration of the smectite. In the present study, electron spin resonance (ESR) investigations of the orientation and mobility of clay intercalated anions under different degrees of relative humidity have been carried out. The anion of Fremy's salt, peroxyl amine disulfonate (PADS) was used as a nitroxide spin probe to examine the rate of tumbling of the exchange anion to determine the diffusion of organic molecules into the intracrystal environment of the The nitroxide spin probes are intersalated system. observed to tumble rapidly enough in aqueous solution at 25°C to average completely anisotropies in q and hyperfine splitting (A) values. The properties of dilute aqueous solution of K<sub>2</sub> (PADS) have been studied and rapid rotational correlation times,  $\tau_p \approx 3 \times 10^{-12}$  sec, have been found [166-169]. Unlike other commonly used nitroxides, [PADS]<sup>2-</sup> has the advantage that its slow motional and rigid spectra are not inhomogeneously broadened by unresolved intramolecular proton dipolar interactions. Also, contributions from intermolecular electron-nuclear dipolar interactions are negligible since the linewidths are the same for H<sub>2</sub>O and D<sub>2</sub>O [166].

 $\operatorname{Zn}(\operatorname{phen})^{2+}_3/\operatorname{SO}^{2-}_4$ -hectorite intersalate (2 equivalent CEC) was synthesized and the nitroxide spin probe is doped into the anion interlayers at about 2% level of exchange, and used to estimate the interlamellar mobility. It has been found that the doping level affects the spectrum of probe adsorbed on clay [30].

It is likely that spin exchange is enhanced by the concentration of probe ions in certain interlamellar regions, a phenomenon of ion segregation (demixing) that is not uncommon. Very low loading levels on the exchange sites (less than 2% of AEC) are therefore preferable to avoid unnecessary line broadening and spin exchange.

The asymmetrical three-line spectrum of the nitroxide spin probe [PADS]<sup>2-</sup> in DMSO solution and, also, its rigid-limit spectrum are shown in Figs. (19) and (20). The spectra of Fig. (21) for PADS <sup>2-</sup>-doped hectorite intersalate demonstrate some loss of rotational mobility on the clay at 98% and 52% relative humidity and on the vacuum dry clay. The anistropic behavior becomes more pronounced as the relative humidity of equilibration is reduced.

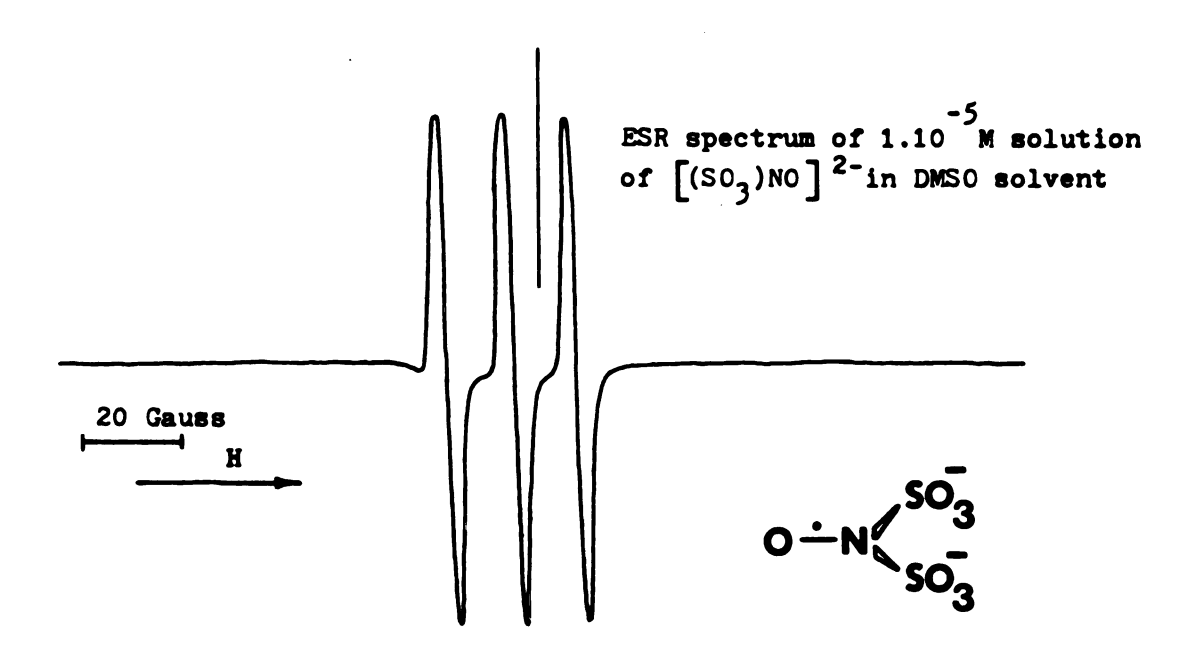


Figure 19 ESR spectrum at  $20^{\circ}\text{C}$  of the nitroxide spin probe, (PADS)<sup>2-</sup>, in DMSO solvent. The vertical line on this spectrum represents the position of g = 2.00.

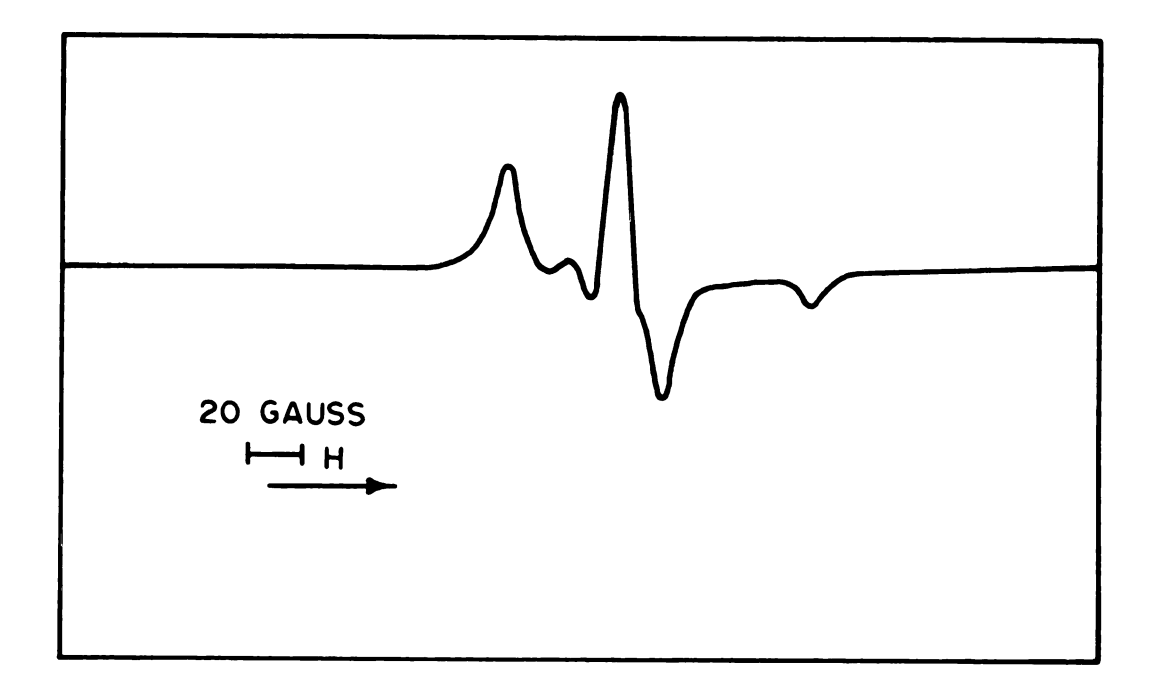


Figure 20 Rigid-limit x-band ESR spectrum of PADS; the field increases to the right.

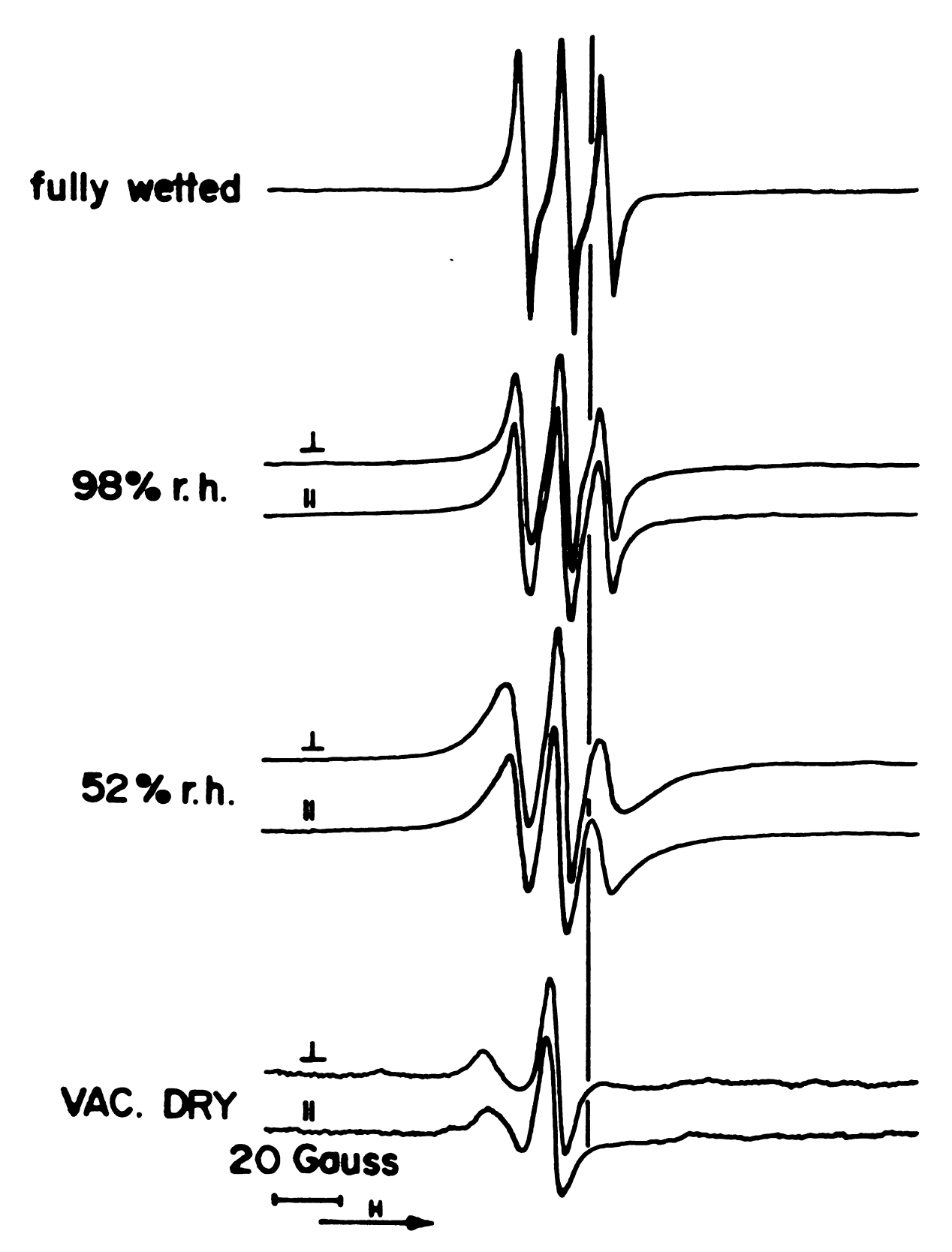


Figure 21 ESR spectra at 20°C of the nitroxide spin probe,  $(PADS)^{2-}$  doped at the 2% exchange level into  $Zn(phen)^{2+}/SO^{2-}_4$ -hectorite at different relative humidity. A free electron signal at g=2.0023 is shown.

The ESR spectra of adsorbed probe reported here do not necessarily reflect interlayer solvent viscosities, since rotational correlation times are modified by specific surface interactions in addition to the properties of the solvent. For example, by using Equations (43) and (44) to estimate  $\tau_c$  for adsorbed [PADS]<sup>2-</sup> under wetted conditions, values of about  $3.85 \times 10^{-10}$  sec. are obtained [see Fig. (21)]. These values are ~100 times lower than the value observed in the aqueous state [166-168]. However, larger values for  $\tau_{c}$  are found for the 1 orientation of the clay films in the magnetic field compared to the | orientation. This is a result of some anisotropic rotation of the probe in the interlayer. In addition, the variation in  $\tau_{c}$  values for samples with different relative humidities can be related to the interlamellar space limitation. The resulting basal spacing suggest that increasing the relative humidity gives the anion more room to move much faster (Table 7). Under fully wetted conditions, the X-ray basal spacing is 33 Å which may allow enough space for the [PADS]<sup>2-</sup> molecules to tumble quite rapidly (i.e.  $\sim 3 \times 10^{-10}$  sec) and take on appreciable solution-like properties.

Spectra were analyzed in the simplest possible manner following the approach of Stone et al. [170] in the following form:

Basal d(001) Spacing for (PADS) 2--Exchanged Hectorite Intersalates of Different Relative Humidity.  $^a$ 

Δd(001), (Å) <sup>b</sup>	23.4	21.9	18.0	16.3
Basal Spacing d(001) (Å)	33.0	31.5	27.6	25.9
(%) Relative Humidity	Fully Wetted	86	52	Vac. Dry

 $^b$ The van der Waals thickness for the silicate layers is  $\sim\!\!9.6$  Å;  $\Delta d$ (001) is the difference between d(001) for the collapse layers and the intercalate.  $^a_{\rm z}$  (phen) $_3$  SO $_4$  -hectorite intersalates were doped with ~2% (PADS) $^2$  on the exchange sites.

$$\tau_{C1} = -2211W_0R - /H_0 \tag{43}$$

$$\tau_{c2} = 0.65W_0(R_+-2) \tag{44}$$

$$R_{\pm} = \left[ \left( h_0 / h_{+1} \right)^{\frac{1}{2}} \right] \pm \left[ \left( h_0 / h_{-1} \right)^{\frac{1}{2}} \right] \tag{45}$$

If the difference and sum of  $(h_0/h_{-1})^{\frac{1}{2}}$  and  $(h_0/h_{+1})^{\frac{1}{2}}$ are taken, the above independent equations for the determination of  $\tau_c$  (correlation time) can be obtained —one containing the  $c_1$  term and the other containing the  $\boldsymbol{c}_2$  term. These two estimates of  $\boldsymbol{\tau}_{_{\mathbf{C}}}$  are not generally identical [169].  $\tau_{cl}$  and  $\tau_{c2}$  are correlation (tumbling) times in nanoseconds,  $\mathbf{W}_0$  is the linewidth of the central peak (G), and  $H_{\Omega}$  is the magnetic field (G) corresponding to the central resonance line, where  $h_0$ , +1, -1 = the height of the middle, low, and high field peaks, respectively. The correlation time,  $\boldsymbol{\tau_{_{\mathbf{C}}}}\text{, was taken as}$ the average of  $\tau_{cl}$  and  $\tau_{c2}$ , a procedure which seemed to reduce random error. The equations used to obtain  $\tau_{c}$ are strictly valid only for isotropic rotation, however, they are useful for comparative purposes in studying anisotropic rotation at surfaces [165]. The calculated values of  $\tau_{c}$  are given in Table 8 for the hectorite intersalates at different relative humidity. The values of  $\tau_c$  are in the range of 1-6  $\times$  10<sup>-9</sup> sec, meaning that the tumbling mobility of the [PADS]<sup>2-</sup> is reduced by a factor of 400-1000 when compared with the probe in aqueous solution. But this is relatively rapid motion of spin probes at the surfaces [171].

Table 8. Calculated Rotational Correlation Times (nsec) of PADS<sup>2-</sup> Doped into Zn(phen)<sub>3</sub>SO<sub>4</sub>-Intersalate of Hectorite Clay. <sup>a,b</sup>

	_	orrelati 3 <sup>)</sup> 2 <sup>NO</sup> ] <sup>2-</sup>			
Relative Humitidy of Samples (%r.h.)	$^{\tau}c_{1}$		•	τc <sub>2</sub>	
		10		1_	
98	1.20	1.39	2.92	3.31	
52	1.23	5.15	4.81	11.35	

<sup>&</sup>lt;sup>a</sup>Amount of PADS<sup>2-</sup> doped into the intersalate were % 2 of the A.E.C.

 $<sup>^{</sup>b}$  Self supported film of the intersalate (3 × 12 mm) were made.

 $<sup>^{</sup>c}\|$  and I represent the orientation of the hectorite films to the magnetic field, H.

#### B. Catalytic Properties of the Intersalates

A new type of heterogeneous catalysis termed "triphase catalysis" has recently been introduced [83]. The underlying feature which distinguishes this from other forms of heterogeneous catalysis is that the catalyst and each of the reactants are located in separate phases. This principle has been successfully applied to certain aqueous phase-organic phase reactions employing a solid phase catalyst.

The ease with which  $XO_4^{2-}$  anions can be replaced in  $M(\text{chel})_3^{2-}/XO_4^{2-}$ -hectorite intersalates suggested that these compounds may be effective catalysts in a triphase reaction system involving anionic nucleophiles. Moreover, since the intersalates are well ordered, it was felt that substrate size or shape selectivity might be observed.

In the present work the kinetics of one such triphase catalyzed process was examined in detail. Anions such as halides and carboxylates as well as cyanide function well under triphase catalysis conditions utilizing smectite intersalates for the catalysis. They were found to be efficiently transported to the organic phase by the phase transfer agent and, once there, behave as potent nucleophilic species in a variety of displacement reactions. Several systems were identified in which anions were involved in the displacement reaction of

organic substrate in the presence of different types of layered silicate intersalates. An illustration of the three-phase system is presented in Fig. (22).

#### 1. Kinetics of the Halogen Exchange

Among all available procedures for exchanging halogen in organic halides, only a few have proven to be useful for converting alkyl bromides to alkyl chlorides [172,173]. It was found that the triphase catalysis technique using smectite intersalates furnishes a convenient method for carrying out such transformations. Halogen ion displacement on different n-butyl halides were conducted in 50-mL culture tubes [(Fig. (23)] using procedures described in the Experimental Section. Rates of reactions were monitored by following the disappearance of the starting n-butyl halide from the organic phase. Clean pseudo first-order kinetics were observed and in spite of the inherent complexity of these systems, the reproducibility of observed rate constants,  $k_{obs}$ , were good. Only one type of reaction product was detected. Figure (24) illustrates typical kinetics data. Examples showing the utility of triphase catalyzed halogen exchange are provided in Table (9).

In the classical mechanism of phase-transfer catalysis, the nucleophilic substitution reaction [Equation (46)] occurs in the organic phase and is the rate-determining step.

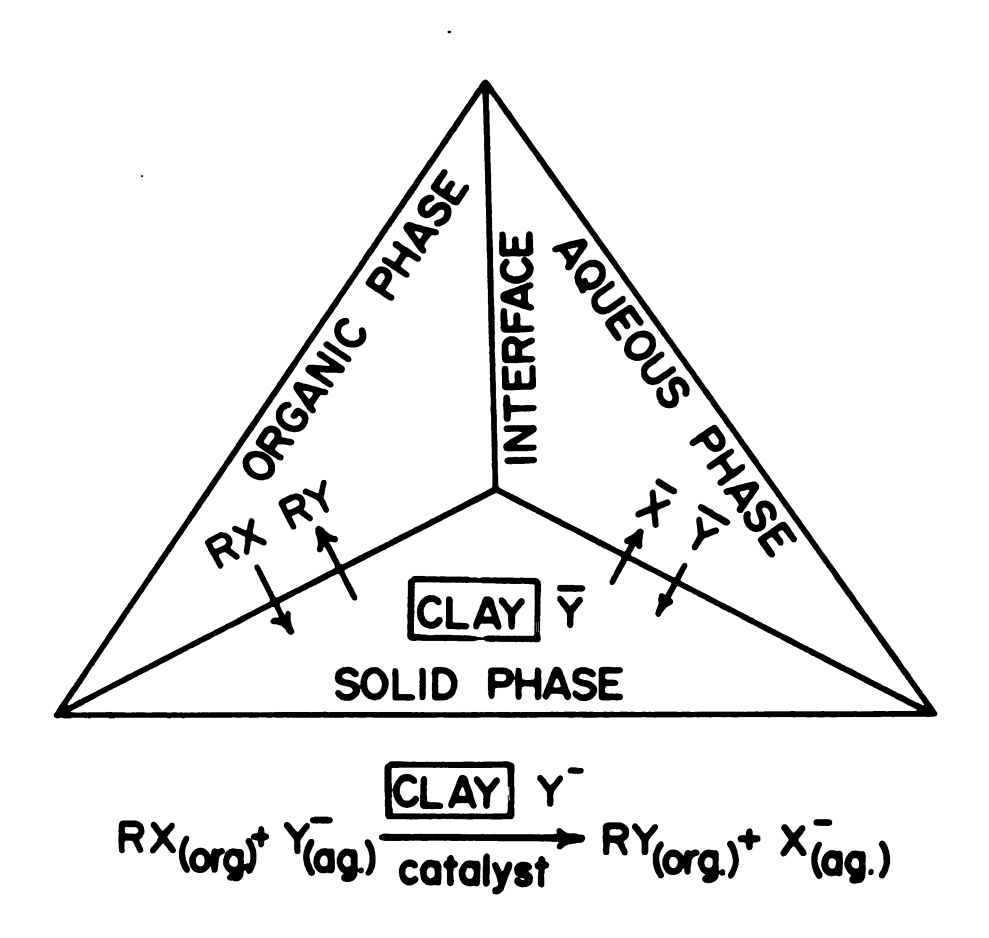


Figure 22 Schematic representation of the three-phase system, using smectite intersalate as a solid phase.

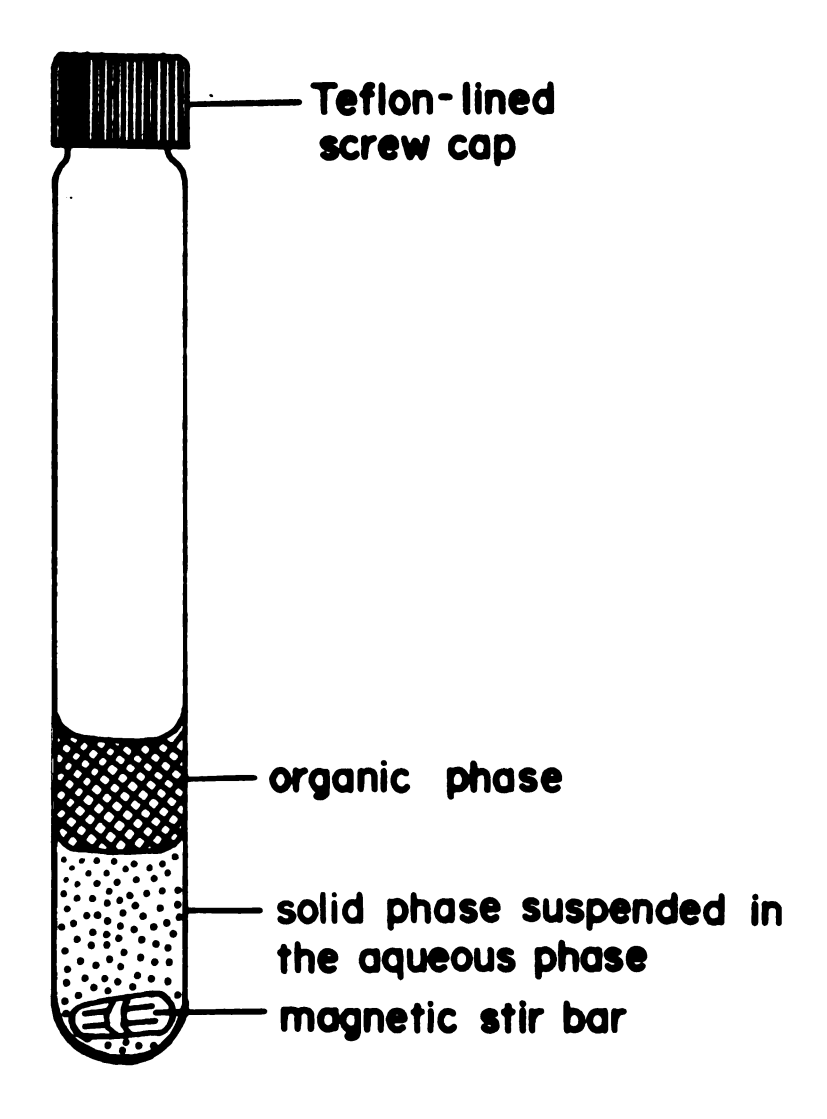


Figure 23 Experimental set-up for triphase catalytic reactions. Corning N° 9826 Culture table (20  $\times$  150 mm) containing organic, aqueous, and solid phase; a teflon coated magnetic stirring bar ( $^{10}/_{16} \times ^5/_{16}$  in. octagonal bar with pivot ring) is shown.

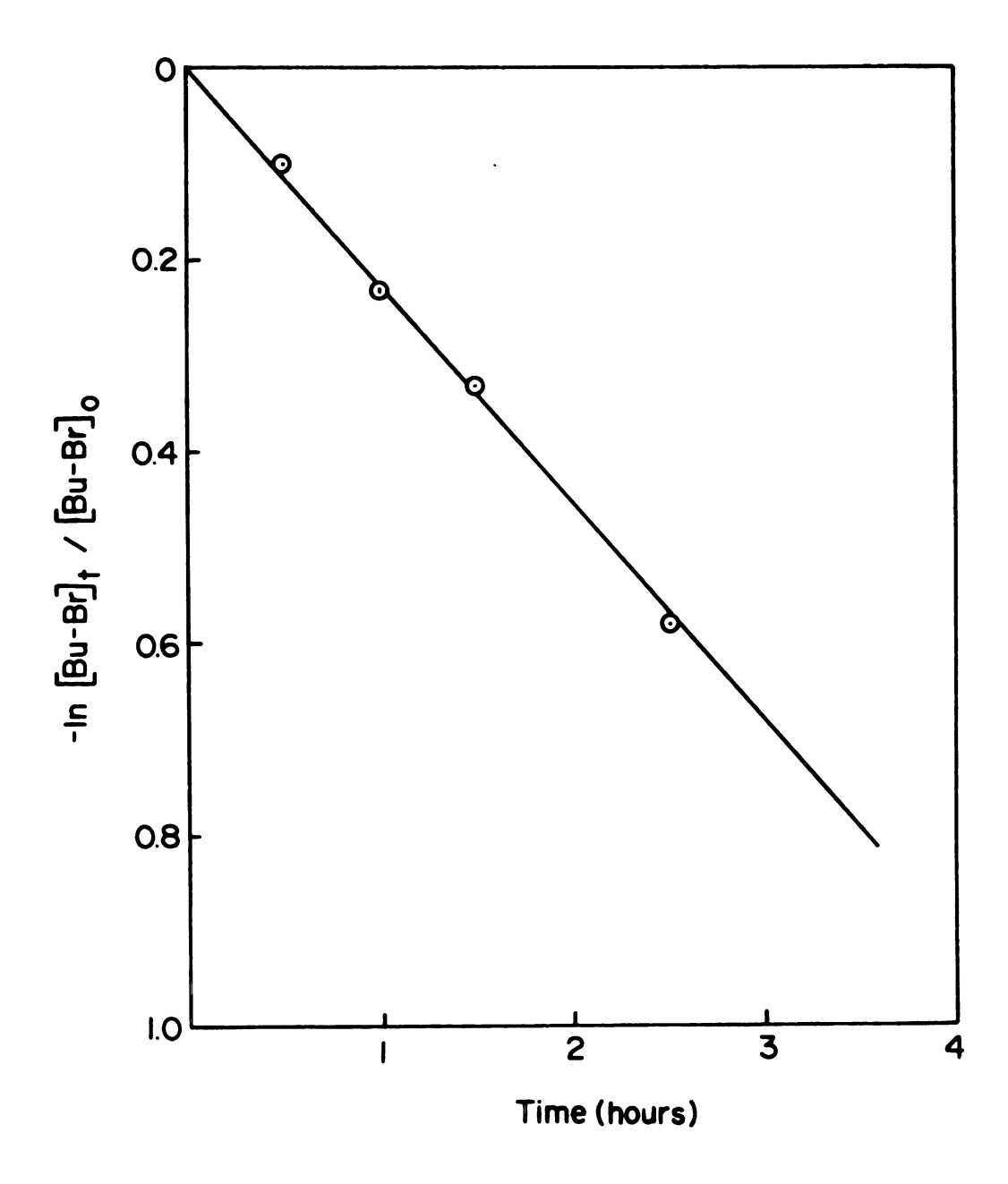


Figure 24 Plot of ln(unreacted) butyl bromide in the organic phase as a function of time for the reaction of 2 mL of 0.5 M n-butyl bromide in toluene with 3.0 mL of an aqueous 3.3 M NaCl catalyzed by 0.069 meq of Ni(phen) 2+/SO<sub>4</sub> ion pair in Laponite at 90°C.

Phase-Transfer Catalzyed Halide Displacement Reactions at $90^{\circ}\mathrm{C}$ with Ni(phen) $_3^{2+}/\mathrm{SO}_4^{2-}$ -Laponite Intersalates as Catalysts.	10 <sup>2</sup> k <sub>obs</sub> (hr <sup>-1</sup> )	22.8	1.92	1.66	0.27
alzyed Halide Dis ponite Intersala	Product	\ \ \	C1	\ \ \	$\longrightarrow_{\operatorname{Br}}$
Phase-Transfer Catalzyed Halide Displacement Reaction i (phen) $^{2+}_3/{ m SO}^2_4$ -Laponite Intersalates as Catalysts. $^a$	Reactant	→ Br	→ Br	C1	<b>₩</b> c1
Table 9.					

<sup>a</sup>Reaction condition: 1 mmol alkyl halide in 2 ml/toluene, 10 mmol sodium halide in 3 ml  $_{1}^{4}$  No. 0.069 meq of Ni(phen)  $_{2}^{2}$  -Laponite catalyst.

$$Rx(org) + \overline{y}(org) \xrightarrow{k[Q^+]} Ry(org) + \overline{x}(org)$$
 (46)

$$\overline{x}(\text{org}) + \overline{y}(\text{aq}) \qquad k[Q^{\dagger}] \qquad \overline{x}(\text{aq}) + \overline{y}(\text{org})$$
 (47)

For most entering and leaving groups, catalyst regeneration by exchange between the aqueous (aq) and organic (org) phases [Eq. (47)] is so rapid that it has no effect on reaction rates. Undoubtedly, in the case of intersalation compounds equation more complex than (46) and (47) must be considered, taking into account any processes of adsorption and/or diffusion,

$$Rx (org) + \overline{clay} \overline{y} \stackrel{k}{\rightleftharpoons} Rx \cdot \overline{clay} \overline{y} \stackrel{k}{\rightleftharpoons} Ry$$

$$\cdot \overline{clay} \overline{x} \stackrel{k}{\rightleftharpoons} Ry (org) + \overline{clay} \overline{x}$$
(48)

$$\overline{y}(aq) + \overline{clay} \, \overline{x} \xrightarrow{k_d} \, \overline{y} \cdot \overline{clay} \, \overline{x} \xrightarrow{k_e} \, \overline{x}$$

$$\cdot \overline{clay} \, \overline{y} \xrightarrow{k_f} \, \overline{x}(aq) + \overline{clay} \, \overline{y} \qquad (49)$$

where  $\[ \overline{\text{clay}} \] \overline{\text{x}} \]$  and  $\[ \overline{\text{clay}} \] \overline{\text{y}} \]$  represent the supported complex salt in the  $\overline{\text{x}}$  and  $\overline{\text{y}}$  forms, respectively;  $Rx \cdot \overline{\text{clay}}$ ,  $Rx \cdot \overline{\text{clay}} \]$ ,  $Rx \cdot \overline{\text{clay}} \]$  and  $Rx \cdot \overline{\text{clay}} \]$  represent Rx, Ry,  $\overline{y}$  and  $\overline{x}$  in the environment of the third solid phase. Processes b, c, d, and f are controlled by adsorption (through their respective constants  $k_{b-f}$ ), by diffusion, or by both. Process e, however, is controlled by the reactivity

of the nucleophile at the surfaces of the intersalate. In reality, the situation may be even more complex than (48) and (49) the continuity of the two liquid phases up to the catalytic center is not guaranteed. Here, the concentration of nucleophile in the aqueous phase, does not affect the reaction rate (Table 10) as dramatically as it would if the

Table 10. Dependence of  $k_{obs}$  on the Amount of Sodium Chloride Present.<sup>a</sup>

NaCl (mmol)	10 <sup>2</sup> k <sub>obs</sub> (hr <sup>-1</sup> )
12	2.05
10	1.92
8	1.83
6	1.96

<sup>&</sup>lt;sup>a</sup>Reaction of 1 mmol n-butyl bromide in 2 ml of toluene with the indicated amount of sodium chloride dissolved in 3 ml of water catalyzed by 0.69 meq of Ni(phen) $^{2+}/SO_4^{2-}$ Laponite intersalate at 90°C.

diffusion of the nucleophile toward the clay surfaces was the step controlling the regeneration of catalytic centers. The assumption is that the anion exchange equilibria whereby anions are transferred from aqueous to solid phase are very fast relative to the rate of the solid phase displacement reaction. This assumption will, of course, not be correct if one greatly slows the rate of phase mixing. Therefore in all the reactions carried out, the reaction mixtures were always stirred vigorously.

The result shows that the coefficient for desorption of the ion pairs in aqueous media is extremely low (i.e.  $\sim 10^{-10}$  mole<sup>2</sup>/L<sup>2</sup> at 25°C), it is even smaller in nonaqueous media. In order to study the significance of complex desorption and also to ensure that the displacement reactions were being catalyzed by the solid phase, the reaction of chloride ion with 1-bromobutane in the presence of Ni(phen) $_{3}^{2+}/SO_{4}^{2-}$ -hectorite was repeated, but stopped after a 20% yield of 1-chlorobutane was obtained. portion of both the aqueous phase and the organic phase was filtered and transferred to a second tube, which, along with the original tube, was heated for an additional period of time at 90°C. Analysis of the product mixture in the tube containing the clay catalyst showed an increased yield of 1-chlorobutane. In the absence of the clay catalyst, however, the yield of 1-chlorobutane remained unchanged.

Under triphase reaction conditions with the intersalate as catalyst, some intercalated  $SO_4^{2-}$  ions are replaced by halogen from the aqueous phase and this intercalated halogen is accessible for reaction with adsorbed alkyl halide.

X-ray diffraction measurements show the basal d(001) spacing of the solid phase is retained after the displacement reaction. Therefore, the intersalation phase remains intact throughout the reaction.

It is interesting to note that despite some limitations, the clay intersalates are quite competitive with polymer supported systems (see Table 11).

A plot of k<sub>obs</sub> for displacement of iodide ion (aqueous phase) in 1-bromobutane (organic phase) as a function of the catalyst amount yielded a straight line, [Fig. (25)]. These data indicate that the catalyst efficiency remains constant. Thus the diffusion of reactants or of products across the various liquid-liquid and liquid-solid is not rate limiting.

Since [I ] >> [1-bromobutane] the complete kinetic equation can be written in the following form:

$$-d[1-bromobutane]/dt = k_{obs}[1-bromobutane]$$
 (50)

An examination of the dependency of the observed pseudo first- order rate constant (kobs) for the reaction of Cl with 1-bromobutane (organic phase) on the chloride concentration revealed that a two-fold increase in the amount of sodium chloride produced no change in the observed rate of reaction (Table 10). Therefore, the Cl concentration at the surface of the intersalate is constant and anion exchange at the intersalate is not rate limiting.

The kinetics features here bear a resemblance to that observed for the displacement of cyanide ion on 1-bromooctane using well known "phase-transfer catalysis" technique as well as recently developed triphase

RY &

97

q 06

a	Temp. Eq. RX/Eq of (°C) Catalyst	90 14.5	3.8
tions.	Tem (°(	6	110
nge Reac	Time (hr)	16	09
logen Excha	Product (RY)	→ Br → I	→ Br → I
isfer Catalyzed Halogen Exchange Reactions. $^a$	Reactant (RX)	$\longrightarrow$ Br	> Br
Phase Transfer	st	Ni (phen) $\frac{2^+}{3}/\mathrm{SO}_4^2$ -Laponite	
	Catalyst	3 / so <sub>4</sub> .	$R_{f 4}N^+$ -polymer $^{m c}$
Table 11.		Ni (phen	R4N+-po

aConditions used here are described in the experimental section.  $^b{
m S.L.}$  Regen, J. Org. Chem., 42, 875 (1977).

Polystyrene Resin

 $R = CH_2N(CH_3)_2(n-C_4H_9)Cl;$  12% ring substitution. 24

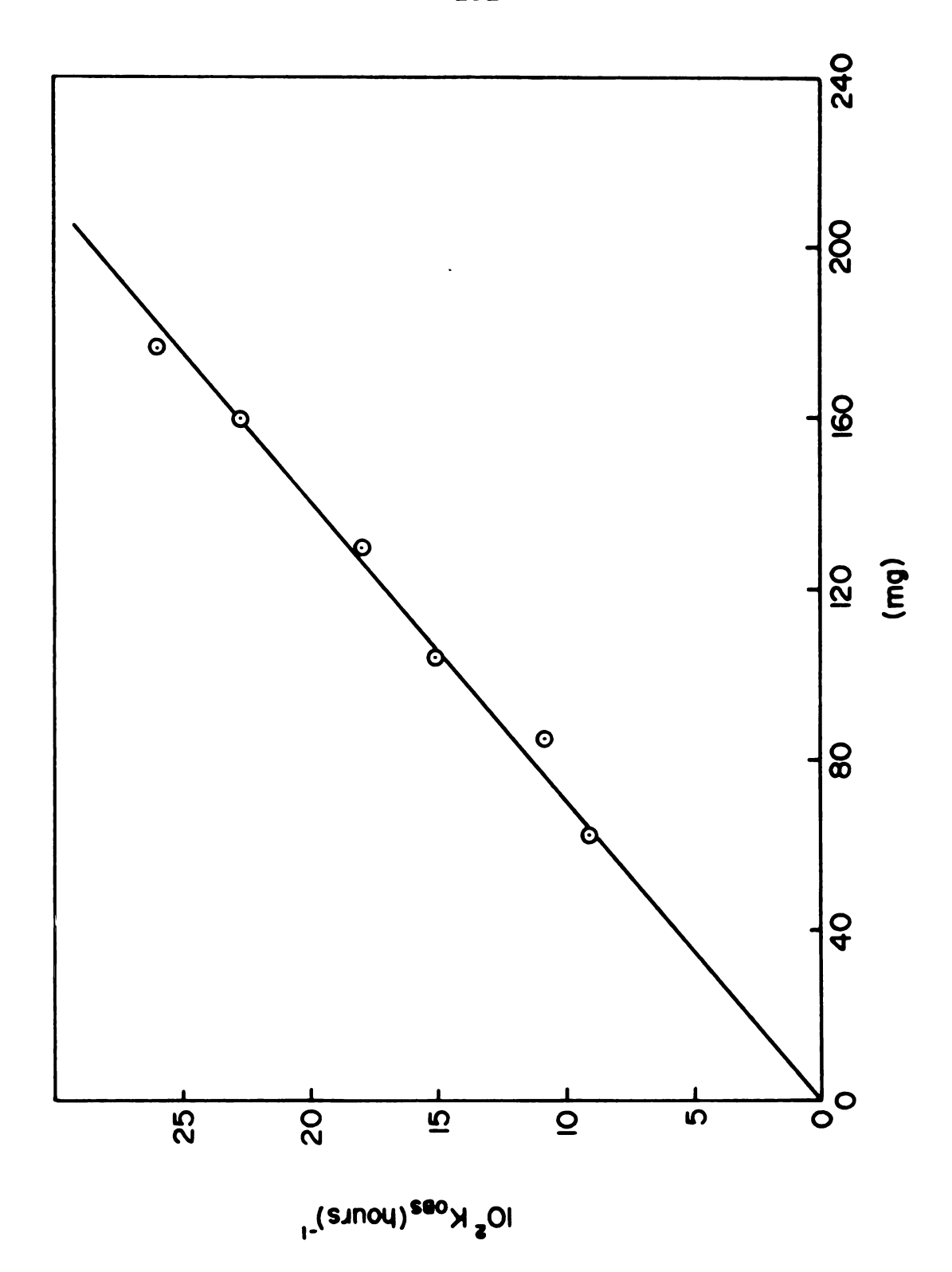


Figure 25 Plot of  $10^2$   $k_{\mbox{obs}}$  as a function of the amount of catalyst used. The catalyst and reaction conditions were similar to those described in Figure 24.

catalysis [103,48]. In all these systems, the rate of nucleophilic displacement exhibits a pseudo first-order dependency on the alkyl halide concentration and is also linearly dependent on the amount of catalyst used. For the phase-transfer reaction it has been proposed that the organic-soluble catalyst acts by repeatedly bringing cyanide ions located in an aqueous phase into the bulk organic phase where the displacement occurs. It has also been suggested that micellar catalysis in which micelles could bring small amounts of aqueous sodium cyanide into the organic phase in a form suitable for displacement reaction is of negligible importance.

The effect of substrate polarity on reaction rate was examined using 1,8-dibromooctane and 1-bromooctane as substrates. A pseudo first-order plot for replacement of Br by Cl in 1,8-dibromooctane is shown in Fig. (26). Although the carbon number is the same as 1-bromooctane, the rate of displacement reaction is enhanced almost by 4 times. 1,8-Dibromooctane is a more polar substrate and perhaps it has a higher affinity toward the surface of the catalyst than 1-bromooctane. Therefore, the rate of reaction can be influenced by the polarity of the substrate as well as its size.

Table 12 provides the pseudo first-order rate constants,  $k_{\rm obs}$ , for the reaction of butyl bromide in various organic solvents with aqueous NaCl in the presence of Ni(phen) $_3^{2+}$ /SO $_4^{2-}$ -hectorite as catalyst. Included in the table, for

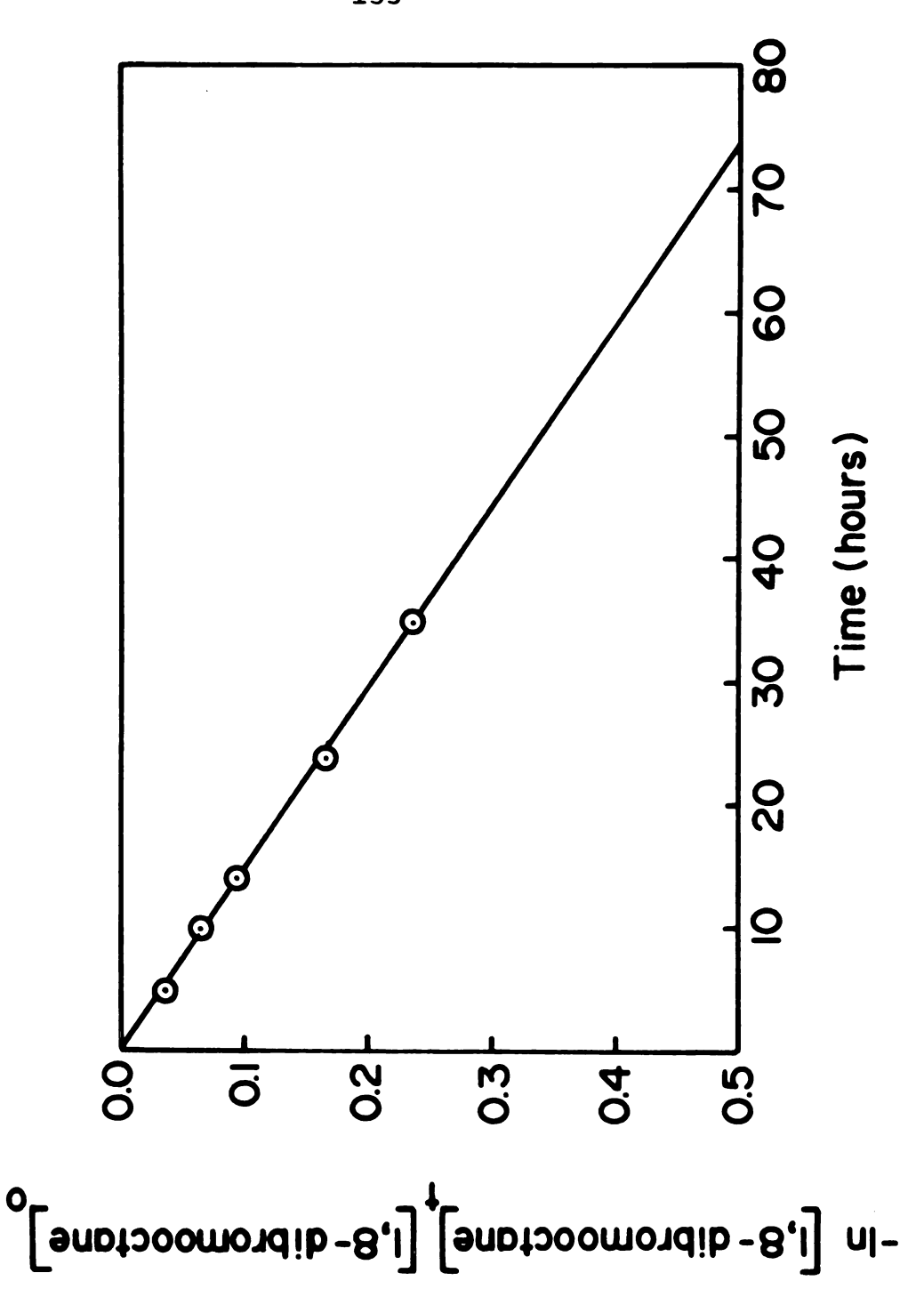


Figure 26 Plot of ln(unreacted) 1,8-dibromooctane in the organic phase as a function of time for the reaction of 2 mL of 0.5 M 1,8-dibromooctane in toluene with 3.0 mL of an aqueous 3.3 M NaCl catalyzed by 0.069 meq of Ni(phen) 3/504 ion pair in natural hectorite at 90°C.

Table 12. Kinetics Data for the Reaction of Butyl Bromide and Aqueous NaCl at  $90^{\circ}C^{a}$ .

Catalyst	Organic Phase	10 <sup>2</sup> k <sub>obs</sub> (hr <sup>-1</sup> )
Ni(phen) $\frac{2+}{3}$ /SO $\frac{2-}{4}$ -hectorite	С <sub>6</sub> н <sub>5</sub> Сн <sub>3</sub>	1.9
	. с <sub>6</sub> н <sub>6</sub>	2.0
	1,2-C <sub>2</sub> H <sub>4</sub> Cl <sub>2</sub>	1.9
	1,2-C <sub>6</sub> H <sub>4</sub> Cl <sub>2</sub>	2.1
Ni(phen) $\frac{2}{3}$ -hectorite	C6H5CH3	0.09
Na <sup>+</sup> -hectorite	C <sub>6</sub> H <sub>5</sub> CH <sub>3</sub>	0.24
Ni(phen) <sub>3</sub> SO <sub>4</sub>	C6H5CH3	<0.05

<sup>&</sup>lt;sup>a</sup>Reaction conditions: 1 mmol butylbromide in 2 mL organic solvent, 10 mmol NaCl in 3 mL H<sub>2</sub>O, 0.069 meq. catalyst.

comparison, are the  $k_{\mbox{\scriptsize obs}}$  values for the same reaction using homoionic Ni(phen)3+-hectorite and Na+-hectorite as catalysts and Ni(phen) 3SO as a liquid-liquid biphase catalyst. Little activity is observed with Ni(phen) 3SO4 under biphase conditions, yet when the salt is intercalated in hectorite, significant catalytic activity is observed. Also, it is noteworthy that the activity of Ni(phen) $_{3}^{2+}/SO_{A}^{2-}$ hectorite is insensitive to the nature of the organic However, phosphonium-based polymers as triphase catalysts exhibited a modest dependence on the nature of the organic solvent employed. It was suggested [174] that the organic solvent can control the extent of swelling which dilates the mesh of the resin which, in turn, allows a greater accessibility of the reagents to the catalytic sites [124]. Since the clay catalyst is swelled much better by H<sub>2</sub>O than by any organic solvent, the effect of organic solvent on reaction rate is insignificant. organic solvent could influence the adsorption equilibria for reactants on the surfaces. Also the organic solvent could influence the nature of the microenvironment at the active sites and, therefore, affect the free energy of activation. However, such factors do not seem to be important for the clay catalyst system.

The low activity of Ni(phen) $_3$ SO $_4$  under biphase conditions presumably arises from the low solubility of Ni(phen) $_3^{2+}$ /Cl $_2^-$  ion pairs in the organic phase. In marked contrast to the intersalated catalyst, homoionic

Ni (phen) 3<sup>2+</sup>-hectorite and Na<sup>+</sup>-hectorite are relatively poor phase transfer catalysts for halide replacement in butyl bromide. These results are similar to those given in earlier reports of the phase transfer properties of homoionic smectite clays in displacement reactions involving anionic nucleophiles [134,128]. In all of these cases, however, the catalytic activity undoubtedly results from the small anion exchange capacity (<5 meq/100 g) of smectite clays which is believed to result from the replacement of some structural hydroxyl groups at the edges of the clay platelets [175]. Some adsorption of cationanion pairs may also contribute to the observed catalytic activity, but unlike the intersalated complexes, these ion pairs would exist only in low concentration at external surface sites.

When natural hectorite complex was adopted for the catalysis in some cases the reproducibility of the kinetic reactions from batch to batch was poor. However, for the synthetic hectorites, as expected, this was not the case. For this reason all reaction done with natural hectorite in a series were performed by using the same batch in order to obtain consistent results.

## 2. Substrate Size and Shape Selectivity

The possibility of substrate size and shape selectivity with Ni(phen) $_3^{2+}/SO_4^{2-}$ -hectorite as a phase transfer catalyst, was investigated for the conversion of alkyl bromides to alkyl chlorides. A range of hydrocarbons from  $C_3$  to  $C_{16}$ 

were examined. Table 13 provides the values of k<sub>obs</sub> for the intersalated catalyst under triphase conditions. Indicated in the table are the rate constant obtained for the same reaction using tricapryl methyl ammonium chloride as a catalyst under biphase reaction conditions. It can be seen that the reaction rates under biphase conditions are very similar, as expected. However, the intersalated catalyst is more than 140 times more reactive toward the smallest substrate (1-bromopropane) than the largest substrate (1-bromophexadecane) in the series.

It is possible that the apparent size selectivity of the intersalated catalyst is related to the ability of the substrate to adsorb in the interlayer region occupied by Cl. The degree to which the substrate penetrates the interlayer, however, probably is limited to a distance of a few molecular diameters, because adsorption of alkyl bromides to the intersalate is undetectably low. This latter observation is consistent with the fact that the 001 spacing of the intersalate is little changed by the adsorption of water or alkyl bromide.

There is an alternative explanation for the apparent size selectivity of the intersalate based on selective adsorption at the edge sites of the intersalate. Since under triphase conditions the intersalate prefers to be wetted by the aqueous phase rather than the organic phase, the extent of edge site adsorption may decrease with increasing hydrophobicity and size of the alkyl chain.

Pseudo First-Order Rate Constants ( $10^2 {
m k}_{
m obs}$  (hr $^{-1}$ )) for the Reaction of Table 13.

 $^{\alpha}$  Reaction conditions: 1 mmol of organic substrate in 2 mL toluene, 10 mmol NaCl in 3 mL  $_{\rm H_2O}$ , 0.069 meg catalyst.

The possibility of shape selectivity was examined for the series of normal and branched alkyl bromides. The pseudo first-order rate constants are plotted as a function of the alkyl carbon number for the Ni(phen) $_3^{2+}$ /SO $_4^{2-}$ -hectorite catalyst system in Fig. (27). The results show that the rate constants  $(k_{obs})$  decrease as the alkyl carbon number increases for both normal and branched alkyl bromides. The value of  $k_{obs}$  for the branched alkyl bromides was lower than for normal alkyl bromides with the same carbon number. However, the observed rate differences for the anion substitution reaction of normal and branched-chain alkyl halides are small. Despite the apparent size over the  $C_3$ - $C_{16}$  range, a dramatic shape selectivity is not observed for isomers of the same carbon number.

Moreover, the k<sub>obs</sub> for the reaction of 1-bromo-3-phenylpropane with NaCl is relatively high, considering the attachment of the large phenyl group as well as the carbon number in the chain. This latter observation is somewhat contrary to what is expected on the basis of shape discrimination. On the other hand this result is consistent with the result shown in Fig. (27). It is possible that the adsorption of the substrates on the surface of the intersalated catalyst is dependent more on polarity than on size or shape. Nonetheless, shape selectivity clearly is observed for two substrates with the same carbon number. This shape selectivity is a

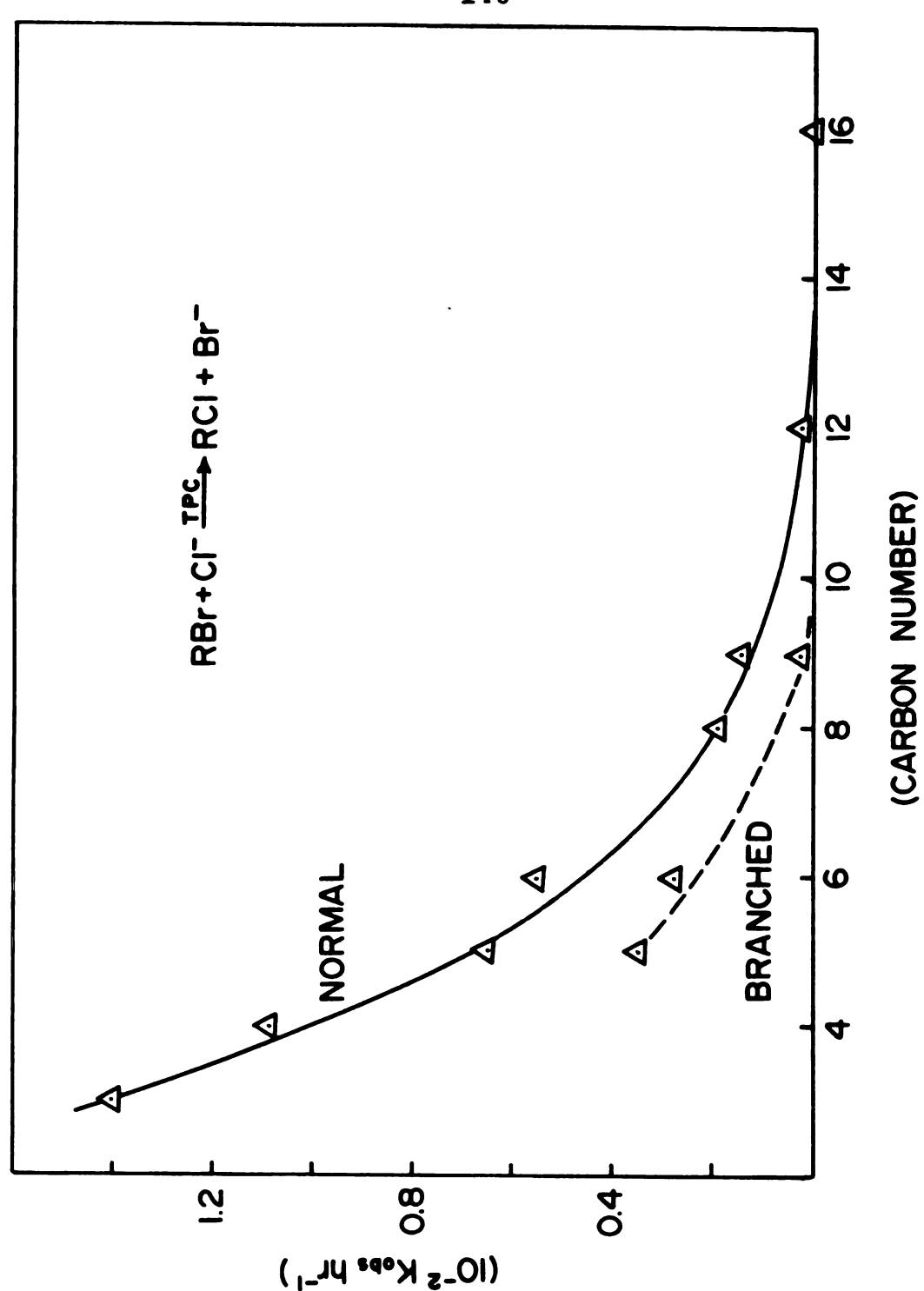


Figure 27 Selectivity induced by the hectorite intersalate catalyst on the pseudo first-order rate constants of Br-Cl exchange for normal and branched alkyl bromides with aqueous NaCl as a function of the number of carbon atoms in the alkyl chain. For the reaction conditions see Table 13, footnote a.

real possibility in the design of new intersalated catalysts.

#### 3. Structural Modification

Several different iron (II) complexes of 1,10phenanthroline and its derivatives were prepared and they
were intersalated in natural hectorite. These intersalates
were then used for the nucleophilic displacement reaction
of some alkyl bromides with sodium chloride in triphase
catalysis to explore the reactivity of intersalated
catalysts in this type of reaction. Figure (28) provides
an edge view of the intersalated catalyst to illustrate the
consequences of the modification of the cation structure.
The influence of different chelate ligands on the reactivity
of the intersalated catalysts is given in Table 14.

The results indicate that changing the ligands of the interlayers cation can actually change the reactivity of the intersalated catalyst. For example, when bathophenanthroline was used in place of phen ligand, the pseudo first-order rate constant for the halogen exchange reaction increased six-fold. Bathophenanthroline is the bulkiest organic ligand in the series with perhaps the highest lipophilic character. This may facilitate the adsorption of the organic substrate at the surface. In the case of 3,4,7,8-tetramethyl-1,10-phenanthroline ligand with 4 methyl group instead of 2 phenyl, the rates of the reactions were doubled. The same improvement in rate of reactions were observed for both substrates (1-bromooctane and 1-bromobutane), which is consistent with

for the Reaction of	$10^2 k_{\rm obs} (hr^{-1})$	7.3	1.2	2.4	0.47	1.2	0.21	
(10 <sup>-</sup> k <sub>obs</sub> (hr <sup>-</sup> ))	Substrate	${\sim}$ Br	A Br	$\stackrel{\text{Rr}}{\longrightarrow}$	A Br	$\stackrel{}{\sim}$	A Br	
Table 14. Pseudo First-Order Rate Constants ( $10^{\circ}k_{\rm obs}$ (hr $^{\circ}$ ) for the Reaction of Alkyl Bromides with NaCl at $90^{\circ}$ C.	Catalyst	Fe (4,7-diphenyl-phen) $\frac{2^+}{3}/50\frac{2^-}{4}$ -hectorite	Fe (4,7-diphenyl-phen) $\frac{2^+}{3}/50\frac{2^-}{4}$ -hectorite	Fe(3,4,7,8-Me <sub>4</sub> -phen) $\frac{2^+}{3}$ /SO $\frac{2^-}{4}$ -hectorite	Fe(3,4,7,8-Me <sub>4</sub> -phen) $\frac{2^+}{3}$ /SO $\frac{2^-}{4}$ -hectorite	Fe (phen) $\frac{2^+}{3}/50\frac{2^-}{4}$ -hectorite	Fe(phen) $\frac{2^+}{3}/50\frac{2^-}{4}$ -hectorite	

l mmol alkyl bromide in 2 ml toluene, 10 mmol NaCl in 3 ml  $_{2}\mathrm{O};$ <sup>a</sup>Reaction condition: 0.069 meg catalyst.

the results for Ni(phen) $_3^{2+}/SO_4^{2-}$ -hectorite system. However, the improvement in reactivity was modest.

To increase the hydrophobicity of the clay edge surfaces, Ni(phen) $_3^{2+}$ /SO $_4^{2-}$ -hectorite intersalates were treated with Cl (CH<sub>2</sub>) $_3$ Si(OCH $_3$ ) $_3$  (silane coupling agent) and then the intersalated catalyst was used for a similar kinetic reaction. However no substantial change in the rate was observed (i.e. <two times). This result is not too surprising, because the ion pair layer represents  $\sim 50\%$  of the total edge surface area and also the silylated edge sites are somewhat far away from the reaction zone [see Fig. (28)].

## 4. Particle Size Effect

Three clays of different particle size (natural hectorite, synthetic hectorites (Laponite) and fluorohectorite) were intersalated with Ni(phen)<sub>3</sub>SO<sub>4</sub> complex. The resultant intersalates were used as catalysts for the displacement reaction of 1-bromooctane and 1-bromobutane. The results are illustrated in Table 15. It can be seen that as the particle size increases the pseudo first-order rate constant decreases. By increasing the particle size of the intersalated catalysts the ratio of edge surfaces to interlayer surfaces also decreases. If the penetration of the substrate molecule into the interlayer is limited to a very short distance, then all interlayer sites will not be available for the reaction. This factor becomes more significant as we go to a larger

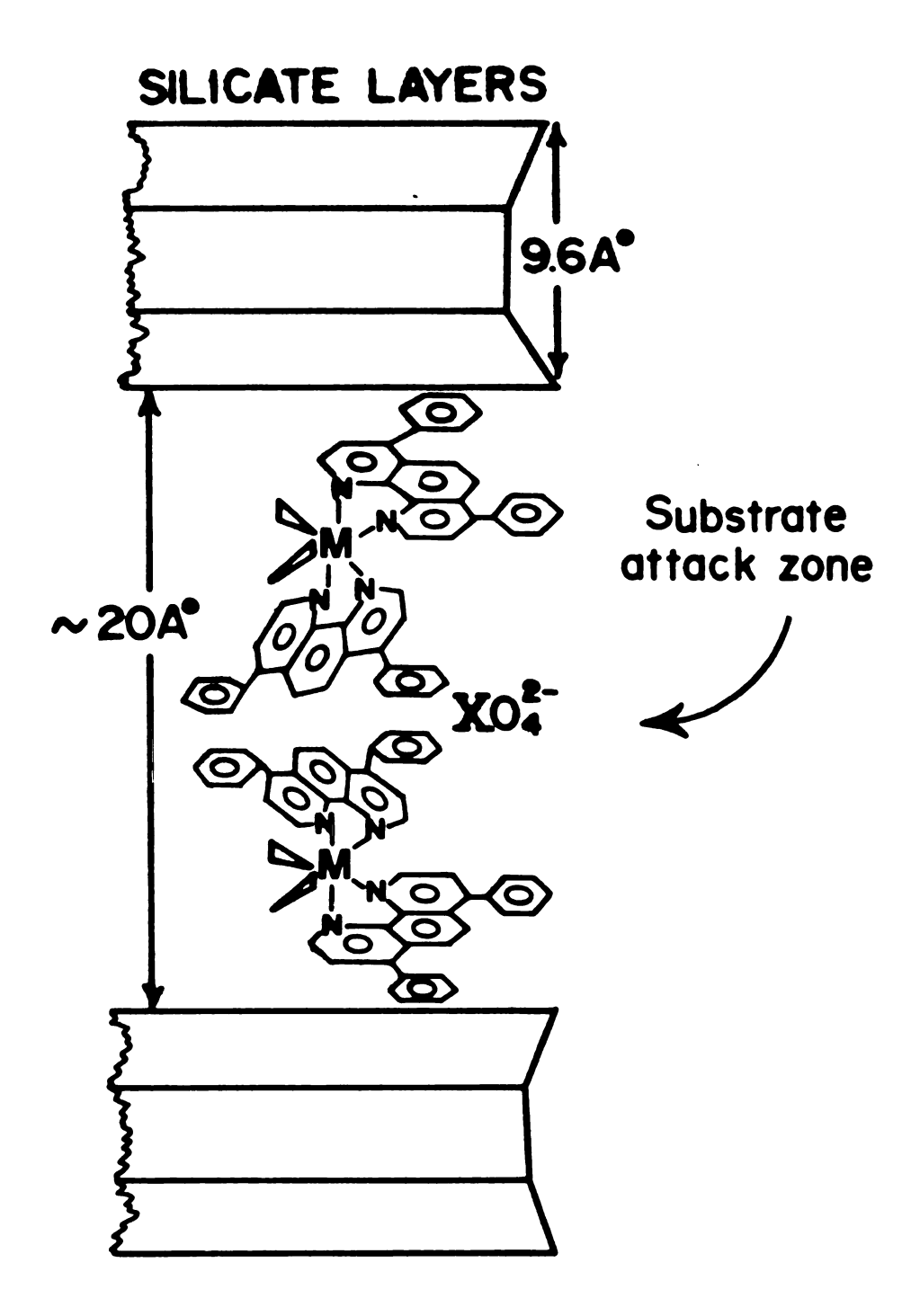


Figure 28 Schematic representation, showing edge view of the intersalated hectorite catalyst and the triphase catalyzed reaction zone.

Effect of Particle Size on Pseudo First-Order Rate Constants  $(10^2 k_{
m obs}~({
m hr}^{-1}))$ for the Reaction of Alkyl Bromides with NaCl at 90°C. Table 15.

(k <sub>obs</sub> )	1.92	0.34	1.1	0.19	0.54	0.08
Particle Size of the Hectorite Used $(\mu)$	0.02	0.02	<2	<2	>>2	>>2
Catalyst	Ni (phen) $\frac{2^+}{3}$ $\frac{2^-}{1}$ -hectorite synthetic, Laponite	Ni (phen) $\frac{2^+}{3}/504^-$ -hectorite synthetic, Laponite	Ni (phen) $\frac{2}{3}$ /SO $\frac{2}{4}$ -hectorite Baroid (B1-26)	Ni (phen) $\frac{2^+}{3}/50\frac{2^-}{4}$ -hectorite Baroid (B1-26)	Ni (phen) $\frac{2^{+}}{3}/50\frac{2^{-}}{4}$ -hectorite synthetic, fluoro-hectorite	Ni (phen) $\frac{2^{+}}{3}/504^{-}$ -hectorite synthetic, fluoro-hectorite
Substrate	→ Br	A Br	≯ Br	A Br	$\stackrel{\text{A}}{\sim}$	A Br

1 mmol substrate in 2 ml toluene, 10 mmol NaCl in 3 ml  $\mathrm{H}_2\mathrm{O}$ , "Reaction condition: 0.069 meg catalyst.

 $^b$ Cation exchange capacity for Laponite, Baroid hectorite and fluoro-hectorite are 55,73 and 193 meq/100 g clay respectively.

particle size. Thus, increasing the edge surface area would favor catalytic reactivity.

### 5. <u>Carboxylate Ion Displacements</u>

Liolta et al. [176] reported that acetate solubilized as the potassium salt in benzene containing 18 crown-6 because sufficiently nucleophilic to react smoothly and quantitatively, even at room temperature, with a wide variety of organic substrates under phase transfer catalysis (PTC) conditions.

Using quaternary ammonium salt under PTC conditions starks [49] obtained high yields of a variety of esters from simple alkyl halides and sodium carboxylates. It was of interest in the present work to examine the properties of clay intersalates for catalytic displacement reaction involving carboxylate ion as a nucleophile. The displacement reaction between benzyl chloride and acetate ion was carried out under triphase conditions by using hectorite intersalate as a catalyst.

$$C_6H_5CH_2C1 + CH_3COO^-M^+ \xrightarrow{Q^+} C_6H_5CH_2OCOCH_3 + MC1$$
 (51)

The yield after a reaction time of 48 hours at 90°C is shown in Table 16. When Na<sup>+</sup>-hectorite was used as a solid phase catalyst, a negligible amount of benzyl acetate was formed. Under identical reaction conditions butyl bromide also reacts with acetate, but the yield of ester is lower than that observed for the benzyl chloride system. This

Table 16. Reaction of Acetate Ion with Organic Substrate a

Substrate	Product	(%) Yield
Benzyl chloride	Benzyl acetate	61
Benzyl chloride	Benzyl acetate	6 <sup>b</sup>
n-C <sub>4</sub> H <sub>9</sub> Br	n-C <sub>4</sub> H <sub>9</sub> OAc	44

Reaction conditions: acetate salt, 1.1 mmol; benzyl
chloride, 1.0 mmol; eq RX/eq Q(+) = 28; toluene, 2 ml;
water, 3 ml; reaction time, 48 hr at 90°C.

is because benzyl chloride is a more reactive substrate than n-butyl bromide.

#### 6. Supported Cetyl Pyridinium Bromide for TC

It is well known that the physical properties of clay can be modified considerably by ion-exchange of quaternary ammonium salts and related compounds [177,178]. On the other hand the adsorption of the cetyl pyridinium ion beyond the exchange capacity of Na and Ca-montmorillonite has also been shown [160].

In the present investigation 2 CEC cetyl pyridinium bromide-hectorite complex has been utilized for triphase catalysis. Cetyl pyridinium bromide was supported on the hectorite clay by the method indicated in the experimental section. The cetyl pyridinium-hectorite system exhibits 20.6 A diffraction peaks at loadings between 73 and 146 meq/100 g. The result is consistent with the data reported by Quirk et al. According to their results [160], the observed maximum in the adsorption isotherm for cetyl

 $<sup>^</sup>b$ Plain clay was used as a solid phase.

pyridinium bromide is 300 meq per 100 g montmorillonite. Therefore, at loading of 146 meq/100 g hectorite there is plenty of room for small anions to be accommodated within the interlayer. Examples illustrating the utility of triphase catalysis for some halogen exchange reactions are provided in Table 17. Here the results are given in terms of % yields. Pseudo first-order rate constant could not be determined, due to micell formation by the catalysis. The cetyl pyridinium salt itself acts as a catalyst in a biphase system. However the yield is lower than the corresponding triphase system (see Table 17).

7. Halogen Exchange Using Organic Salt Intersalates

Several different organic salts (compound 1-4,

see Table 5) were intersalated and the resulting phases
were used as triphase catalysis. The organic salts were
supported on hectorite by the method described in the
Experimental Section.

X-ray diffraction measurement of the basal d(001) spacing confirmed that the compounds were indeed supported (Table 5), and in some cases the X-ray diffraction pattern was very similar to what is found for the metal chelated complex intersalation [see Fig. (16)]. These organic intersalates were used for halide ion displacement in 1-bromobutane and 1-bromooctane. The experiments were conducted in the same manner as described previously in Section B-1. The rate data for the triphase catalyzed

Table 17. Phase Transfer Catalyzed Halogen Exchange Reactions Using Cetyl Pridinium Hectorite Complex (72 hr at  $90^{\circ}$ C).

Reactant	Product	(%) Yield	Form of Catalyst
∕∕ Br	$\sim$ 1	· 98	2CEC hectorite intersalation
<b>∕ C1</b>	<b></b>	59	2CEC hectorite intersalation
∕∕ Br	<b>∕ C1</b>	55	2CEC hectorite intersalation
$\sim$	<b>^</b> c1	9	<pre>1CEC intercalation (homoionic)</pre>
∧∧ Br	^^ c1	39	Aqueous organic betwo-phase system using cetyl pridinium bromide

Reaction condition: Toluene used as solvent, 0.1 gr hectorite clay, 1 mmol of substrate and 6 mmol of appropriate salt were taken.

The amount of quaternary ammonium salt is the same as any other intersalation system.

halogen displacement reactions are provided in Table 18. For all reactions pseudo first-order kinetics were observed. It is worthy to mention here that the difference in the reaction rate going from biphase to triphase systems for all these compounds is not dramatic. In addition, considering factors such as the molecular structure, the degree of layer ordering, the amount of anion present, hydrophobic interactions, ion pairing and the solvation properties of these molecules, it would be very difficult to rationalize the results. From the X-ray diffraction pattern of the Nile blue intersalate it seems that this compound is well ordered and similar to the  $M(chel)_3^{2+}/XO_4^{2-}$ hectorite systems. However, the behavior of the Nile blue intersalate as a phase transfer catalyst was somewhat surprising. The rate of the exchange reactions under triphase conditions is only twice as large as the rate under biphase conditions.

These organic salt-clay systems, like the organometallic-clay system mentioned earlier, show almost the same selectivity toward the longer size alkyl halide. The clay supported organic salts have advantages over the clay supported organo-metallic salts discussed earlier. The utility of transition metal complexes for a wide range of catalytic reaction is limited due to their reactivity with nucleophiles, but organic salts are less sensitive to nucleophiles.

Kinetics Data for the Reaction of Butyl and Octyl Bromide with Aqueous Nacl at 90°C. Table 18.

	Triphase Catalysis 10 <sup>2</sup> k <sub>obs</sub> (hr) <sup>-1</sup>	$\begin{array}{c} b \\ \text{atalysis} \\ (\text{hr})^{-1} \end{array}$	Biphase Catalysis 10 <sup>2</sup> k <sub>obs</sub> (hr)-1	phase Catalysis $^{0.2}$ k $^{0.2}$ (hr) $^{-1}$
Catalyst	Butyl Bromide	Octyl Bromide	Butyl Bromide	Octyl Bromide
$[c_8H_17]_3cH_3N^+c1^-$	35	5.70	25	20
	1.83	0.31	1.42	1.23
(C <sub>2</sub> M <sub>5</sub> ) <sup>4</sup> (C <sub>2</sub> M <sub>5</sub> ) <sup>4</sup> (S <sub>2</sub> M <sub>1</sub> ) SO <sub>4</sub>	69.0	0.11	0.34	0.27
$\begin{bmatrix} c_{H_3} & c_{H_3} \\ -h^{\Theta}(c_{H_2})_6 & h^{\Theta}(c_{H_2})_3 - ]2Br^{-} \end{bmatrix}_{\mathbf{x}}$ $\begin{bmatrix} c_{H_3} & c_{H_3} \\ c_{H_3} & c_{H_3} \end{bmatrix}$	0.53	60.0	0.32	0.25

1 mmol butyl bromide in 2 ml toluene, 10 mmol NaCl in 3 ml  $_{\rm 2}$ O, Reaction conditions: 0.069 meg catalyst.

 $<sup>^</sup>b\mathrm{Triphase}$  catalysts were prepared by reaction of 2.0 CEC equivalent of the indicated salt with Na -hectorite.

# 8. Kinetics of Cyanide Displacement on 1-Bromooctane

Phase transfer catalysis, as well as triphase catalysis procedures have been successfully utilized by several workers [48,83a] in cyanide displacement reactions involving simple alkyl halides.

In the present work, tricapryl methyl ammonium chloride-hectorite complex (0.069 meg) was used as the solid phase along with 3 ml aqueous potassium cyanide (3.33 M) plus 3 ml toluene solution of 1-bromooctane (0.33 M). It was found that heating such heterogeneous mixtures at 90°C resulted in the production of 1-cyanooctane in high yield. The typical procedure is outlined in Chapter II. Despite the complexities of the system, it was found that the above displacement reaction obeyed simple first-order kinetics, i.e., the rate of reaction showed a first-order dependency on the 1-bromooctane concentration. Typical kinetics data for triphase systems as well as biphase are illustrated in Fig. (29). In this respect the kinetic reaction here shows a resemblance to that observed for the displacement of cyanide ion on 1-bromooctane using the well developed "phase transfer catalysis" technique [48]. However, the details of the mechanism for this specific triphase-catalyzed system remains to be established.

As was mentioned earlier, the utility of the transition metal chelates intersalation compound for displacement reactions involving nucleophiles such as cyanide is

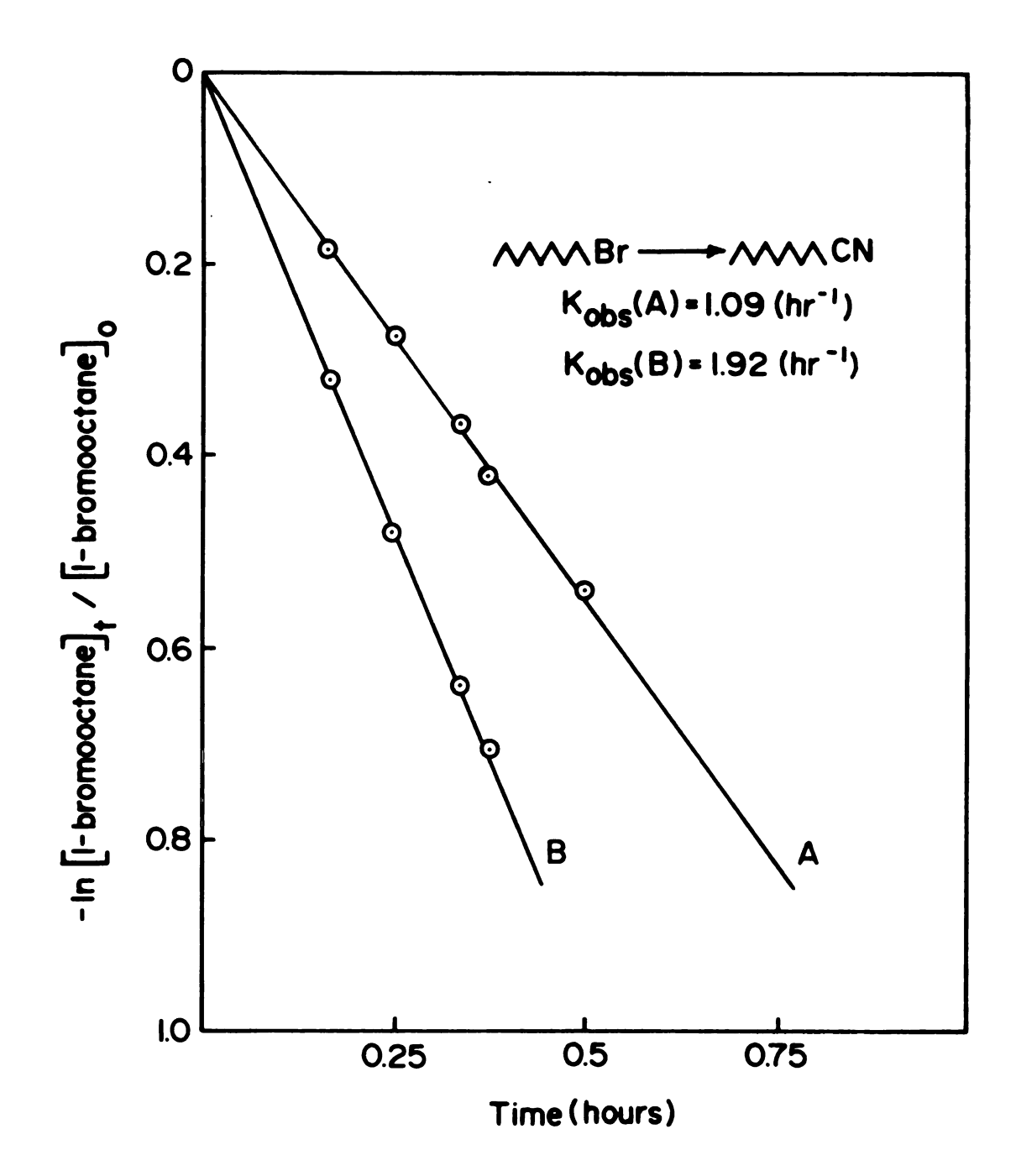
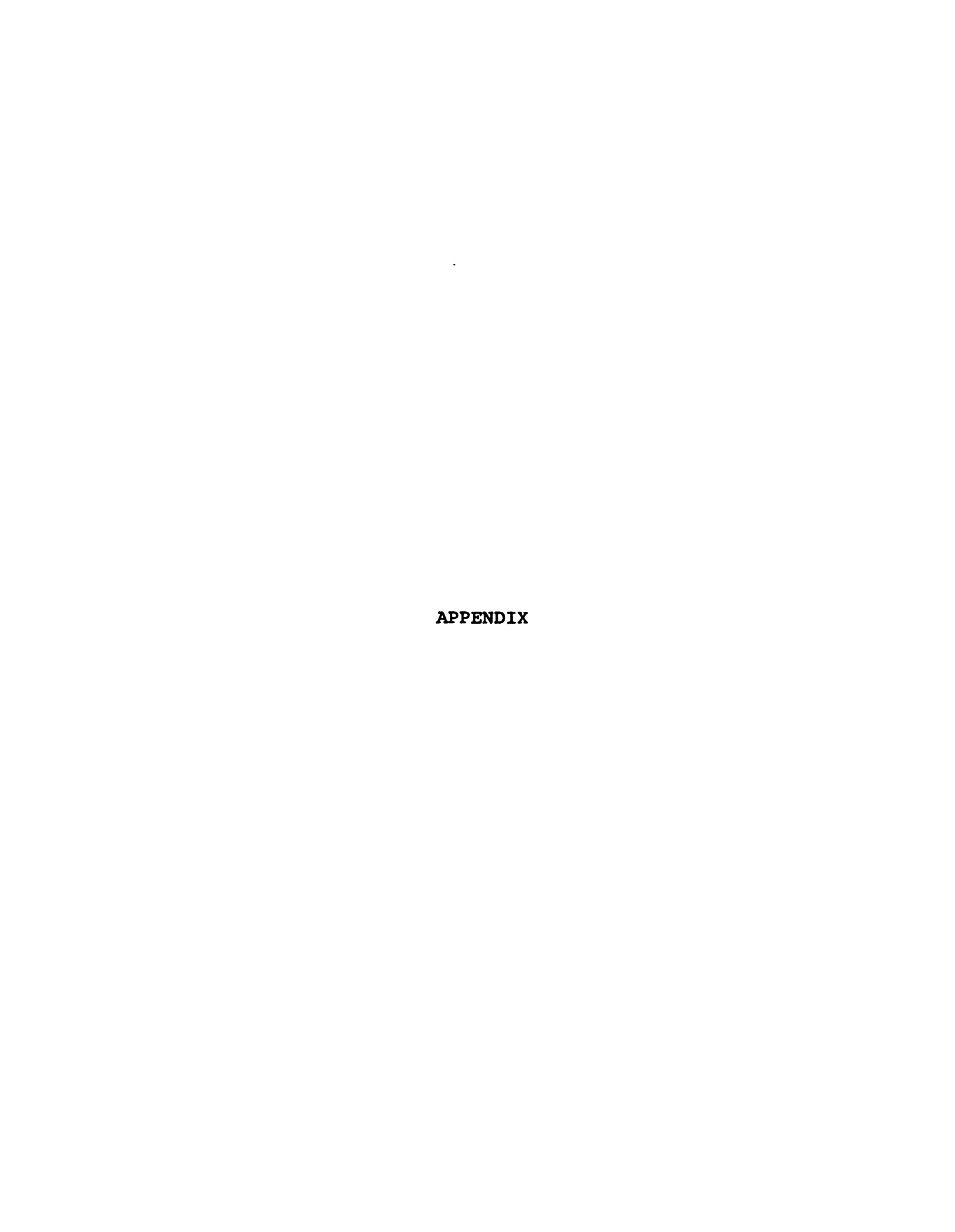


Figure 29 Plot of ln(unreacted) 1-bromooctane in the organic phase as a function of time for the reaction of 2 mL of 0.5 M 1-bromooctane in toluene with 10 mmol of sodium cyanide dissolved in 1 mL of water catalyzed by 0.069 meq of tricapryl methyl ammonium chloride ion pair in hectorite at 90°C.

limited due to the reactivity of these complexes. Herein lies the potential of organic salt intersalates.

.



## **APPENDIX**

A. Calculation of d(001) Basal Spacing Using Bragg Law

The following procedures were used to determine d(001) basal spacing and to assign the orders of reflection obtained.

Equation (52) is the Bragg equation for a cubic system [179].

$$n\lambda = \left[2a_0/(h^2+k^2+1^2)^{\frac{1}{2}}\right] \sin\theta$$
 (52)

The factor  $a_0/(h^2+k^2+l^2)^{\frac{1}{2}}$  in Equation (52) is simply the interplanar spacing d for the plane (hkl). The Bragg equation in its general form is then written

$$n\lambda = 2d \sin \theta \tag{53}$$

Multiplying the equation by  $2\pi$  and dividing by d one can obtain  $2\pi n\lambda/d = 4\pi \sin\theta$  or  $2\pi/d = 4\pi \sin\theta/n\lambda$ . By inserting the value for d we have  $2\pi/d = (2\pi/a_0)n$ . By defining  $2\pi/d = q$ , and  $2\pi/a_0 = m$ , therefore, the equation can be simplified to q = mn or  $2\pi/d = mn$ .

A plot of q versus n can be tried by least square technique to get the best fit of data point for different

order of reflections. Here m is the slope of the line. Thus, the d value when n = 1 or d(001) basal spacing would be equal to  $2\pi/m$ . For example, application of the above procdures using Braggs law for x-ray diffraction pattern of Ni(phen) $_3^{2+}/SO_4^{2-}$ -hectorite system indicate that the true d(001) to be 29.7 (see Fig. 30).

## B. Sample Calculation for the Amount of Catalyst

The amount of Ni(phen) 3SO4 complex needed in order to prepare 2 CEC of 0.1 g of natural hectorite (with 2 CEC of 73 meq/100 g) is as follows: Ni(phen) $_3$ SO $_4$ , 7 H $_2$ O  $\Rightarrow$  F.W. = 947.3 g/mole or 473.7 g/eq. 73 meq  $\times$  0.1 g hectorite/100 g = 0.073 meq of the complex needed for 1 equivalent CEC of 0.1 g hectorite or  $(7.3 \times 10^{-5} \text{ eq})$ .  $7.3 \times 10^{-5}$  eq × 2 (factor for 2 CEC) × 473.7 g/eq = 0.0692 g of Ni(phen) 3SO4, 7 H2O needed for 2 equivalent CEC of 0.1 g hectorite. Now,  $7.3 \times 10^{-5}$  eq of  $SO_4^{2-}$  should be subtracted from the total complex (i.e. 0.0692 g) needed for 2 equivalent CEC. Hence  $7.3 \times 10^{-5}$  eq × (48 g/eq  $SO_A^{2-}$ ) = 0.0035 g  $SO_A^{2-}$  that will wash out of the clay and 0.0692 g - 0.0035 g = 0.0657 g of complex cation and ion pair in 0.1 g of hectorite. Therefore 0.1 g hectorite + 0.0657 g = 0.1657 gr of Ni(phen) $_{3}^{2+}/SO_{4}^{2-}$ hectorite intersalate would contain 0.073 meg of ion pair which is taken to function as a catalyst. In other words, we need 146 meq of Ni(phen) $_{3}^{2+}$  and 73 meq of SO $_{4}^{2-}$ 

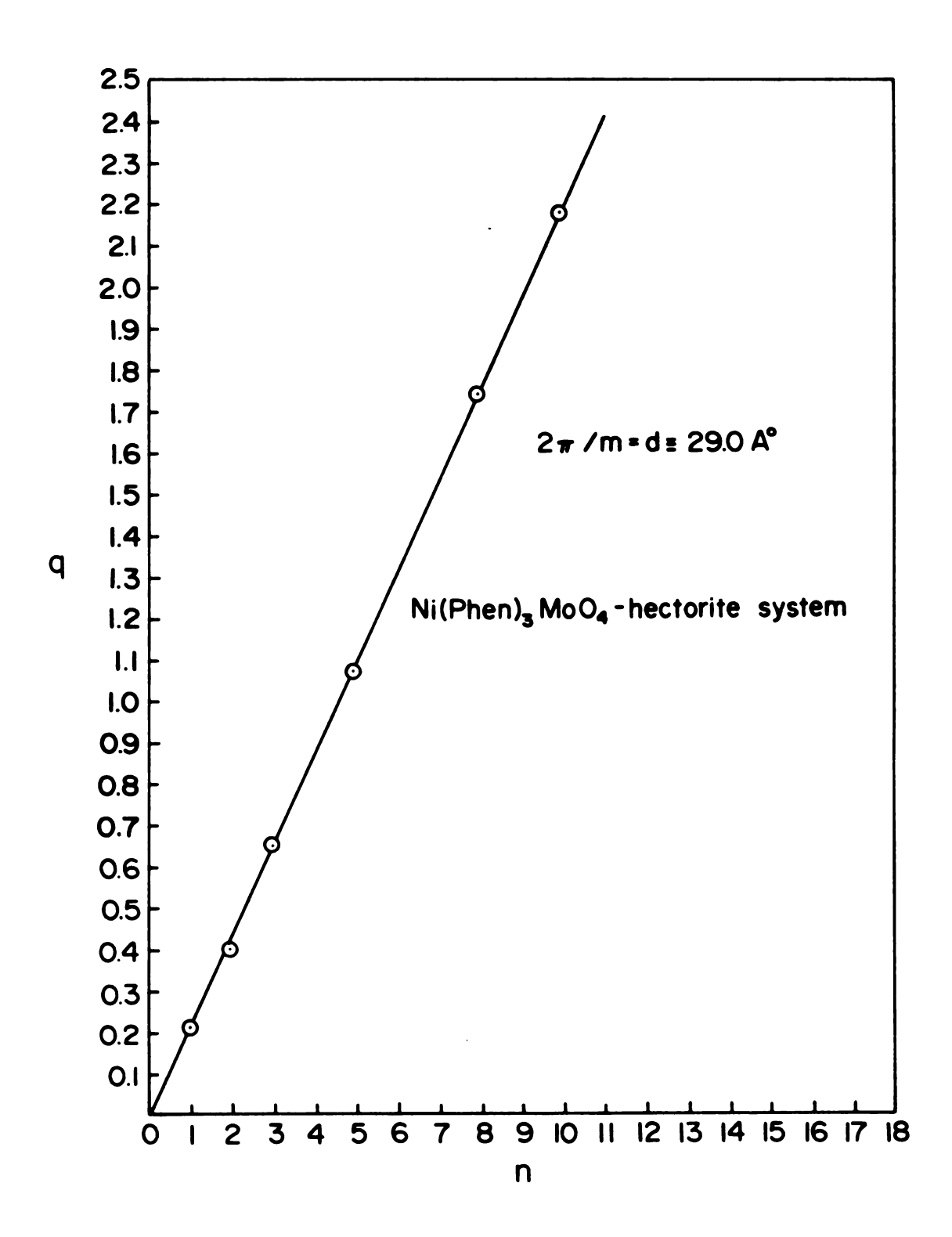


Figure 30 Plot of  $2\pi/d$  (d is basal spacing) versus n (order of reflection), using least square fitting technique.

to prepare 0.1657 g of Ni(phen) $_3^{2+}/\text{SO}_4^{2-}$ -hectorite intersalate.

LIST OF REFERENCES

## LIST OF REFERENCES

- 1. G. Brown, Ed., X-Ray Identification and Crystal Structure of Clay Minerals, Mineralogical Society, London, 1961.
- 2. G.W. Brindly and G. Brown, Eds., Crystal Structures of Clay Minerals and Their X-Ray Identification, Mineralogical Society, London, 1980.
- 3. H. Van Olphin, "An Introduction to Clay Colloid Chemistry", 2nd ed., John Wiley, New York, 1977, chapter 7.
- 4. J.D. Russell and A.R. Frazer, Clays and Clay Minerals 19, 55 (1971).
- 5. Thomas J. Pinnavaia, Intercalated Clay Catalysts, Science 220, 365-371 (1983).
- 6. M.M. Mortland, J.J. Fripiat, J. Chaussidon, and Uytterhoeven, J. Phys. Chem. 67, 248 (1963).
- 7. B.S. Snowder and Woessner, J. Colloid. Interface Sci. 30, 54 (1969).
- 8. D.H. Solomon and D.G. Hawthorne, Chemistry of Pigments and Fillers, John Wiley & Sons, New York, (1983).
- 9. B.K.G. Theng, "The Chemistry of Clay-Organic Reactions", Johy Wiley & Sons, New York, (1974).
- 10. M.M. Mortland, Adv. Agron. 22, 75 (1970).
- 11. M.M. Mortland, Trans. 9th Intern. Congr. Soil Sci. 1, 691 (1968).
- 12. G. Lagaly and A. Weiss, The Layer Charge of Smectite Layer Silicates., Proceedings of the International Clay Conference, Mexico City, pp. 157-172 (1975).
- 13. G. Lagaly, G. Schön and A. Weiss, Kolloid Zeitschrift und Zeitschrift für Polymere 250, 667-674 (1972).

- 14. H. Suquet, C. delaCalle, H. Pezerat, Clays Clay Miner. 23, 1 (1975).
- 15. J.J. Fripiat and M.I. Cruz-Cumplido, Ann. Rev. Earth Plant Sci. 2, 239 (1974).
- 16. A. Shimoyama and W.D. Johns, Nature Phys. Sci. 232, 140 (1971).
- 17. W.D. Johns and A. Shimoyama, Amer. Ass. Petrol. Geol. Bull. 56, 2160 (1972).
- 18. G.W. Bailey and J.L. White, Residue Rev. 32, 29 (1970).
- 19. M. Schnetzer and H. Kodama in "Minerals in Soil Environments", J.B. Dixon and S.B. Weeds, Eds., Soil Science Society of America, Madison, WI, 1977, Chapter 21.
- 20. J.E. Bernal, "The Physical Basis of Life", Rutledge and Kegan Paul, London, 1951.
- 21. M. Paecht-Horowitz, J. Berger, A. Katchalsky, Nature 228, 6361 (1970).
- 22. M. Paecht-Horowitz, Angew. Chem. Int. Ed. Engl. 12, 349 (1973).
- 23. J.J. Fripiat and G. Poncelet, Adv. Org. Geochem. Proc. 6th Intern. Meet., 875 (1974).
- 24. N. Lahav, D. White, S. Chang, Science 201, 67 (1978).
- 25. D.H. White and J.C. Erickson, J. Mol. Evol. <u>16</u>, 279 (1980).
- 26. (a) T. Endo, M.M. Mortland and T.J. Pinnavaia, Clays and Clay Minerals 28, 105 (1980); (b) T. Endo, M.M. Mortland and T.J. Pinnavaia, Clays and Clay Minerals 29, 153 (1981).
- 27. Ming-Shin Tzou, Ph.D. Dissertation, Chemistry Department, Michigan State University, 1983.
- 28. D.E. Woessner, J. Mag. Res. 39, 297 (1980).
- 29. T.J. Pinnavaia in "Advanced Techniques for Clay Mineral Analysis", J.J. Fripiat, Ed., Elsevier, New York, 1981, pp. 139-161.

- 30. M.B. McBride in "Advanced Chemical Methods for Soil and Clay Mineral Research", J.W. Stucki and W.L. Banwart, Eds., Reidel, Holland, 1980, pp. 423-450.
- 31. W.E.E. Stone in "Advanced Techniques for Clay Mineral Analysis", J.J. Fripiat, Ed., Elsevier, New York, 1981, pp. 71-112.
- 32. J.J. Fripiat, "Advanced Techniques for Clay Mineral Analysis" Elsevier, Amsterdam (1981).
- 33. P.L. Hall in "Advanced Techniques for Clay Mineral Analysis", J.J. Fripiat, Ed., Elsevier, New York, pp. 51-75 (1981).
- 34. W.E.E. Stone, in "Advanced Techniques for Clay Mineral Analysis", J.J. Fripiat, Ed., Elsevier, New York, pp. 71-112 (1981).
- 35. B.K.G. Theng, "Formation and Properties of Clay-Polymer Complexes", Elsevier Scientific Publishing Company, New York (1979).
- 36. V.J. Thielman and J.L. McAtee Jr., Clays & Clay Minerals 23, 173 (1975).
- 37. V.E. Berkheiser and M.M. Mortland, Clays and Clay Minerals 25, 105-112 (1977).
- 38. R.A. Schoonheydt, J. Pelgrims, Y. Heroes and Jan. B. Uytterhoeven, Clay Minerals 13, 435 (1978).
- 39. M.F. Traynor, M.M. Mortland, and T.J. Pinnavaia, Clays and Clay Minerals 26, 318 (1978).
- 40. R.H. Loeppert, M.M. Mortland, and T.J. Pinnavaia, Clays and Clay Minerals 27, 201 (1979).
- 41. H. Van Olphen, "An Introduction to Clay Colloid Chemistry", 2nd ed., Wiley-Interscience, New York, p. 70 (1977).
- 42. D.M. Clementz and M.M. Mortland, Clays & Clay Miner. 22, 223 (1974).
- 43. M.M. Mortland and V.E. Berkheiser, Clays and Clay Miner. 24, 60 (1976).
- 44. R.H. Loeppert, R. Raythatha, M.M. Mortland, and T.J. Pinnavaia, Preprints, Catalysis Soc. 6th North American Meeting, Chicago, (1979).

- 45. R.H. Loeppert and M.M. Mortland, Clays and Clay Minerals. 27, 373 (1979).
- 46. C.M. Starks, J. Amer. Chem. Soc. 93, 195 (1971).
- 47. C.M. Starks and D.R. Napier (to Continental Oil Company) U.S. patent 3,992,432 (1976); British patent 1,227,144 (197); French patent 1,573,164 (1969); Australian patent 439,286 (196), Netherlands patent 6,804,687 (1968).
- 48. C.M. Starks and R.M. Owens, J. Amer. Chem. Soc. <u>95</u>, 3613 (1973).
- 49. C.M. Starks and C. Liotta, "Phase Transfer Catalysis", Principles and Techniques, Academic Press, New York, (1978).
- 50. J. Jarrouse, C.R. Hebd. Seances Acad. Sci., Ser. C 232, 1424 (1951).
- 51. DuPont, British patent 632,346 (1949).
- 52. P. Edwards (to American Cyanamid), U.S. Patent 2,537,981 (1951).
- 53. Pest Control. Ltd., British patent 692,774 (1953).
- 54. R. Kohler and H. Pietsch (to Henkle), German patent 944,995 (1956).
- 55. H. Rath and U. Einsele, Melliand Textilber 40, 526 (1959); C.A. 53, 16531 (1957).
- 56. H.B. Copelin and G.B. Crance (to DuPont), U.S. patent 2,779,781 (1957).
- 57. Farbenfabriken Bayer, German patent 959,497 (1957); C.A. <u>53</u>, 13665 (1959).
- 58. B. Graham (to Ethyl Corp.), U.S. patent 2,866,802 (1958).
- 59. G. Maercker, J.F. Carmichael, and W.S. Port, J. Org. Chem. 26, 2681 (1961).
- 60. Gavaert Photo-Produce N.V., Belgian patent 602,793 (1961); C.A. 59, 11491 (1963).
- 61. B.E. Jennings (to ICI), British patent 907,647 (1962).

- 62. M.A. Iskenderov, V.V. Korshak, and S.V. Vinogradova, Vysokomol, Soedin 4, 637 (1962); C.A. 58, 9239 (1962).
- 63. W.S. Port, British patent 912,104 (1962).
- 64. R.W. Kay (to Distillers, Ltd.), British patent 916,772 (1963).
- 65. F. Nerdel, British patent 1,052,047 (1966).
- 66. B.C. Oxenrider and R.M. Hetterly (to Allied Chem.), U.S. patent 3,297,634 (1967).
- 67. M. Makosza and B. Serafinowa, Rocz. Chem. <u>39</u>, 1223 (1965).
- 68. N.A. Gibson and J.W. Hosking, Aust. J. Chem. <u>18</u>, 123 (1965).
- 69. H.E. Hennis, L.R. Thompson, and J.P. Long, Ind. Eng. Chem. Prod. Res. Dev. 7, 96 (1968).
- 70. A Brändström and U. Junggren, Acta Chem. Scand. 23, 2204 (1969).
- 71. C.L. Liotta and H.P. Harris, J. Amer. Chem. Soc. <u>95</u>, 2250 (1974).
- 72. E.V. Dehmlow, Angew. Chem. Inst. Edn. 16, 493 (1977).
- 73. H. Schnell, Angew. Chem. 68, 633 (1956).
- 74. N.O. Bodin, et al. Antimicrob. Agents Chemother. 8, 518 (1965).
- 75. Beecham Group Ltd., British patent 1,364,672 (19 ).
- 76. Chem. Eng. Prog. Symp. 26, 66 (1970).
- 77. A. Molin, Dissertation (Ph.D.) Department of Chemical Technology, Royal Institute of Technology, 5-100 44 Stockholm, Sweden.
- 78. P.S. Hallman, B.R. McGarvey, and G. Wilkinson, J. Chem. Soc. A.P. 3143 (1968).
- 79. D.S. Allam and W.H. Lee, J. Chem. Soc. A.P. 426 (1966).
- 80. V.L. Kheifets, N.A. Yakovleva, and B. Yakrasilschik, Zh. Prikl. Khim. (Lenningrad).
- 81. J.E. Gordon and R.E. Kutina, J. Amer. Chem. Soc. 99, 3903 (1977).

- 82. E.J. Fendler and J.H. Fendler, Adv. Phys. Org. Chem. 8, 271 (1970).
- (a) S.L. Regen, J. Amer. Chem. Soc. 97, 5956 (1975); (b) S.L. Regen, J. Amer. Chem. Soc. 98, 6270 (1976); 83.

  - (c) S.L. Regen, J. Org. Chem. 42,  $87\overline{5}$  (1977).
- S.L. Regen, Angew. Chem. 18, 421-429 (1979). 84.
- 85. D. Landini, A. Maia, F. Montanari, J. Amer. Chem. Soc. 100, 2796 (1978).
- 86. Euchen Conference on Phase-Transfer Catalysis and Related Topics, Gargano (Italy), 1978.
- 87. M. Makosza, E. Bialecka, Tetrahedron Lett., 183 (1977).
- 88. (a) W.P. Weber, G.W. Gokel: Phase-Transfer Catalysis in Organic Synthesis, Springer, Berlin (1977); (b) E.V. Dehmlow, Angew Chem. 89, 521 (1977); (c) E.V. Dehmlow, Angew Chem. Int. Ed. Engl. 16, 493 (1977); (d) A. Brändström, Adv. Phys. Org. Chem. 15, 267 (1977).
- 89. E.H. Cordes, R.B. Dunlap, Acc. Chem. Res. 2, 329 (1969).
- 90. C.A. Bunton, Prog. Solid State Chem. 8, 239 (1973).
- 91. F.M. Menger, J. Amer. Chem. Soc. 92, 5965 (1970).
- 92. J.M. Brown, and J.A. Jenkins, Chem. Comm. 1976, 458 (1976).
- 93. M. Cinquini, S. Colonna, F. Montanari, and P. Tundo, Chem. Comm. 1976, 392 (1976).
- 94. H. Molinari, F. Montanari, and P. Tundo, Chem. Comm. 1977, 639 (1977).
- 95. P. Tundo, Synthesis 1978, 315 (1978).
- 96. M. Tomoi, O. Abe, M. Ikeda, K. Kihara, and H. Kakiuchi, Tetrahedron Lett. 1978, 3031 (1978).
- H. Serita, N. Ohtani, and C. Kimura, Kobunshi 97. Ronbunshu 35, 203 (1978).
- 98. H.J.M. Dou, R. Gallo, P. Hassanaly, and J. Metzger, J. Org. Chem. 42, 4275 (1977).
- 99. P. Tundo, Chem. Comm. 1977, 641 (1977).

- 100. J. Smid, S. Shah, L. Wong, and J. Hurley, J. Amer. Chem. Soc. 97, 5932 (1975).
- 101. S. Shah and J. Smid, J. Amer. Chem. Soc. <u>100</u>, 1426 (1978).
- 102. E. Blasius and P.G. Maurer, Makromol. Chem. <u>178</u>, 649 (1977).
- 103. S.L. Regen, in "Catalysis in Organic Synthesis" (G.V. Smith, Ed.), Academic Press, New York, 1977, p. 119.
- 105. E. Chiellini and R. Saloro, Chem. Comm. <u>1977</u>, 231 (1977).
- 106. E. Chiellini, R. Saloro, and S.D. Antone, Makromol. Chem. 178, 3165 (1977).
- 107. S. Colonna, R. Fornasier, and U. Pfeiffer, J. Chem. Soc. Perkin I, 1978, 8 (1978).
- 108. T. Yamashita, H. Yasueda, N. Nakatani and N. Nakamura, Bull. Chem. Soc. Japan 51, 1183 (1978).
- 109. T. Yamashita, H. Yasueda, and N. Nakamura, Bull. Chem. Soc. Japan 51, 1247 (1978).
- 110. (a) S. Ohashi and S. Inoue, Macromol. Chem. <u>150</u>, 105 (1971); (b) S. Ohashi and S. Inoue, Macromol. Chem. 160, 69 (1972).
- 111. S. Inoue, S. Ohashi, and Y. Unno, Polymer J. 3, 611 (197).
- 112. S.L. Regen and L. Dulak, J. Amer. Chem. Soc. <u>99</u>, 623 (1977).
- 113. S.L. Regen, J. Amer. Chem. Soc. 99, 3838 (1977).
- 114. M. Tomoi, T. Takubo, M. Ikeda, and H. Kakiuchi, Chem. Lett. 1976, 473 (1976).
- 115. H. Normant, Angew. Chem. Int. Edn. 6, 1046 (1967).
- 116. J.E. Shaw, D.Y. Hsia, G.S. Parries, and T.K. Sawyer,
   J. Org. Chem. 43, 1017 (1978).
- 117. F. Rolla, W. Roth, L. Horner, Naturwissenschaften 64, 377 (1977).

- 118. (a) C.G. Armistead, A.J. Tiler, F.H. Hambleton, S.A. Mitchel and J.A. Hochey, J. Phys. Chem. 73, 3947 (1969); (b) W.A. Aue and C.R. Hastings, J. Chromotogr. 42, 319 (1969); (c) H. Colin and G. Gviochon, ibid 141, 289 (1977); (d) P. Roumeliotis and K.K. Unger, ibid 149, 211 (1978).
- 119. J.F. Fritz and J.N. King, Anal. Chem. 48, 570 (1976).
- 120. I. Haller, J. Amer. Chem. Soc. 100, 8050 (1978).
- 121. A.C. Zettlemoyer and H.H. Hsing, J. Colloid Interface Si. 58, 263 (1977).
- 122. P. Tundo and Paolo Venturello, J. Amer. Chem. Soc. 101, 6606 (1979).
- 123. S.L. Regen and C. Koteel, J. Amer. Chem. Soc. <u>99</u>, 3837 (1977).
- 124. I. Halasz, and P. Vogtel, Angew. Chem. Int. Ed. Engl. 19, 24-28 (1980).
- 125. R.K. Iler, "The Chemistry of Silica", Wiley, New York, chapters 5 and 6, (1979).
- 126. P. Tundo, Paolo Venturello, and E. Angeletti, J. Amer. Chem. Soc. 104, 6551-6555 (1982).
- 127. P.C.H. Posher, Angew. Chem. Int. Ed. Engl. <u>17</u>, 487 (1978).
- (a) S.L. Regen, S. Quici, S. Liaw, J. Org. Chem. 44, 2029 (1979); (b) G. Bram, T. Fillebeen-Khan, and N. Geraghyt, Synth. Comm. 10, 279-289 (1980); (c) E. Angeletti, P. Tundo, P. Venturello, J. Chem. Soc., Chem. Comm. 1127 (1980).
- 129. M.M. Egorov et al., Zh. Fiz. Khim. <u>36</u>, 1882 (1962).
- 130. R.K. Iler, J. Colloid Interface Sci. <u>55</u>, **25** (1976).
- 131. T.J. Pinnavaia, R. Raythatha, J.G.S. Lee, L.J. Holloran, and J.F. Hoffman, J. Amer. Chem. Soc. 101, 6891 (1979).
- 132. R. Raythatha and T.J. Pinnavaia, J. Catal. <u>47</u>, 80 (1983).
- 133. J.M. Thomas in "Intercalation Chemistry", M.S. Whittingham and A.J. Jacobson, Eds., Academic Press, New York (1982) Chapter 3.

- 134. P. Monsef-Mirzai and W.R. McWhinnie, Inorg. Chem. Acta 52, 211 (1981).
- 135. F.T. Bingham, J.R. Sims and A.L. Page, Soil Sci. Soc. Am. Proc. 29, 670 (1965).
- 136. C. McAuliffe, M.S. Hall, L.A. Dean, and S.B. Hendricks, Soil Sci. Am. Proc. 12, 119 (1947).
- 137. J.L. Ahlrichs, Bonding of Organic Polyanions to Clay Minerals, Dissertation Abstracts 22, 2121 (1962).
- 138. S.K. De and R.K. Jaim, J. Indian Chem. Soc. <u>41</u>, 379 (1964).
- 139. M.B. McBride, T.J. Pinnavaia and M.M. Mortland, Am. Mineral 60, 66 (1975).
- 140. G. Jacobs, F. Speeke, Acta Cryst. 8, 67 (1955).
- 141. (a) R.A. Inskeep, J. Inorg. Nucl. Chem. <u>24</u>, 763 (1962); (b) Inorganic Syntheses, Vol. p. 228.
- 142. The iron reagents, third edition, published by G.F. Smith Chemical Company, 1980.
- 143. G.F. Smith, Anal. Chem. 23, 925 (1951).
- 144. Lewis J. Clark, Anal. Chem. 34, 348 (1962).
- 145. Man-Sheung Chan, J. Barry Deroos and Arthur C. Wahl, J. Phys. Chem. 77, 2163 (1973).
- 146. R.S. Vagg, R.N. Warrener and E.C. Walton, Aust. J. Chem. 20, 1841 (1967).
- 147. P.J. Taylor and A.A. Schilt, Inorganica Chimica Acta 5, 691 (1971).
- 148. (a) T.D. George and W.W. Wendlandt, J. Inorg. Nucl. Chem. 25, 395 (1963; (b) A. Braver, Ed., "Handbuch der Praparativen Anorganischen Chemie" Ferdinand Enke Verlag, Stuttgart, Germany (1954).
- 149. F.H. Burstall and R.S. Nyholm, J. Chem. Soc. 3570-3579 (1952).
- 150. Inorganic Synthesis 1, 37 (1939).

- 151. R.A. Schoonheydt, J. Pelgrims, Y. Heroes, and J.B. Uytterhoeven, Clay Minerals 13, 435 (1978).
- 152. A. Wada, N. Sakake, and J. Tanaka, Acta Cryst. B32, 1121 (1976).
- 153. J. Baker, L.M. Englehardt, B.N. Figgis, and A.H. White, JCS Dalton, 530 (1975).
- 154. P. Krumholz, Inorg. Chem. 4, 612 (1965).
- 155. R.A. Palmer and T.S. Piper, Inorg. Chem. <u>5</u>, 864 (1966).
- 156. J. Hidaka and B. Douglas, Inorg. Chem. 3, 1180 (1964).
- 157. P. Day and N. Sanders, J. Chem. Soc. (A), 1530 and 1536 (1967).
- 158. T. Ito, N. Tanaka, I. Hanazaki, and S. Nagakura, Bull. Chem. Soc. Japan 41, 365 (1968).
- 159. S.F Mason, Inorgamica Chemica Acta Reviews 1-3, 89 (1968).
- 160. D.J. Greenland and J.P. Quirk, Clays and Clay Minerals 9, 484 (1962).
- 161. M. Mesrogli and G. Lagaly, Proceedings of the International Clay Conference, Italy, p. 201 (1982).
- 162. D.M. Clementz, T.J. Pinnavaia, and M.M. Mortland, J. Phys. Chem. 77, 196 (1973).
- 163. M.B. McBride, T.J. Pinnavaia, and M.M. Mortland, Am. Mineral. 60, 66 (1975).
- 164. W.H. Quayle and T.J. Pinnavaia, Inorganic Chemistry 18, 10 (1979).
- 165. M.B. McBride, J. Phys. Chem. 80, 196 (1976).
- 166. R.G. Kooser, W.V. Volland, and J.H. Freed, J. Chem. Phys. 50, 5243 (1969).
- 167. W.H. Schreurs and G.K. Fraenkel, J. Chem. Phys. 34, 756 (1961).
- 168. Z. Luz, B.L. Silver, and C. Eden, J. Chem. Phys. 44, 4421 (1966).

- 169. L.J. Berliner, "Spin Labeling, Theory and Application, Academic Press, New York, 1976.
- 170. T.J. Stone, T. Buckman, P.L. Nordio, and H.M. McConnell, Proc. Nat'l. Acad. Sci. USA 54, 1010 (1965).
- 171. S.A. Goldman, G.V. Bruno, C.F. Polnaszek, and J.H. Freed, J. Chem. Phys. <u>56</u>, 716 (1972).
- 172. G.H. Schmid and D.G. Garratt, Can. J. Chem. <u>52</u>, 1807 (1974).
- 173. G.H. Schmid, V.M. Csizmadia, V.J. Nowlan, and D.G. Garratt, Can. J. Chem. 50, 2457 (1972).
- 174. S.L. Regen, J. Heh, and J. McLick, J. Org. Chem. 44, 1961 (1979).
- 175. F.T. Bingham, J.R. Sims, and A.L. Page, Soil Sci. Soc. Amer. Proc., 29, 670 (1965).
- 176. C.L. Liolta, H.P. Harris, M. McDermott, T. Gonzalez, and K. Smith, Tetrahedron Lett., 2417 (1974).
- 177. K.F. Clare, Nature 160, 828 (1947).
- 178. F.X. Grossey, and L.J. Woolsey, Ind. Eng. Chem. 47, 2253 (1955).
- 179. P. Harold Klug and Leroy E. Alexander, "X-ray Diffraction Procedures for Polycrystalline and Amorphous Materials", John Wiley and Sons, Inc., New York, 1974.

